Petrogenesis of Neoproterozoic Granitoids and Related Rocks from the Seychelles: the Case for an Andean-type Arc Origin

L. D. ASHWAL[1]*, D. DEMAIFFE[2] AND T. H. TORSVIK[3]

[1]DEPARTMENT OF GEOLOGY, RAND AFRIKAANS UNIVERSITY, PO BOX 524, AUCKLAND PARK 2006, SOUTH AFRICA

[2]DÉPARTEMENT DES SCIENCES DE LA TERRE ET L'ENVIRONNEMENT, UNIVERSITÉ LIBRE DE BRUXELLES, CP 160/02, AV. F. D. ROOSEVELT 50, B-1050 BRUSSELS, BELGIUM

[3]GEOLOGICAL SURVEY OF NORWAY, PO BOX 3006 LADE, N-7002, TRONDHEIM, NORWAY

The Seychelles islands consist of undeformed and unmetamorphosed, metaluminous monzogranites and granodiorites of Neoproterozoic age (∼ 750 Ma). Subsolvus, and lesser hypersolvus granitoids are crosscut by coeval dolerite dykes, dominantly of olivine tholeiite composition. Field relations suggest that mixing between granitoid and doleritic magmas generated a variety of minor intermediate rocks that occur as irregular masses and enclaves; their compositions plot as linear arrays between those of dolerites and granitoids. Two groups of granitoids can be distinguished based on colour, chemistry and isotopic signature. Mahé Group granitoids are grey, with relatively low incompatible element concentrations and primitive isotopic signatures that cluster at $\varepsilon_{Nd\,750} = +2\cdot85 \pm 0\cdot17$ and $I_{Sr\,750} = 0\cdot7031 \pm 0\cdot0008$ (some samples with impossibly low $I_{Sr} <0\cdot700$ were affected by open-system processes). Praslin Group granitoids are characteristically red to pink, with Rb >180 ppm, U >4·2 ppm, Th >20 ppm, Pb >30 ppm, and correspondingly evolved and variable isotopic signatures ($\varepsilon_{Nd,\,T} = +0\cdot80$ to $-3\cdot71$ and $I_{Sr,\,T} = 0\cdot7032–0\cdot7263$). Both groups of granitoids appear to have been derived from a mixed source dominated by a juvenile, mantle-derived component, with variable amounts of an ancient, possibly Archean, silicic source constituent or contaminant. Potential source materials are unexposed in the Seychelles, but the juvenile component may resemble ∼ 750 Ma intermediate to mafic metavolcanic rocks of NW Madagascar or NE India; candidates for the ancient silicic component, whose signature is slightly enhanced in granitoids of the Praslin Group, may be represented by 2·5–3·3 Ga tonalitic gneisses of the Banded Gneiss Complex in Rajasthan (NW India), or by similar materials present in central–northern Madagascar. Seychelles dolerites show variable Nd and Sr isotopic compositions ($\varepsilon_{Nd\,750} = +5\cdot46$ to $-0\cdot87$; $I_{Sr\,750} = 0\cdot7021–0\cdot7061$) that can be modelled as basaltic magmas derived from depleted mantle, variably contaminated (0–15%) by Archaean silicic crust. All petrologic, petrographic, geochemical, isotopic and chronologic data for Neoproterozoic magmatic rocks of the Seychelles, coupled with palaeomagnetic data indicating its position at the margin of the Rodinia supercontinent at ∼ 750 Ma, are at least consistent with, if not suggestive of, a continental or Andean-type arc setting. We argue, therefore, that the conventionally accepted notion of an extensional (i.e. rift or plume) setting for Seychelles magmatism is vulnerable.

INTRODUCTION

The Seychelles (Figs 1 and 2), correctly interpreted by both Wegener (1924) and Du Toit (1937) as a continental fragment left behind after Gondwana break-up, have long been considered as a geological curiosity, representing small, but conspicuous granitic islands in the Indian Ocean, at least 1000 km from the prominent continental land masses of Madagascar or Africa. About 25 of the >100 islands in the Seychelles archipelago

consist almost entirely of Late Precambrian granitic basement, the largest of which (Mahé Island, $\sim 140\,km^2$) contains mountainous topography reaching an altitude of nearly 1 km; the remaining islands are coralline, with and without sand cays (Baker, 1963). Seismic studies indicate a crustal thickness of ~ 33 km (Davies & Francis, 1964; Laughton et al., 1970), and the extent of the Seychelles 'microcontinent' (e.g. Davies, 1968; Plummer & Belle, 1995), albeit mainly submerged, can be approximated at $\sim 40\,000$–$45\,000\,km^2$ based on its topographic expression (Fig. 1). Considerations that the Seychelles might be contiguous with the African mainland, but separated from it by an intervening subsident basin (e.g. Baker & Miller, 1963), were denied by seismic evidence for the existence of oceanic crust in the Somali Basin (Francis et al., 1966; Matthews & Davies, 1966).

Our interest in the Seychelles and other former continental fragments of Gondwana, such as Madagascar, relates to current efforts in refining a more precise fit of Gondwana components, and developing an increased understanding of the details of Gondwana assembly and break-up. Accordingly, we extensively sampled Seychelles rocks for detailed geochronological, geochemical and palaeomagnetic analysis. We report here the results of our petrologic, geochemical and isotopic studies of Late Precambrian igneous rocks from the Seychelles, and discuss their origin in terms of magmatic and tectonic processes. Palaeomagnetic and geochronological results are published elsewhere (Torsvik et al., 2001a; Tucker et al., 2001).

SEYCHELLES GEOLOGY

Introduction

The memoir of Baker (1963) remains the definitive work on the geology of the Seychelles. Although later workers, including the present authors, have supplemented this effort as described below, Baker's observations, measurements and maps represent the most comprehensive basis for all subsequent studies. Simply stated, Seychelles geology consists of an assortment of Late Precambrian undeformed granitic rocks crosscut by doleritic dykes (Fig. 3a; Baker, 1963, 1967). Metamorphic and sedimentary rocks are completely absent. The youngest Seychelles igneous rocks include syenites, alkaline gabbros and granites, and trachytic tuffs in a Mid-Palaeocene (63.2 ± 1 Ma, Rb–Sr, Dickin et al., 1986) alkaline ring complex exposed only on Silhouette and North Islands (Fig. 2) (Devey & Stephens, 1992); these Deccan-related magmatic rocks are not considered further in this paper.

Granitoid rocks

Baker (1963, 1967) distinguished three types of Precambrian granitoids: grey granite (typified by the granitic rocks exposed on Mahé Island), 'faintly gneissose' grey granite (Île au Cerf and Ste. Anne), and 'reddish' granite (Praslin and La Digue). Textural varieties include porphyritic facies (western Mahé, Marianne), aplitic rocks (Fregate), and zones in which amphibolite and/or diorite enclaves and xenoliths are present (e.g. northern Mahé). Baker considered all of the granitoid rocks as cogenetic facies of a single intrusion, with the slightly foliated varieties having formed during magmatic flow, possibly near the margins of the intrusion. Contacts between the major or varietal granitoid types have not been identified, mainly because of poor exposures in the heavily vegetated mountainous interiors of most Seychelles islands.

Baker's geological map of Mahé was revised by Suwa et al. (1983) and Hoshino & Suwa (1983), who distinguished a region of 'gneissose' granodiorite in northern Mahé, and correlated the grey and pink to reddish granites of Mahé, Praslin and La Digue, which they collectively considered to represent a main, central intrusive mass. They also linked the porphyritic varieties in northwestern Mahé with those on Marianne, Fregate and several smaller islands, in what was proposed as a marginal facies of the intrusion. As discussed below, our work corroborates some, but not all of these correlations, and we hesitate to characterize mappable rock units with the generally poor level of exposure available in the Seychelles, and the resulting absence of clear contact relations. A first-order observation made by Weis & Deutsch (1984) is that the typical grey granitoids of Mahé are geochemically and isotopically distinct from the reddish to pinkish varieties of Praslin, La Digue and other islands; we concur with and elaborate upon this bipartite subdivision below. The geological and sample location map shown in Fig. 2 is simplified from the published maps of Baker (1963) and Suwa et al. (1983), and shows the distribution of 'grey' and 'pink' granitoid types, which we refer to as the Mahé and Praslin Groups, respectively. With the exception of the two large areas of porphyritic grey granitoids on western Mahé, we have chosen not to distinguish areas with common textural properties in Fig. 2 (e.g. porphyritic, aplitic, subsolvus vs hypersolvus varieties).

Doleritic dykes

Doleritic dykes (up to 80 m thick, average 0·5–2 m) are present throughout the Seychelles islands; most are near vertical with strikes of N20–70°W, clustering at N40°W (Baker, 1963; Devey & Stephens, 1991; Torsvik et al., 2001a). Age data are sparse, but there is some indication that both Late Proterozoic and Late Cretaceous dykes exist, with the latter possibly restricted to Praslin. K–Ar results for Mahé dykes yield ages between 312 ± 6 Ma and 654 ± 55 Ma (Baker & Miller, 1963; Dickin et al.,
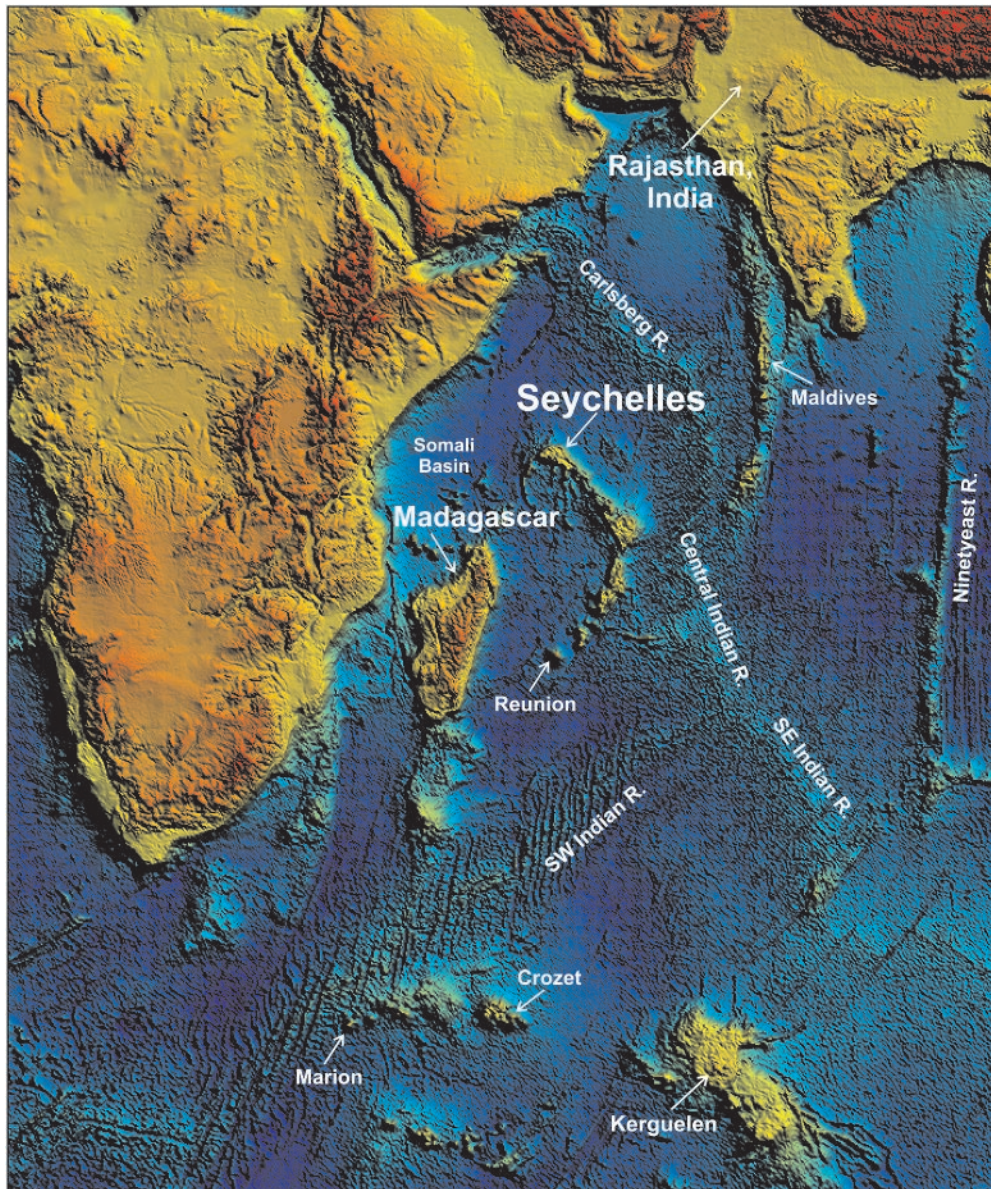
Fig. 1. Indian Ocean topography from global digital elevation model (Smith & Sandwell, 1997), showing Seychelles, other relevant tectonic features, and localities mentioned in the text.

1986; Hargraves & Duncan, 1990), although most of these ages are considered disturbed as a result of Ar loss. An important result from a granophyric patch in a 10 m thick dolerite dyke from southwestern Mahé (U–Pb zircon age of 750·2 $\pm$ 2·5 Ma) demonstrates the coevality of granitoid and at least some dolerite magmatism in the Seychelles (Torsvik *et al.*, 2001*a*). Precambrian dykes are dominantly olivine tholeiites, and have been partly to completely altered to assemblages of amphibole (hornblende and/or actinolite), chlorite, epidote and white mica. New petrographic, chemical and isotopic data for Precambrian dykes are reported here.

Geochronology of Precambrian magmatic rocks

The Late Precambrian age of Seychelles granitoids was first established by Miller & Mudie (1961), who obtained a K–Ar age of 663 $\pm$ 17 Ma (recalculated using new decay constants, Dalrymple, 1979) for biotite in a pink granite from Mahé. Numerous isotopic studies since then, using a variety of techniques [summarized by Plummer (1995) and Tucker *et al.* (2001)], yield a range of ages between 625 $\pm$ 25 Ma (Rb–Sr microcline, Wasserburg *et al.*, 1963) and 780 $\pm$ 100 Ma (U–Pb zircon, multigrain fractions, Michot & Deutsch, 1977). The latest and
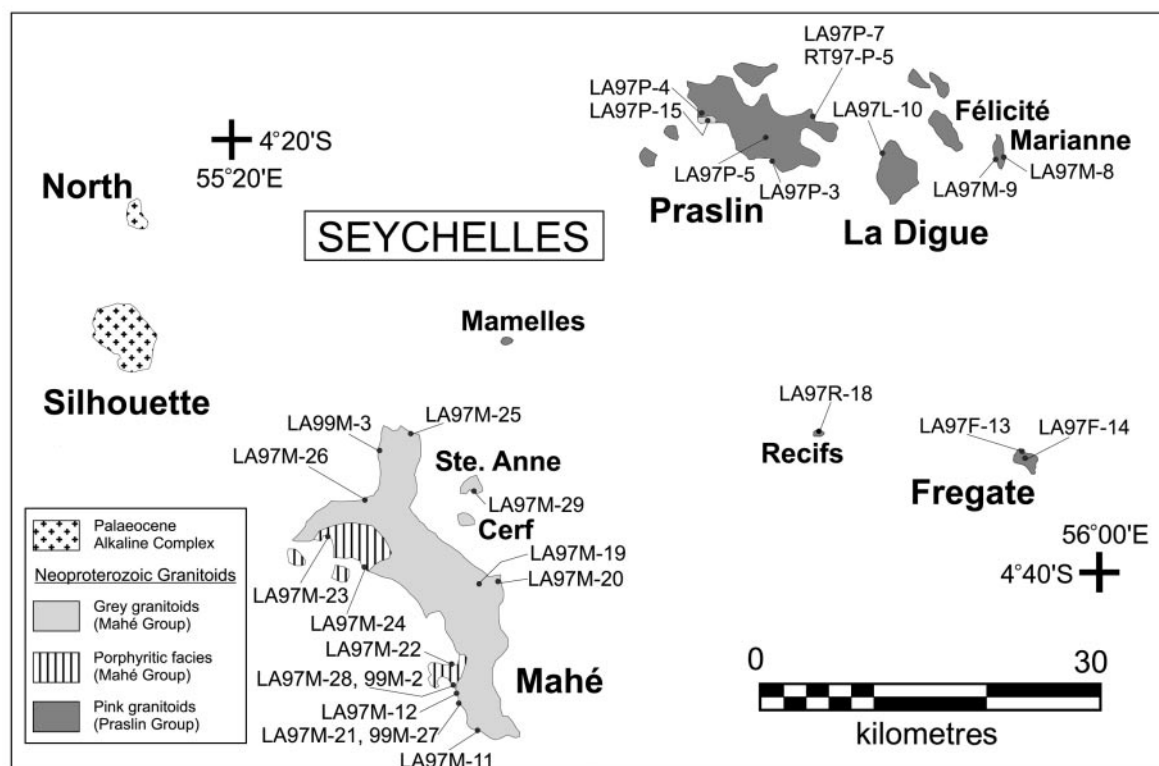
Fig. 2. Geological map of the Seychelles showing sample locations [modified from Baker (1963) and Suwa *et al.* (1983)]. Smaller islands have been omitted for clarity. We have distinguished the large areas of porphyritic grey granitoids of western Mahé; because of poor inland exposures, the boundaries shown are only approximate. Small regions of porphyritic granitoids, as well as other textural variants, occur elsewhere on Mahé and several other islands, but their extent and contact relations are not known. The distinction between Mahé and Praslin Group granitoids is made on the basis of colour, geochemistry and isotopic compositions, as discussed in the text.

most reliable effort, using U–Pb single zircon abrasion methods, yields concordant magmatic crystallization ages between 750 and 755 Ma for 19 individual granitoids from Mahé, Praslin, La Digue, Fregate and Mammelles (Stephens *et al.*, 1997; Tucker *et al.*, 2001). Reliable ages outside this range were obtained from Marianne (759 Ma), Ste. Anne (764 Ma), Recifs (809 Ma) (Tucker *et al.*, 2001) and eastern Mahé (703 Ma) (Stephens *et al.*, 1997). The vast majority of Late Precambrian magmatic rocks in the Seychelles, therefore, were produced at 752 $\pm$ 4 Ma (n = 19, Tucker *et al.*, 2001), although magmatism lasted for $\sim$100 my.

ANALYTICAL METHODS

Major and trace element compositions (Tables 1 and 2) were determined by standard X-ray fluorescence (XRF) techniques as follows. Slabs representative of each whole rock (generally >20 g) were trimmed of weathering rinds and powdered in a carbon steel vessel. For major elements, $\sim$0·35 g of sample was mixed with $\sim$2 g lithium tetraborate (Spectroflux), fused in a Pt–Au crucible for 2 h at 1000°C, and cast into a glass bead. For

trace elements, $\sim$10 g of sample was compressed into a pellet. Analyses were carried out on Philips 1404 and X'Unique II instruments housed at the University of Natal, Durban, Department of Geology. Instrumental uncertainties are as follows: $\pm$0·2% for SiO_2, CaO, TiO_2 and P_2O_5; $\pm$0·3% for MgO; $\pm$0·5% for Al_2O_3, Fe_2O_3 and MnO; $\pm$2% for Na_2O; $\pm$2% for Rb; $\pm$3% for Zr, Sr, Nb and Y; $\pm$5% for Zn, Cu, Ni, Cr, Ce and Nd; $\pm$10% for Sc, Pb, V, Ga, Co As and S; $\pm$20% for Ba, U and Th. Replicate analyses of sample LA97M-26C (Table 1) are in excellent agreement for both major and trace elements.

Trace elements, including rare earth elements (REE), were also analysed by inductively coupled plasma emission mass spectrometry (ICP-MS) at Musée Royal de l'Afrique Central, Dépt. de Géologie, Tervuren, Belgium, using a VG elemental Plasmaquad instrument. Details of the analytical procedures have been given by André & Ashchepkov (1996). Precision of these measurements is better than $\pm$5% for concentrations $\geq$1 ppm, and $\pm$10–15% for concentrations in the range 0·1–1 ppm. There is excellent agreement between trace element concentrations determined by XRF and ICP-MS
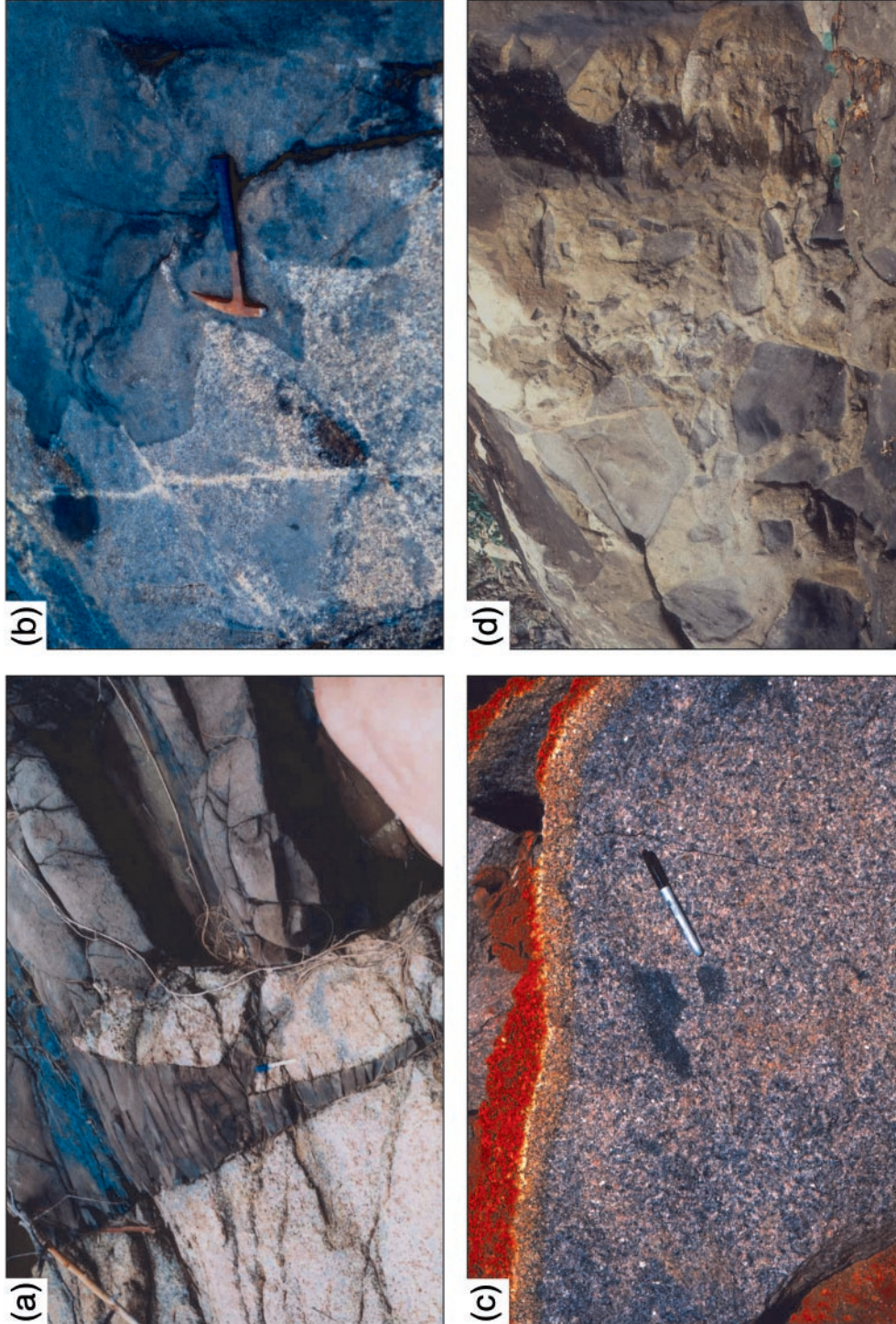
Fig. 3. Outcrop photographs illustrating magmatic features of Seychelles granitoids, dolerites and intermediate rocks. Locations are shown in Fig. 2. (a) Dolerite dyke with complex bifurcations and well-developed chilled margins, crosscutting granitoids at locality LA-97M-28, SW Mahé. The dyke pictured is an offshoot from a larger dyke ∼13 m thick, the central portions of which contain coarse granophyric patches (sample LA99M-2). (b) Irregular masses of mafic-rich intermediate rocks (right, samples LA97M-26B,C) showing lobate contacts with porphyritic quartz diorite (left, sample LA97M-26A). These relations are interpreted as having resulted from magmatic intermingling between coeval granitoid and dolerite intrusive rocks. Thin aplitic dykes (sample LA97M-26D) crosscut quartz diorites at left centre of photo. Bel Ombre locality, NW Mahé. (c) Rounded enclaves of 'amphibolite' (sample LA97M-25B) within hornblende–biotite granodiorite (sample LA97M-25A). Northern tip of Mahé. (d) Angular xenoliths of intermediate lithologies, mainly hornblende–biotite quartz diorite (sample LA99M-3B) within biotite granodiorite (sample LA99M-3A). Exposures north of Sunset Beach Hotel, NW Mahé.

Table 1: Major and trace elements for granitoids and intermediate rocks from the Seychelles

Mahé Group granitoids

Mahé

Sample:	LA99M-2	LA99M-3B	LA97M-11B	LA97M-20	LA97M-22	LA97M-23	LA97M-24A	LA97M-25A	LA97M-26D
Lithology:	Hypersolvus amph. granite	Hb–Bi quartz diorite	Hypersolvus amph. granite	Bi–Hb granite	Porphyritic Hb–Bi granite	Porphyritic Hb–Bi granodiorite	Porphyritic Hb–Bi granite	Hb–Bi granodiorite	Aplitic granite
U–Pb age (Ma):[a]			750.9 ± 2.0		748.4 ± 1.2	751.1 ± 1.7	750.8 ± 1.2		
SiO_2	75.65	58.01	75.72	70.69	75.46	72.29	73.84	72.79	77.63
TiO_2	0.19	0.94	0.24	0.49	0.24	0.39	0.32	0.33	0.07
Al_2O_3	12.29	17.27	11.77	13.53	12.34	13.81	12.98	13.54	12.62
Fe_2O_3*	2.39	8.07	2.49	3.40	2.20	2.80	2.52	2.88	0.43
MnO	0.08	0.17	0.09	0.10	0.07	0.07	0.07	0.10	0.01
MgO	0.08	2.86	0.02	0.54	0.16	0.57	0.29	0.41	0.00
CaO	0.35	6.40	0.49	1.42	0.84	2.02	1.29	1.40	0.68
Na_2O	4.19	4.59	4.17	4.50	4.08	4.27	4.09	5.26	3.60
K_2O	4.62	1.50	4.58	4.60	4.61	3.61	4.30	2.84	5.00
P_2O_5	0.01	0.30	0.02	0.17	0.02	0.09	0.06	0.08	0.01
LOI	0.35	0.44	0.28	0.00	0.44	0.45	0.30	0.09	0.17
Total	100.20	100.55	99.87	99.43	100.46	100.37	100.06	99.72	100.22
mg-no.[b]	0.306	0.824	0.096	0.677	0.490	0.729	0.603	0.653	0.000
Ba	1044	629	1213	864	1083	966	1178	1966	334
Rb	92.8	43.1	119.5	94.9	151.7	119.5	127.5	46.8	127.4
Sr	22.2	458.2	22.1	157.9	56.4	132.4	91.1	140.9	39.4
Ga	20	21	20	18	17	16	18	15	12
Nb	11.8	5.5	13.8	14.7	14.6	13.2	12.2	5.8	7.5
Hf	10.3	7	11.4	12.5	10.2	6.8	8.8	11.2	2.8
Zr	330	211	426.2	444.6	307.3	213.8	266.4	423.3	60.1
Y	62.7	41.8	79.2	46.4	63.1	52	58.3	37.1	17.3
Th	15.5	6.8	15.6	18.6	19.3	18.2	14.4	7.4	19.7
U	3.4	1.4	2.8	2.5	3.8	4.2	2.9	1.3	5.4
Ta	0.8	0.3	1.5	1.4	2.4	2.2	1.6	1.4	1.9
W	1.2	1.5	324	304	869	552	392	600	488
Cr	0.9	1.6	0	0	0	0	0	0	0
Ni	1.6	1.3	0	0	0	0	0	0	0
Co	0	18	68	68	150	96	75	102	95
Sc	6.2	24.9	7.5	9.9	5.2	7.6	8.1	10.4	1.5
V	0.53	59.6	4.3	1.05	7.8	26	14.4	10.4	0.6
Cu	0.9	7.7	0	0	0	0	0	0	0.3
Pb	15.6	9.4	6	9.8	21	18.3	18.7	13.5	28.7
Zn	96.1	97.6	69.4	99.9	66.8	49.6	66	84.8	3.6
La	62.59	27.07	64	108.09	48	36	44	50	18.82
Ce	131.56	60.12	132	204.74	100	73	91	100	35.42
Pr	16.45	7.95	16.4	22.51	12.1	8.7	11	12.1	3.55
Nd	63.37	33.73	62	79.26	45	32	41	44	11.57
Sm	12.33	7.21	12.1	12.55	8.7	6.5	8	7.5	2.07
Eu	2.21	2.16	2.1	2.2	1.37	1.04	1.44	1.99	0.28
Gd	11.97	7.53	12.3	10.86	8.7	6.5	8.6	7	2.04
Tb									
Dy	10.83	7.05	12.1	8.65	9	6.9	8.6	6	2.29
Ho	2.39	1.6	2.7	1.91	2.1	1.6	1.98	1.35	0.57
Er	6.38	4.2	7.4	5	5.9	4.6	5.5	3.4	1.71
Yb	6.98	3.84	7.7	5.29	6.2	5.3	5.9	3.5	2.33
Lu	1.06	0.6	1.21	0.84	0.93	0.78	0.89	0.6	0.37
S	230	969	34	404	93	22	31	114	174
As	1	0	1	5	5	4	3	1	8

	Mahé Group granitoids		Praslin Group granitoids								
	Praslin	Ste. Anne	Praslin		La Digue	Marianne	Fregate				Recifs
Sample:	LA97P-15	LA97A-29	LA97P-4	RT97P-5	LA97L-10	LA97M-9	LA97F-13A	LA97F-13B	LA97F-13C	LA97F-14	LA97R-16
Lithology:	Amphibole granodiorite	Hypersolvus amph. granite	Porph. granite	Hb–Bi granite	Hb–Bi granite	Amph granite	Aplitic Bi granite	Biotite granite	Porph. aplitic amph. granite	Biotite granite	Biotite granophyre
U–Pb age (Ma):[a]	752·5±3·2	764·2±1·4		752·9±4·0	750·5±1·8	758·8±2·0			754·7±1·9	752·0±1·7	808·8±1·9
SiO_2	73·32	75·87	74·74	73·90	75·55	68·01	77·99	71·67	73·11	71·11	75·31
TiO_2	0·31	0·08	0·19	0·21	0·25	0·49	0·15	0·37	0·30	0·51	0·28
Al_2O_3	13·14	12·53	12·36	12·81	12·21	14·58	12·18	14·50	13·22	14·30	12·42
Fe_2O_3*	2·83	1·23	2·41	2·30	2·04	4·77	0·69	2·39	3·06	3·33	2·30
MnO	0·10	0·04	0·05	0·04	0·04	0·10	0·03	0·16	0·06	0·08	0·04
MgO	0·36	0·35	0·04	0·07	0·19	0·39	0·00	0·39	0·05	0·52	0·07
CaO	1·37	0·80	0·90	1·00	0·85	2·41	0·32	1·13	0·88	1·61	0·65
Na_2O	5·51	3·74	3·86	3·69	3·09	3·81	3·77	4·84	3·42	4·22	3·14
K_2O	2·57	5·20	5·04	5·58	5·46	4·76	4·97	4·48	5·45	4·22	5·88
P_2O_5	0·07	0·02	0·02	0·03	0·04	0·11	0·01	0·10	0·03	0·13	0·03
LOI	0·13	0·43	0·57	0·43	0·92	0·30	0·13	0·39	0·24	0·40	0·87
Total	99·71	100·29	100·18	100·06	100·64	99·74	100·24	100·42	99·82	100·43	100·99
mg-no.[b]	0·627	0·790	0·180	0·287	0·552	0·519	0·000	0·683	0·177	0·673	0·287
Ba	1770	225	227	119	230	1359	182	441	838	729	366
Rb	40·6	158·6	252·4	277·1	352·5	133·6	204·8	206·6	191·7	221·4	383·7
Sr	135·7	35·3	36	36·5	35·2	163·6	11·2	80·1	53·6	114·8	24·9
Ga	17	27·8	24	20	16	18	17	19	21	21	20
Nb	6·6	6·3	33·8	21·8	15·6	13·9	15·5	29·3	17·9	33·1	21·2
Hf	11·2	8·2	13·3	11	7·4	14	5·4	6·6	13	9·7	13·5
Zr	413·3	62·9	379·7	335·7	201	481·5	131·6	191·7	445·2	317·7	404·2
Y	41·8	84·3	122·2	92·2	74·1	47·8	80·8	126·2	84·7	69·5	127·3
Th	7·2	15	45·5	38	61	29	24·3	26·1	30	38	46
U	1·3	3·2	8·5	6·1	10·2	3·2	5·6	4·4	4·4	5·9	6·5
Ta	1·1	0·8	3·2	2·8	2·5	1·6	2·2	2·1	2·1	3·5	3·5
W	394	23	283	563	508	356	539	288	565	535	1048
Cr	0	2·1	0	0	0	0	0	0·7	0	0	0
Ni	0	1	0	0	0	0	0	0	0	0	0
Co	71	182·8	65	93	93	66	111	65	105	91	181
Sc	11·7	7·3	2·6	3·7	3·6	15·6	1·4	15	7·5	8·5	7·2
V	10·2	1·9	0·1	2·6	5·8	10·5	0·1	10·3	1·1	21	3·3
Cu	0	0	0	0	0	0	0	0	0	0	0
Pb	12·8	25·1	35·6	36	42	24	32·7	38·3	31	30	43
Zn	67·9	75·3	103·7	67	41·6	82·7	36·4	122·3	72·4	86·5	74·4
La	44	46·8	82·92	81	72	118	56·25	51·59	93	87	83
Ce	89	104·94	177·02	167	142	223	120·98	120·73	180	163	177
Pr	11·2	14·05	21·56	20	15·9	25	15·01	15·41	22	18	22
Nd	43	57·05	81·77	72	53	85	55·6	60·49	79	61	84
Sm	8	13·05	17·2	14·3	10·2	12·5	12·8	14·92	14·9	11·2	18·1
Eu	1·97	0·9	1·12	1·3	0·6	2·2	0·88	1·24	1·71	1·49	1·28
Gd	7·8	13·71	17·62	14·2	9·5	10·2	12·26	16·7	14·3	10·4	18·4
Tb											
Dy	7	13·23	19	13·5	10·2	8·1	11·3	18·22	13·2	10·6	19·2
Ho	1·54	2·85	4·31	3	2·3	1·69	2·39	4·12	2·9	2·4	4·3
Er	3·9	6·95	12·11	8·2	6·4	4·3	6·4	11·4	7·6	6·7	11·7
Yb	3·8	5·9	11·92	8·1	6·6	4·3	6·43	10·68	7·3	7	11·5
Lu	0·59	0·9	1·73	1·16	0·97	0·64	0·92	1·56	1·1	1·06	1·67
S	113	115	0	7	3	45	1910	3393	91	140	29
As	1	1·4	11	10	14	6	12	13	8	8	13

Table 1: continued

	Intermediate rocks						
	Mahé						
Sample:	LA99M-3A	LA97M-24B	LA97M-25B	LA97M-26A	LA97M-26B	LA97M-26C	LA97M-26C
Lithology:	Biotite grdiorite	Porph. Hb–Bi grdiorite	Amphibolite	Porph. Hb Qtz diorite	Mafic Hb Qtz diorite	Rexl Mafic Hb Qtz diorite	Replicate
U–Pb age (Ma):[a]				752·4±3·3	753·0±1·4		
SiO_2	73·12	69·35	61·04	58·50	57·40	51·58	51·68
TiO_2	0·26	0·49	0·87	0·79	0·80	1·36	1·35
Al_2O_3	14·07	14·78	17·28	18·46	16·13	17·11	17·18
Fe_2O_3*	2·04	3·78	5·38	6·96	8·85	9·42	9·21
MnO	0·06	0·10	0·30	0·12	0·18	0·15	0·14
MgO	0·43	0·79	1·74	2·00	3·87	6·01	6·04
CaO	1·78	2·46	3·94	6·80	7·17	8·79	8·65
Na_2O	4·11	4·83	7·62	4·94	4·09	3·49	3·29
K_2O	3·41	3·23	1·26	1·11	1·16	1·40	1·58
P_2O_5	0·06	0·15	0·37	0·38	0·28	0·41	0·42
LOI	0·42	0·76	0·06	0·29	0·48	1·71	1·68
Total	99·76	100·72	99·86	100·35	100·41	101·42	101·22
mg-no.[b]	0·736	0·734	0·810	0·791	0·852	0·894	0·896
Ba	886	717	699	585	541	542	
Rb	116·6	136·1	23·1	32·3	34·3	33·9	
Sr	178·8	160·2	190·5	563·8	407·4	1072·2	
Ga	15	17	19	20	19	21	21
Nb	5·2	12·1	16·3	4·7	4·6	2·8	2·9
Hf	4·4	8·3	8·4	10	2·3	2·9	
Zr	122	301·3	311·9	350·8	63	134·9	137·3
Y	27·5	51·4	89·4	35·5	42·5	21·1	23·2
Th	11·7	15·8	4·1	3·9	2	4·3	
U	2·7	2·9	1·2	0·9	0·4	0·8	
Ta	0·5	0·7	0·5	0·4	0·7	0·2	
W	0·9	1·5	1·25	168	307	73	
Cr	0·2	0	0	0	0	86·7	83·7
Ni	0·8	0·6	0	0	0	34·9	39·2
Co	4	3	6	49	75	52	27
Sc	5·2	8·6	23·5	20·7	33·2	28·6	29·9
V	8·41	30·7	12·2	66·3	171	147·9	
Cu	0	0	0	0	0	21·4	27·1
Pb	16·6	19	13·1	8·3	7·1	5·5	
Zn	29·6	75	178·7	81·1	101·2	89·2	88·8
La	34·69	35·03	25·67	22·8	21	30·51	
Ce	80·07	79·72	70·69	51·53	51	66·24	
Pr	7·96	10·07	11·63	6·79	7·5	9	
Nd	27·33	39·97	58·88	29·48	33	38·12	
Sm	4·49	7·91	15·82	6·23	7	7·02	
Eu	0·92	1·62	3·57	1·97	1·77	2·39	
Gd	4·44	7·56	17·65	6·68	7·1	5·73	
Tb							
Dy	4·13	7·38	15·59	5·56	6·5	3·9	
Ho	0·97	1·66	3·33	1·23	1·46	0·78	
Er	2·8	4·62	8·2	3·3	3·9	1·89	
Yb	3·31	4·91	7·02	3·11	3·7	1·65	
Lu	0·52	0·74	1·07	0·46	0·56	0·26	
S	365	159	722	280	612	894	878
As	0	4	2	0	0	0	0

[a]U–Pb ages by TIMS (Tucker *et al.*, 2001).
[b]Calculated with FeO as 0·85 of total Fe.
*Total Fe as Fe_2O_3.
grdiorite, granodiorite. Rexl, recrystallized.

Table 2: Major and trace elements for dolerite dykes from the Seychelles

	Mahé							Marianne	Fregate
Sample:	LA97M-11A	LA97M-12	LA97M-21	LA97M-24C	LA97M-27	LA97M-28B	LA97M-28C	LA97M-8	LA97F-13D
Lithology:	Partly altered dolerite/gabbro	Partly altered dolerite	Partly altered dolerite	Extensively altered dolerite	Partly altered dolerite	Partly altered dolerite	Partly altered gabbro/dolerite	Altered dolerite	Partly altered basalt/dolerite
U–Pb age (Ma):[a]							$750 \cdot 2 \pm 2 \cdot 5$		
SiO_2	45·94	45·87	47·90	46·92	48·18	45·77	45·89	52·30	49·35
TiO_2	2·81	2·86	1·82	2·27	1·90	2·83	2·84	1·29	2·33
Al_2O_3	14·27	14·13	15·27	15·32	15·35	14·12	14·32	17·26	14·93
Fe_2O_3*	16·78	16·81	12·43	13·20	12·68	16·70	16·86	9·84	12·13
MnO	0·25	0·25	0·19	0·19	0·20	0·25	0·25	0·17	0·18
MgO	6·14	6·16	8·84	8·41	8·64	5·90	5·89	5·44	6·53
CaO	9·03	9·21	8·98	9·42	8·85	9·13	9·18	7·25	9·20
Na_2O	2·85	2·73	2·38	2·80	2·24	2·75	2·80	3·55	2·90
K_2O	1·02	0·98	1·53	0·78	1·37	1·82	1·06	2·39	1·44
P_2O_5	0·57	0·56	0·41	0·58	0·43	0·60	0·54	0·26	0·67
LOI	0·93	1·79	2·69	2·29	3·02	1·35	1·57	2·12	1·10
Total	100·59	101·35	102·44	102·18	102·86	101·22	101·20	101·87	100·76
mg-no.[b]	0·784	0·784	0·876	0·863	0·871	0·778	0·776	0·846	0·842
Ba	400·7	439	328·1	493·9	316·1	549·4	460.	858.	518.
Rb	25	39·4	99·6	16·2	77·8	70·9	30	90·8	57·2
Sr	325·2	331·9	250·4	554·4	273·5	279·8	308·1	597·8	355·3
Ga	24	25	17	21	18	25	24	19	21
Nb	7·9	6·9	5·1	7·1	6·4	7·6	6·9	2·9	14·5
Hf	5·5	5·4	4	4·3		5·8	5·3	3	8·7
Zr	212·8	207·9	167·9	178·3	177·1	214·6	209·1	110·2	357·4
Y	49	47·9	32	33·1	52·2	48·7	47	26·6	48·5
Th	1·4	1·4	1·7	2·7	6·4	1·6	1·2	3·2	5·1
U	0·3	0·3	0·4	0·5	3·5	0·3	0·3	0·6	1
Ta	0·4	0·6	0·2	0·3		0·4	0·6	0·2	1·1
W	2	4·6	1·8	2·2		2·3	4·5	5·2	3·9
Cr	16·7	23·6	372·8	341·6	362·7	35·4	24·9	47·3	240·4
Ni	52·9	48·8	138·6	145·6	143·4	47·9	48·7	34·6	90·9
Co	52	48	50	46	52	43	46	30	39
Sc	38	36·5	27·5	34·4	30·9	37	35·5	39·1	33·9
V	284·1	329	159·2	200·8	219·3	194·9	338	255	232
Cu	31·5	25	21·7	15·9	20·8	34·4	28·1	43·4	21
Pb	4·5	60	3·7	3·8	8	3·5	3·7	8·4	11·7
Zn	149·1	123·7	81	109·5	106·3	138·8	134·5	83·7	100·6
La	17·87	17	17·15	26·73	6·1	19·14	17	15	38
Ce	44·38	42	40	60·29	29	47·8	41	32	85
Pr	6·32	6·3	5·43	8·27		6·84	6·3	4·4	11·4
Nd	30·17	29	23·98	35·69	20	32·75	29	20	48
Sm	7·58	7·1	5·5	7·33		7·93	7	4·3	9·6
Eu	2·93	2·6	1·95	2·73		2·89	2·5	1·45	2·8
Gd	8·59	8·1	5·98	7·35		9·27	8·1	4·7	9·4
Dy	7·83	7·6	5·33	5·54		8·44	7·5	4·2	7·8
Ho	1·75	1·67	1·15	1·14		1·84	1·67	0·94	1·68
Er	4·59	4·3	3·04	2·85		4·89	4·3	2·4	4·1
Yb	4·1	4·1	2·66	2·47		4·27	4	2·3	3·7
Lu	0·61	0·61	0·41	0·34		0·66	0·6	0·36	0·58
S	2323	1665	1656	203	885	1674	982	2636	1540
As	0	0	0	0	0	0	0	2	1

[a]U–Pb age by TIMS (Torsvik *et al.*, 2001*a*).
[b]Calculated with FeO as 0·85 of total Fe.
*Total Fe as Fe_2O_3.

methods. However, we consider as superior the XRF analyses of those trace elements (Ga, Nb, Zr, Y, Cr, Ni, Co, Sc, Cu, Zn, S) potentially less soluble because of refractory trace minerals such as zircon. All other trace element concentrations reported in Tables 1 and 2 (Ba, Th, U, V, Pb, Hf, Ta, W, REE) represent analyses by ICP-MS.

Samples for Rb–Sr and Sm–Nd isotopic analysis were dissolved in mixed HF–HNO_3 (10:1), and chemical separation of Rb, Sr, Sm and Nd was carried out by cation-exchange chromatography; procedural blanks were <1 ng. Sr and Nd isotopic ratios were measured on a VG Sector 54 multicollector thermal ionization mass spectrometer housed at the Université Libre de Bruxelles, Belgium. Replicate analyses of the MERCK Nd standard gave an average $^{143}Nd/^{144}Nd$ value of $0{\cdot}512742 \pm 8$ (normalized to $^{146}Nd/^{144}Nd = 0{\cdot}7219$), and measurements of NBS 987 yielded an average $^{87}Sr/^{86}Sr$ value of $0{\cdot}710247 \pm 7$ (normalized to $^{86}Sr/^{88}Sr = 0{\cdot}1194$). On the basis of routine laboratory replicate analyses, $^{147}Sm/^{144}Nd$ and $^{87}Rb/^{86}Sr$ ratios are reproducible to better than $0{\cdot}2\%$ and $0{\cdot}5\%$, respectively. Rb–Sr and Sm–Nd concentrations, isotopic data and parameters derived therefrom are given in Table 3. Isochron regressions were carried out using Isoplot/Ex (Ludwig, 1999), assuming blanket uncertainties of $0{\cdot}6\%$ for $^{87}Rb/^{86}Sr$ and $0{\cdot}01\%$ for $^{87}Sr/^{86}Sr$. For older isotopic data (Michot & Deutsch, 1977; Yanagi et al., 1983), blanket uncertainties of $1{\cdot}0\%$ for $^{87}Rb/^{86}Sr$, and the reported within-run precisions (expressed as percent) for $^{87}Sr/^{86}Sr$ were used. Epsilon Nd values were calculated assuming $^{147}Sm/^{144}Nd = 0{\cdot}1967$ and $^{143}Nd/^{144}Nd = 0{\cdot}512638$ for CHUR.

RESULTS

Our sample suite consists of 26 granitoids and related rocks from Mahé, Praslin, La Digue, Marianne, Fregate, Recifs and Ste. Anne, and nine dolerite dykes from Mahé, Marianne and Fregate. Locations are shown in Fig. 2; brief field and petrographic descriptions of individual samples, with GPS coordinates, are given in an electronic Appendix, which may be downloaded from the *Journal of Petrology* Web site at http://www.petrology. oupjournals.org. Estimated modes and CIPW norms are given in Tables 4 and 5.

Field relations and lithologies

The subdivision of Seychelles granitoids on the basis of colour, with Mahé specimens being dominantly grey, and those from Praslin, La Digue and other islands being dominantly pink or reddish, is corroborated by our observations (Fig. 2). Our specimens from Fregate and

Recifs are also dominantly pink to reddish in colour. Minor pink granite of Mahé includes subsolvus (specimen LA97M-20) and hypersolvus (LA99M-2, LA97M-11B, LA97A-29) varieties. In part, the colour distinction is related to the modal abundance of alkali- or K-feldspar, which is commonly, but not invariably pinkish as a result of iron staining along grain boundaries and cleavage planes, and/or the presence of finely disseminated Fe-oxide (probably haematite) as sub-micron sized, dust-like inclusions. Weis & Deutsch (1984) suggested that the pink to reddish granitoids of Praslin and La Digue, which are chemically and isotopically distinct from those typical of Mahé, acquired their coloration as a result of hydrothermal alteration. The grey granitoid of Praslin (LA97P-15) has a chemical and isotopic signature resembling material from Mahé.

On the northern end of Mahé, the granitoids display a variety of complex relations, including the presence of abundant xenoliths and enclaves, in some cases exhibiting flow alignment, and there is evidence for multi-phase magmas of granitic, mafic and intermediate composition (Fig. 3b–d). This northern region of Mahé has been considered sufficiently distinctive to warrant a separate map unit, designated either as the 'gneissose' (e.g. Suwa et al., 1983, 1994) or 'northern' (P. Plummer, personal communication, 1997) granite. Xenoliths within granitoid host rocks are either angular or rounded (Fig. 3c and d), commonly in the size range 5–10 cm across [although Baker (1963) reported 'rafts' up to 15 m across], and range in composition from amphibolite (sample LA97M-25B) to quartz diorite (LA97M-3B) to porphyritic grano-diorite (LA97M-24B). At the Bel Ombre locality of northwestern Mahé (LA97M-26), complex intermingling features are present between quartz dioritic rocks of variable colour index. Here, finer-grained mafic inter-mediate rocks (LA97M-26B, 26C) occur as irregular masses and patches, commonly showing lobate contacts (Fig. 3b) with host porphyritic quartz diorite (LA97M-26A). That these intermediate rocks might represent the results of hybridization between granitoid and mafic magmas was initially suggested by Baker (1963); we support this interpretation, and provide geochemical evidence below.

Nearly all dolerite dykes display sharp contacts with host granitoids. Complex bifurcations commonly occur near dyke terminations (Fig. 3a). Well-developed chilled margins have been observed in dykes up to 10 m thick (e.g. LA97M-28); at this locality coarse (plagioclase laths up to 3 mm across, with sub-ophitic pyroxene oikocrysts up to 6 mm) granophyric patches occur near the dyke centre (sample LA97M-28C). In some cases contacts with surrounding granitoids are sheared and hydrothermally altered to epidote- and/or amphibole-rich assemblages. Most Seychelles dolerites are aphyric, with typical grain size of 0·1–0·2 mm, although Frankel (1969) described

Table 3: Rb–Sr and Sm–Nd isotopic data

Sample	Lithology	U–Pb age (Ma)	Rb (ppm)	Sr (ppm)	$^{87}Rb/^{86}Sr$	$^{87}Sr/^{86}Sr$	$I_{Sr\,750}$	Sm (ppm)	Nd (ppm)	$^{147}Sm/^{144}Nd$	$^{143}Nd/^{144}Nd$	$\varepsilon_{Nd\,750}$*	T_{DM} (Ma)*†
Mahé Group granitoids													
LA99M-2	Hypersolvus amph. granite		92.75	22.2	12.2302	0.828110 ± 10	0.697163	12.3	63	0.1180	0.512337 ± 11	1.68 ± 0.42	1195
LA99M-3A	Biotite granodiorite		116.6	178.75	1.8901	0.723055 ± 7	0.702818	4.5	27	0.1008	0.512301 ± 8	2.64 ± 0.16	1057
LA97M-11B	Hypersolvus amph. granite	750.9 ± 2.0	119.5	22.1	15.8899	0.868072 ± 6	0.697940	12.1	62	0.1180	0.512396 ± 6	2.84 ± 0.12	1099
LA99M-20	Bi–Hb granite		94.9	157.9	1.7411	0.720759 ± 13	0.702117	12.6	79	0.0964	0.512288 ± 14	2.80 ± 0.27	1035
LA99M-22	Porphyritic Hb–Bi granite	748.4 ± 1.2	151.7	56.4	7.8325	0.773969 ± 6	0.690108	8.7	45	0.1169	0.512384 ± 10	2.71 ± 0.20	1106
LA97M-23	Porphyritic Hb–Bi granodiorite	751.1 ± 1.7	119.5	132	2.625	0.730260 ± 10	0.702154	6.5	32	0.1228	0.512434 ± 12	3.12 ± 0.23	1094
LA97M-24A	Porphyritic Hb–Bi granite	750.8 ± 1.2	127.5	91	4.0681	0.743958 ± 8	0.700401	8	41	0.1180	0.512401 ± 8	2.94 ± 0.16	1091
LA97M-25A	Hb–Bi granodiorite		46.8	140.9	0.9615	0.713135 ± 13	0.702840	7.5	44	0.1030	0.512332 ± 9	3.02 ± 0.17	1037
LA97M-26D	Aplitic granite		127.4	39.4	9.4322	0.791692 ± 9	0.690702	2.1	11.6	0.1094	0.512247 ± 9	0.74 ± 0.18	1228
LA97P-15	Amphibole granodiorite	752.5 ± 3.2	40.6	136	0.8641	0.712197 ± 8	0.702945	8	43	0.1125	0.512362 ± 12	2.70 ± 0.23	1090
LA97A-29	Hypersolvus amph. granite	764.2 ± 1.4	158.6	35.3	13.1832	0.852435 ± 10	0.711284	13.1	57	0.1389	0.512517 ± 6	3.19 ± 0.12	1166
Praslin Group granitoids													
LA97P-4	Porphyritic granite		252.35	35.95	20.7627	0.936012 ± 13	0.713708	17.2	82	0.1268	0.512238 ± 6	−1.10 ± 0.12	1496
RT97P-5	Hb–Bi granite	752.9 ± 4.0	277	36.5	22.4727	0.947814 ± 11	0.707201	14.3	72	0.1201	0.512201 ± 12	−1.18 ± 0.23	1447
LA97L-10	Hb–Bi granite	750.5 ± 1.8	352.5	35.2	29.9055	1.036489 ± 6	0.716294	10.2	53	0.1163	0.512072 ± 12	−3.34 ± 0.23	1595
LA97M-9	Amphibole granite	758.8 ± 2.0	133.6	163.6	2.3384	0.732296 ± 13	0.706938	12.5	85	0.0889	0.511912 ± 15	−3.83 ± 0.29	1434
LA97F-13A	Aplitic Bi granite		204.8	11.2	56.0048	1.306598 ± 13	0.706961	12.8	57	0.1357	0.512384 ± 9	−1.86 ± 0.17	1663
LA97F-13B	Biotite granite		206.6	80.05	7.5241	0.785600 ± 9	0.705041	14.9	60	0.1501	0.512282 ± 8	−2.48 ± 0.16	1958
LA97F-13C	Porphyritic aplitic granite	754.7 ± 1.9	191.7	53.6	10.4469	0.805684 ± 11	0.693830	14.9	79	0.1140	0.512080 ± 8	−2.96 ± 0.16	1544
LA97F-14	Biotite granite	752.0 ± 1.7	221.4	114.8	5.6103	0.763438 ± 12	0.703369	11.2	61	0.1110	0.512069 ± 12	−2.88 ± 0.23	1514
LA97R-16	Biotite granophyre	808.8 ± 1.9	383.7	24.9	47.0345	1.269553 ± 12	0.765960	18.1	84	0.1303	0.512327 ± 10	0.31 ± 0.20	1394
Intermediate rocks													
LA99M-3B	Hb–Bi Qtz diorite		43.05	458.15	0.2718	0.706749 ± 10	0.703838	7.2	34	0.1280	0.512406 ± 9	2.07 ± 0.17	1214
LA97M-24B	Porphyritic Hb–Bi granodiorite		136.1	160.2	2.4631	0.729111 ± 8	0.702738	7.9	40	0.1194	0.512373 ± 13	2.25 ± 0.25	1154
LA97M-25B	Amphibolite		23.05	190.5	0.3501	0.707213 ± 10	0.703465	15.8	59	0.1619	0.512549 ± 10	1.61 ± 0.19	1609
LA97M-26A	Porphyritic Hb–Bi Qtz diorite	752.4 ± 3.3	32.5	563.8	0.1667	0.705831 ± 10	0.704046	6.2	29	0.1292	0.512327 ± 9	0.40 ± 0.17	1377
LA97M-26B	Mafic Hb Qtz diorite	753.0 ± 1.4	34.3	407	0.2438	0.706712 ± 8	0.704102	7	33	0.1282	0.512350 ± 15	0.95 ± 0.29	1318
LA97M-26C	Rexl Hb–Bi Qtz diorite		33.9	1072	0.0915	0.704570 ± 18	0.703591	7	38	0.1114	0.512440 ± 9	4.33 ± 0.17	960
Dolerites													
LA97M-11A	Partly altered dolerite or gabbro		25	325.2	0.2224	0.706183 ± 8	0.703802	7.6	30	0.1532	0.512634 ± 10	4.11 ± 0.20	1147
LA97M-12	Partly altered dolerite		39.4	331.9	0.3434	0.707401 ± 7	0.703724	7.1	29	0.1480	0.512677 ± 6	5.44 ± 0.12	952
LA97M-21	Partly altered dolerite		99.55	250.35	1.1517	0.718438 ± 19	0.706107	5.5	24	0.1385	0.512418 ± 7	1.29 ± 0.14	1364
LA97M-24C	Extensively altered dolerite		16.2	554.35	0.0845	0.705335 ± 15	0.704430	7.3	36	0.1226	0.512339 ± 11	1.28 ± 0.21	1253
LA97M-28B	Partly altered dolerite		71	280	0.7338	0.709984 ± 10	0.702127	7.9	33	0.1447	0.512662 ± 8	5.46 ± 0.15	939
LA97M-28C	Partly altered gabbro or dolerite	750.2 ± 2.5	30	308	0.2818	0.706762 ± 9	0.703745	7	29	0.1459	0.512664 ± 9	5.39 ± 0.18	952
LA97F-13D	Partly altered basalt/dolerite		57.2	355.3	0.4659	0.710419 ± 9	0.705431	9.6	48	0.1209	0.512221 ± 11	−0.87 ± 0.21	1427
LA97M-8	Altered dolerite		90.8	598	0.4394	0.710193 ± 7	0.705488	4.3	20	0.1300	0.512423 ± 10	2.21 ± 0.20	1211

*Using CHUR parameters $^{147}Sm/^{144}Nd = 0.1967$, $^{143}Nd/^{144}Nd = 0.512638$.
†Using depleting mantle model of DePaolo *et al.* (1991).

Table 4: Estimated modes and CIPW norms of Seychelles granitoids and intermediate rocks

Mahé Group granitoids

	Mahé									Praslin	Ste. Anne
Sample:	LA99M-2	LA99M-3A	LA97M-11B	LA97M-20	LA97M-22	LA97M-23	LA97M-24A	LA97M-25A	LA97M-26D	LA97P-15	LA97A-29
Lithology:	Hypersolvus amph granite	Biotite granodiorite	Hypersolvus amph granite	Bi–Hb granite	Porphyritic Hb–Bi granite	Porphyritic Hb–Bi granodiorite	Porphyritic Hb–Bi granite	Hb–Bi granodiorite	Aplitic granite	Amph granodiorite	Hypersolvus amph granite
Quartz	25	25	25	20	30	22	30	32	30	25	20
K-feldspar	64	29	70	37	35	35	40	35	35	26	75
(type*)	(MM)	(Mm)	(MM)	(Mp)	(Mm)	(Mm)	(Mm)	(Mm)	(Mm)	(Mp)	(M/O M)
(% alteration)	(5%)	(5%)	(5%)	(15%)	(20%)	(5%)	(tr)	(tr)	(tr)	(tr)	(tr)
Plagioclase	5	40		35	27	35	30	27	35	45	
(% sericitization)	(tr)	(10%)		(5%)	(20%)	(10%)	(5%)	(tr)	(5%)	(tr)	
Biotite		4		3	2	3	3	1		tr	tr
Hornblende	5		5	2	3	4	4	3		2	3
(colour)	(dk green)		(dk blue–green)	(green/brown)	(dk green)	(green)	(dk green/brown)	(green)		(green/brown)	(green)
Actinolite							1				
Chlorite									tr		
Sphene	tr	tr		2	2	1	tr	1	tr	2	tr
Epidote	tr	tr									
Apatite	tr	tr	tr	tr	tr	tr	tr	tr		tr	tr
Zircon	tr	tr	tr	tr	tr	tr	tr	tr		tr	tr
Allanite	tr						tr				
Opaques	1	2	tr	1	1	tr	2	1	tr	tr	tr
CIPW norms, 100% anhydrous†											
Q	31·69	31·08	32·25	22·62	31·50	27·74	29·77	26·92	35·94	27·46	31·83
Or	27·43	20·34	27·24	27·45	27·32	21·42	25·55	16·91	29·57	15·31	30·84
Ab	35·54	35·03	35·53	38·37	34·55	36·21	34·73	44·74	30·43	46·89	31·69
An	1·05	8·56		3·12	1·71	7·84	4·34	4·95	3·32	3·53	2·01
Cor		0·50							0·05		
Di	0·57		2·17	2·55	2·05	1·43	1·51	1·35		2·50	1·57
Hy	2·88	3·45	1·95	3·92	1·95	3·86	2·86	3·77	0·46	3·01	1·64
Ol											
Mt	0·47	0·40	0·49	0·67	0·43	0·55	0·49	0·56	0·07	0·55	0·23
Ilm	0·36	0·50	0·46	0·94	0·46	0·74	0·61	0·63	0·13	0·59	0·15
Ap	0·02	0·13	0·04	0·37	0·04	0·20	0·13	0·18	0·02	0·15	0·04
	100·01	99·99	100·13	100·01	100·01	99·99	99·99	100·01	99·99	99·99	100·00
Normative An	2·87	19·64	0·00	7·52	4·72	17·80	11·11	9·96	9·84	7·00	5·96

	Praslin Group granitoids									Intermediate rocks					
	Praslin		Fregate				Recifs	La Digue	Marianne	Mahé					
Sample:	LA97P-4	RT97P-5	LA97F-13A	LA97F-13B	LA97F-13C	LA97F-14	LA97R-16	LA97L-10	LA97M-9	LA99M-3B	LA97M-24B	LA97M-25B	LA97M-26A	LA97M-26B	LA97M-26C
Lithology:	Porph. granite	Bi granite	Aplitic Bi granite	Bi granite	Porph. aplitic amph granite	Bi granite	Biotite granophyre	Hb–Bi granite	Amph. granite	Hb–Bi Qtz diorite	Porph. Hb–Bi granodiorite	Amphibolite	Porph. Hb Qtz diorite	Mafic Hb Qtz diorite	RexI Hb Qtz diorite
Quartz	30	25	35	25	30	26	35	30	20	15	25		8	10	10
K-feldspar	30	35	30	27	35	27	35	35	30	5	22				
(type*)	(Mm)	(Mp)	(Mp)	(Mm)	(Mp)	(Mp)	(Mm)	(Mm)	(Mm)	(Mm)	(Mm)				
(% alteration)	(20%)	(30%)	(40%)	(15%)	(25%)	(40%)	(70%)	(75%)	(50%)	(5%)	(tr)				
Plagioclase	36	27	35	45	30	40	25	30	38	62	40	65	70	60	59
(% sericitization)	(30%)	(40%)	(20%)	(10%)	(5%)	(40%)	(30%)	(50%)	(50%)	(5%)	(5%)	(tr)	(tr)	(5%)	(60%)
Biotite	3	7	tr	3		7	3	2	2	8	4		10	3	6
Hornblende	1	6			5			3	10	8	6	30	9	20	5
(colour)	(green)	(dark green)			(green/brown)			(green)	(bluish green)			(green)	(green)	(green)	(green)
Actinolite															15
Chlorite															
Sphene										tr	2	tr		3	
Epidote	tr							tr	tr		tr				
Apatite		tr	tr	tr	tr		tr		tr	tr			tr	tr	
Zircon	tr	tr	tr	tr	tr		tr	tr	tr	tr				tr	
Allanite														tr	
Opaques	tr	tr	tr	tr		tr	2	tr		2	1	3	3	4	5
CIPW norms, 100% anhydrous†															
Q	30.56	28.49	36.07	22.52	29.05	24.95	32.12	33.95	20.43	5.88	21.46	0.82	6.78	6.52	8.37
Or	29.99	33.20	29.39	26.55	32.46	25.03	34.81	32.45	28.44	8.93	19.18	7.50	6.60	6.92	
Ab	32.82	31.37	31.85	40.98	29.11	35.76	26.56	26.24	32.53	39.03	40.98	64.84	41.98	34.86	29.83
An	1.48	1.88	1.53	4.58	4.22	7.25	2.38	3.29	8.66	22.19	9.11	9.27	25.02	22.38	27.15
Cor			0.02	0.39	0.14	0.13									
Di	2.57	2.60			3.78		0.59	0.62	2.42	6.68	1.93	6.90	5.61	9.83	11.88
Hy	1.70	1.56	0.71	3.60		4.98	2.49	2.49	5.41	13.25	5.35	7.13	10.28	15.58	10.64
Ol															6.75
Mt	0.47	0.45	0.13	0.46	0.60	0.65	0.45	0.40	0.94	1.60	0.74	1.06	1.38	1.76	1.88
Ilm	0.36	0.40	0.28	0.70	0.57	0.97	0.53	0.48	0.94	1.80	0.93	1.66	1.51	1.53	2.61
Ap	0.04	0.07	0.02	0.22	0.07	0.28	0.07	0.09	0.24	0.66	0.33	0.81	0.83	0.62	0.91
	99.99	100.02	100.00	100.00	100.00	100.00	100.00	100.01	100.01	100.02	100.01	99.99	99.99	100.00	100.02
Normative An	4.31	5.65	4.58	10.05	12.66	16.86	8.22	11.14	21.02	36.25	18.19	12.51	37.34	39.10	47.65

*MM, microcline mesoperthite; Mm, microcline microperthite; Mp, microcline perthite; M/O M, microcline or orthoclase perthite.
†Calculated with FeO as 0.85 of total Fe.

Table 5: Estimated modes and CIPW norms of Seychelles dolerite dykes

	Mahé							Marianne	Fregate
Sample:	LA97M-11A	LA97M-12	LA97M-21	LA97M-24C	LA97M-27	LA97M-28B	LA97M-28C	LA97M-8	LA97F-13D
Lithology:	Partly altered dolerite or gabbro	Partly altered dolerite	Partly altered dolerite	Extensively altered dolerite	Partly altered dolerite	Partly altered dolerite	Partly altered gabbro or dolerite	Altered dolerite	Partly altered dolerite
Plagioclase	35	48	40	50	43	40	65	45	40
(% sericitization)	(20–30%)	(50–60%)	(100%)	(60%)	(100%)	(50–60%)	(60–70%)	(~40%)	(~50%)
Clinopyroxene	25	30	30		10	7	15		tr
Fe–Ti oxides	10	5	10	5	7	10	5	3	10
Actinolite	30	15	20	19	40	43	13		15
Chlorite				5				5	10
Epidote				2			tr	10	
Brown amphibole				19				37	15
Brown biotite		2					2		10
*CIPW norms, 100% anhydrous**									
Qz									
Or	6·14	5·90	9·16	4·67	8·20	10·93	6·38	14·29	8·63
Ab	24·50	23·49	20·37	23·94	19·16	21·83	24·08	30·32	24·84
An	23·49	23·80	26·75	27·21	28·07	21·08	23·75	24·31	23·74
Ne						0·95			
Di (wo)	7·80	8·10	6·65	6·95	5·77	8·91	8·09	4·39	7·74
Di (en)	3·84	4·00	4·09	4·20	3·51	4·33	3·91	2·47	4·49
Di (fs)	3·81	3·94	2·17	2·37	1·93	4·42	4·05	1·73	2·88
Hy (en)	2·91	3·77	5·85	4·10	10·35		2·74	5·57	8·35
Hy (fs)	2·88	3·71	3·10	2·31	5·69		2·84	3·91	5·36
Ol (fo)	6·20	5·53	8·71	9·08	5·60	7·45	5·83	3·99	2·59
Ol (fa)	6·78	6·01	5·09	5·65	3·40	8·41	6·67	3·09	1·84
Mt	4·96	4·96	3·66	3·87	3·73	4·92	4·97	2·89	3·57
Ilm	5·43	5·53	3·50	4·36	3·65	5·46	5·49	2·48	4·49
Ap	1·27	1·24	0·91	1·28	0·95	1·33	1·20	0·57	1·48
	100·01	99·98	100·01	99·99	100·01	100·02	100·00	100·01	100·00
Normative An	48·95	50·33	56·77	53·20	59·43	49·13	49·66	44·50	48·87

*Calculated with FeO as 0·8 of total Fe.

mega-porphyritic dolerites from L'Île Longue (a small ~1 km island between Ste. Anne and Cerf, Fig. 2) that contain labradorite megacrysts up to 7 cm across; we encountered a similar occurrence on eastern Mahé (LA97M-19, Fig. 2).

Petrography

Most Seychelles granitoids are uniform, with massive texture, medium grain size (0·5–2 cm), randomly oriented feldspar crystals, and up to 10% brown biotite and/or brown to green hornblende (electronic Appendix; Baker, 1963, 1967; Frankel & Kent, 1964; Suwa *et al.*, 1983). Subsolvus granodiorites and monzogranites predominate, but a significant and unknown volume of hypersolvus monzogranite occurs on Mahé and Ste. Anne. Textural variations include porphyritic types from Mahé (samples LA97M-22, 23, 24A, 24B, 26A), Praslin (LA97P-4) and Marianne (Baker, 1963). On Mahé, two sizeable regions of granitic porphyry (Fig. 2) were distinguished by Baker

(1963); these evidently 'grade imperceptibly' into typical massive Mahé granitoids. In the porphyritic rocks, K-feldspar phenocrysts (1–2 cm across) are either pink (LA97M-22, 24A; LA97P-4) or white (LA97M-23), and the groundmass is usually grey, but is chocolate brown in Praslin sample LA97P-4. Partial development of rapakivi texture has been observed in a few specimens (LA97M-22, 24A; LA97F-13B). Pegmatitic rocks are notably absent in the Seychelles (Baker, 1963, 1967; Frankel & Kent, 1964). Fine-grained (0·5–2 mm) aplitic granitoids are abundant on Fregate (LA97F-13A); these rocks are crosscut by dykes of medium-grained, subsolvus granite up to 50 cm thick (LA97F-13B). Thin aplitic dykes (LA97M-26D) crosscut intermediate rocks (described below) at Bel Ombre on Mahé.

Typical subsolvus granodiorites and monzogranites contain subequal proportions of quartz, K-feldspar (microcline and/or orthoclase microperthite) and plagioclase (some with minor compositional zoning). Magmatic texture is well preserved in most specimens, and consists of subhedral, tabular K-feldspar and plagioclase, with interstitial quartz. In some cases original grain boundaries have been modified to give a recrystallized appearance, perhaps by subsolidus cooling or emplacement of coeval magmas. Mafic minerals include biotite and/or hornblende, which occur as irregular to acicular grains; compositional data have been given by Hoshino (1986). Common accessory minerals include zircon, apatite, sphene, epidote, allanite and/or Fe–Ti oxides (intergrown magnetite and ilmenite, some with up to 32 wt % MnO, Agata & Suwa, 1983). Hypersolvus granites (LA99M-2, 11B; LA99A-29) are dominated by large, irregular grains of mesoperthitic orthoclase and/or microcline; plagioclase is absent or very minor. Mafic silicates in these rocks include hornblende and alkalic amphiboles such as ferrorichterite, commonly with rims of riebeckite (Hoshino & Suwa, 1983; Hoshino, 1986). Other phases said to be present in these and other Seychelles granitoids include Fe-rich clinopyroxenes and fluorite (Hoshino, 1986); we have not found either of these in our specimens.

Phenocrysts in porphyritic granitoids are typically subhedral to irregular, perthitic K-feldspar, both with (LA97M-22, 24A) or without (LA97F-13C) thin, irregular plagioclase rims as partially developed rapakivi texture. Some specimens also contain smaller plagioclase phenocrysts (LA97M-24A, 24B); the reddish porphyry of Praslin (LA97P-4) contains K-feldspar, plagioclase and embayed quartz phenocrysts. Some of the intermediate rocks at Bel Ombre (LA97M-26A) contain only plagioclase phenocrysts with irregular quartz inclusions. Aplitic rocks (LA97M-26D; LA97F-13A, 13C) are fine grained and equigranular, generally with very low colour index. The biotite granophyre of Recifs (LA97R-16) is distinct, consisting of radiating intergrowths of K-feldspar and quartz, surrounding subhedral plagioclase.

Excluding the well-preserved, olivine-bearing dolerite dykes of Praslin, which are probably of Late Cretaceous age, the remainder of Seychelles dolerites, which are presumed or demonstrated to be of Precambrian age, have been variably altered to assemblages of secondary minerals. These include the seven dolerite dykes in our sample suite from Mahé, and individual specimens from Marianne and Fregate, as well as those described by Baker (1967, $n = 3$) and Devey & Stephens (1992, $n = 2$) from Mahé and other islands. Magmatic texture and mineralogy is best preserved in Mahé sample LA97M-11A, in which randomly oriented laths and elongate, skeletal crystals of plagioclase are partly surrounded by pinkish Ti-rich augites, and lesser Fe–Ti oxides. Pyroxenes in this specimen have been partly replaced by fine-grained, pale green actinolite, and the original groundmass has been completely converted to an extremely fine-grained assemblage of actinolite, Fe–Ti oxides and brown biotite. Most other dolerite samples show variable, but higher degrees of sericite development (after plagioclase) and amphibole replacement of pyroxene. In some specimens (e.g. LA97M-24C, LA97M-28B), primary feldspars and pyroxenes have been almost completely replaced by secondary minerals, including sericite, amphiboles (both brown hornblende and pale green actinolite), chlorite, epidote and Fe–Ti oxides (Table 5).

Major, minor and trace element chemistry

Major, minor and trace element compositions of Seychelles granitoids and intermediate rocks are given in Table 1; data for dolerites appear in Table 2. For the compositional diagrams based on major elements (Figs 4–6), data obtained in this study were combined with previously published chemical analyses of Seychelles granitoids (Baker, 1963, 1967; Suwa *et al.*, 1983, 1984) and dolerite dykes (Baker, 1963, 1967; Devey & Stephens, 1992). We include here the first published set of trace element data for Seychelles granitoids and intermediate rocks (Table 1, Figs 7–10).

Granitoids

Excluding the intermediate rocks, which are discussed below, Seychelles granitoids show a limited, but significant variation of major element chemical compositions, with SiO_2 ranging from 68 to 78 wt % (average $73·86 \pm 2·25$ wt %, $n = 30$). In terms of normative or modal mineralogy, the compositions straddle the boundary between monzogranite and granodiorite (Fig. 4); most samples have higher normative or modal plagioclase than K-feldspar. The most 'granitic' samples [i.e. highest normative or/(or + pl) or K/(K + Na)] include the Recifs pink biotite granophyre (LA97R-16), the pink to reddish granites of La Digue and Praslin (LA97L-10,
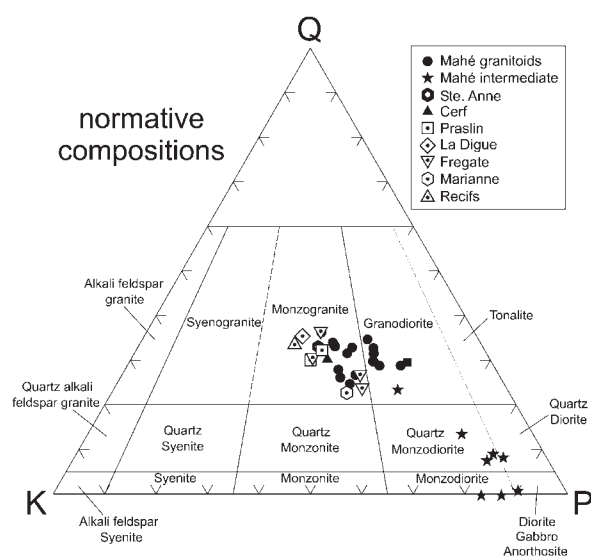
Fig. 4. Normative compositions of Seychelles granitoid and intermediate rocks, plotted on the granitoid classification diagram of Streckeisen (1976). Q, normative quartz; P, normative albite + anorthite; K, normative orthoclase. The lower left apex is plotted as K-feldspar rather than alkali feldspar to allow direct comparison of the normative compositions of subsolvus and hypersolvus granitoids. Mahé Group granites are plotted with filled symbols, those of the Praslin Group with open symbols. Data from this study, Baker (1963) and Suwa et al. (1983, 1984). All norms calculated with FeO = 85% of Fe total.
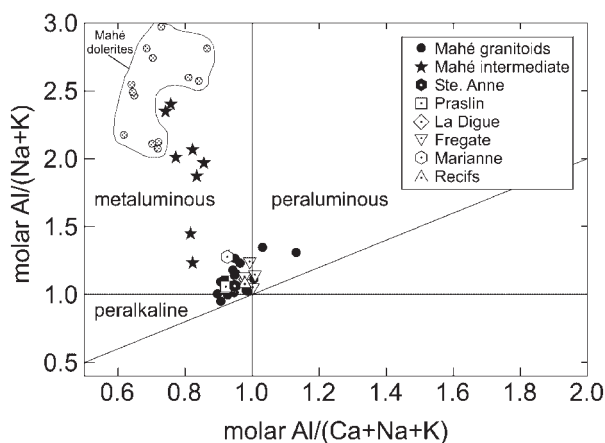
Fig. 5. Diagram of molar $Al/(Na + K)$ vs $Al/(Ca + Na + K)$ (from Maniar & Piccoli, 1989) showing metaluminous character of Seychelles granitoids. Data for Mahé dolerites and intermediate rocks are shown for comparison.

LA97P-4, P-5), the aplitic granites of Fregate and Mahé (LA 97F-13A, 13C; LA97M-26D), and the hypersolvus granites of Mahé and Ste. Anne (LA97M-11B, LA99M-2, LA97A-29). Normative or modal colour index (percent mafic minerals) is generally <10, and there is a tendency for the more potassic samples to have lower colour

index. The vast majority of Seychelles granitoids are metaluminous–peralkaline, and peraluminous compositions are absent or insignificant (Fig. 5). It is misleading, therefore, to describe Seychelles granitoids as chemically alkaline (Weis & Deutsch, 1984; Hoshino, 1986; Suwa et al., 1994) or even 'mildly' alkaline (Stephens & Devey, 1992; Plummer, 1995).

Collectively, Seychelles granitoids show 'normal' variation trends of decreasing Al_2O_3, MgO, $Fe_2O_3^T$, CaO, P_2O_5, TiO_2 and MnO with increasing SiO_2 (Fig. 6). Both Na_2O and K_2O show substantial scatter, with no apparent trends (Fig. 6). There is considerable overlap amongst granitoids from all Seychelles islands for most major elements except perhaps for the alkalis; it should be kept in mind, however, that this compilation, which includes all published data ($n = 30$), represents incomplete sample coverage for most islands except perhaps Mahé ($n = 18$). Nevertheless, it is apparent that the red to pink granites from Praslin have higher K_2O and lower Na_2O than those from Mahé (Fig. 6), a point noted by Weis & Deutsch (1984), based on additional, but regrettably unpublished rock analyses. In terms of alkali abundances, samples from La Digue, Fregate, Recifs and Marianne resemble Praslin granitoids, but a single specimen of grey granodiorite from Praslin (LA97P-15) is chemically akin to the grey granitoids of Mahé.

This chemical distinction between Mahé grey granitoids and the dominantly red to pink granitoids from other islands (notably Praslin, La Digue, Recifs, Marianne and Fregate) is significant, and is best expressed in terms of trace element concentrations and isotopic compositions (Weis & Deutsch, 1984), as discussed below. Accordingly, we distinguish two types of granitoids, referred to hereafter as the Mahé Group (which includes the single grey granodiorite from Praslin, LA97P-15), and the Praslin Group [which includes the red to pink granitoids from Praslin, La Digue, Fregate, Recifs and Marianne (Fig. 2)]. The hypersolvus granitoids from Mahé (LA97M-11B, LA99-2) and Ste. Anne (LA97A-29) are chemically and isotopically akin to those of the Mahé Group. In most cases, the chemical and/or isotopic distinction between Mahé and Praslin Group granitoids is clear, but a few specimens share properties of both groups; these are discussed individually below.

Mahé Group granitoids have lower concentrations of incompatible elements than those of the Praslin Group, as illustrated in Harker plots (Fig. 7) and spider diagrams (Fig. 8). In general, increasing concentrations of Rb, Th, U and Pb are found in the sequence: Mahé—Fregate—Praslin—La Digue (Figs 7 and 9). The Marianne granite and Recifs granophyre are also variably enriched in incompatibles. Mahé granitoids are generally enriched in Ba (Fig. 7) and Sr relative to those from other islands, and available data allow Mahé Group granitoids (excluding aplite dyke LA97M-26D) to be
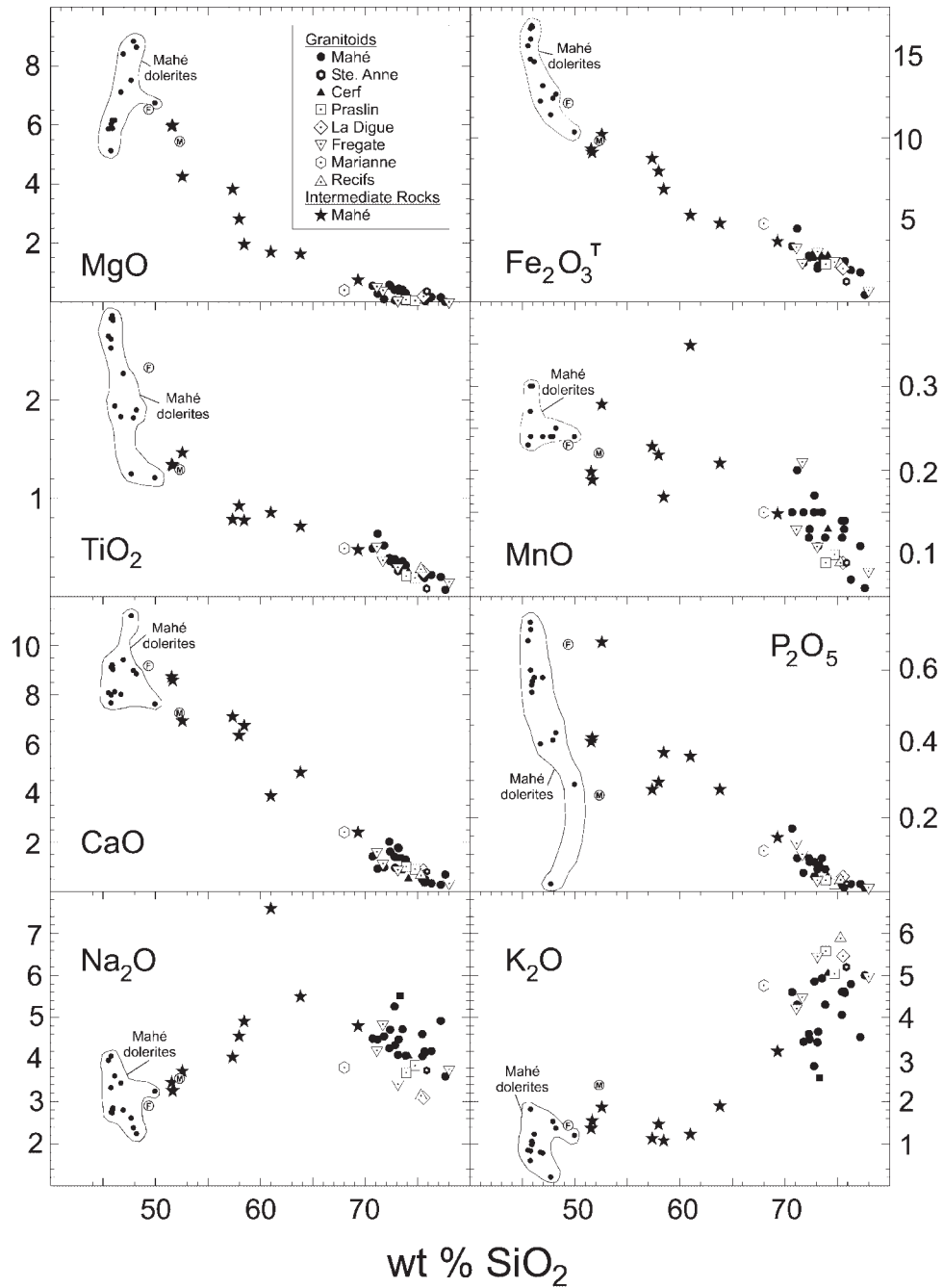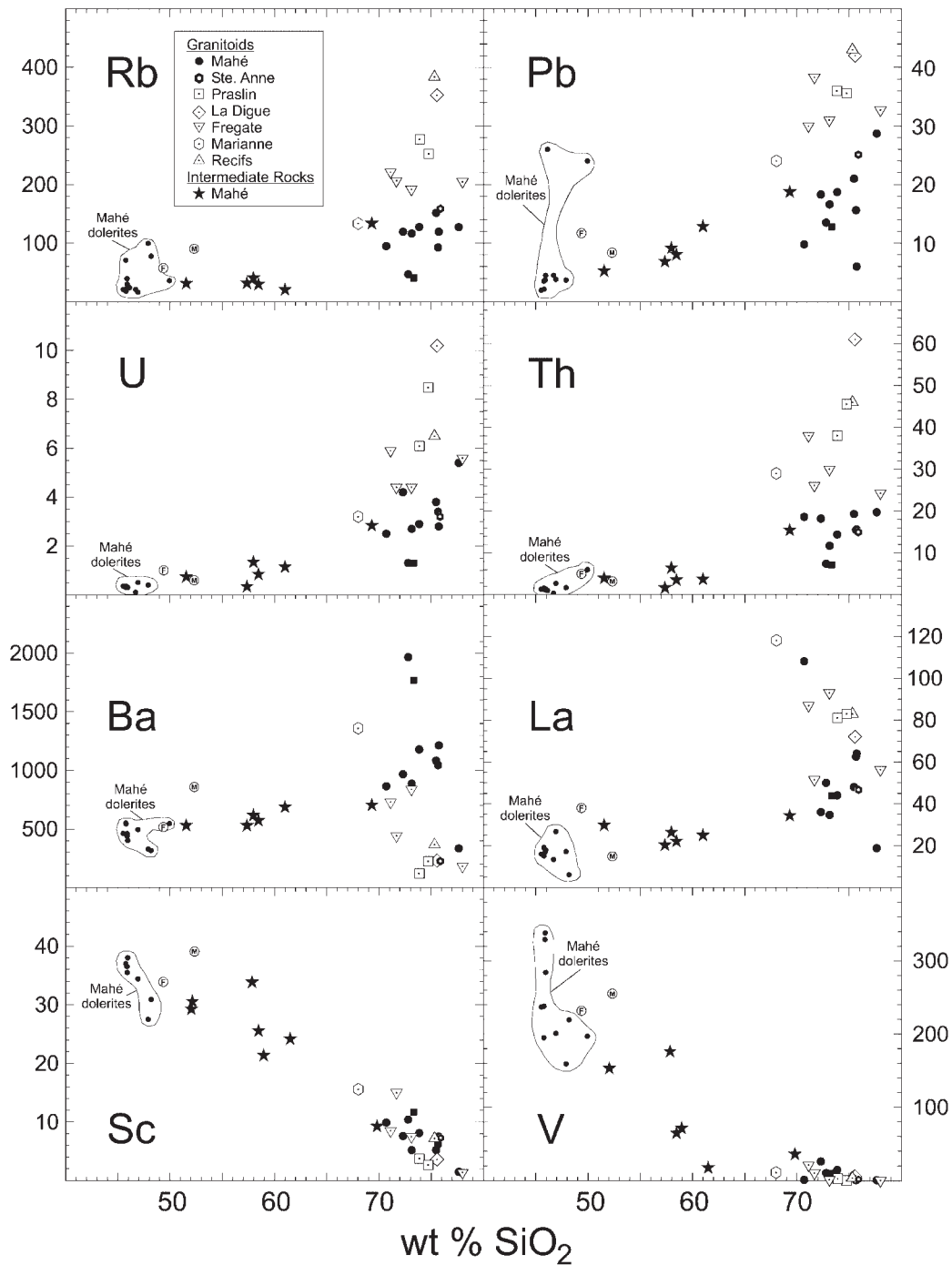
Fig. 6. Harker diagrams showing variation of major element oxides with silica, for Seychelles granitoids, intermediate rocks and dolerites. Granitoids of the Mahé Group are shown as filled symbols, those of the Praslin Group as open symbols; locations are given in the inset at upper left. Compositional fields for Mahé dolerites are outlined; data points for individual dolerite specimens from Fregate (F) and Marianne (M) are circled. Data for granitoids are from this study ($n = 26$), Baker (1963, 1967; $n = 5$) and Suwa *et al.* (1983, 1984; $n = 7$). Data for dolerites are from this study ($n = 9$), Baker (1967; $n = 3$) and Devey & Stephens (1992, $n = 2$).

characterized as follows: Rb <180 ppm, Th <20 ppm, Pb <30 ppm, U <4·2 ppm, Nb <15 ppm and Ba >840 ppm (Fig. 7, Table 1). Granitoids from Mahé, Fregate, Praslin, La Digue, Recifs and Marianne are readily

distinguished on a variety of inter-element plots, most notably Rb vs Th or U vs Pb (Fig. 9). Increases in SiO_2 among granitoids are accompanied by marked decreases in Sc and V, and vague increases in Rb and Pb for Mahé

Fig. 7. Harker diagrams showing variation of trace elements (in ppm) with silica, for Seychelles granitoids, intermediate rocks and dolerites. Granitoids of the Mahé Group are shown as filled symbols, those of the Praslin Group as open symbols; locations are given in the inset at upper left. Compositional fields for Mahé dolerites are outlined; data points for individual dolerite specimens from Fregate (F) and Marianne (M) are circled. All data are from this study.

granitoids; other trace elements such as Ba and Th do not correlate with silica content (Fig. 7).

The REE in most Seychelles granitoids, including both Mahé (Fig. 10a) and Praslin (Fig. 10b) Groups, show similar abundance levels (La 100–300 times chondrites; Lu 15–50 times chondrites) and pattern shapes [steeper light REE (LREE) and flatter heavy REE (HREE)]. All samples show negative Eu anomalies. A few Mahé
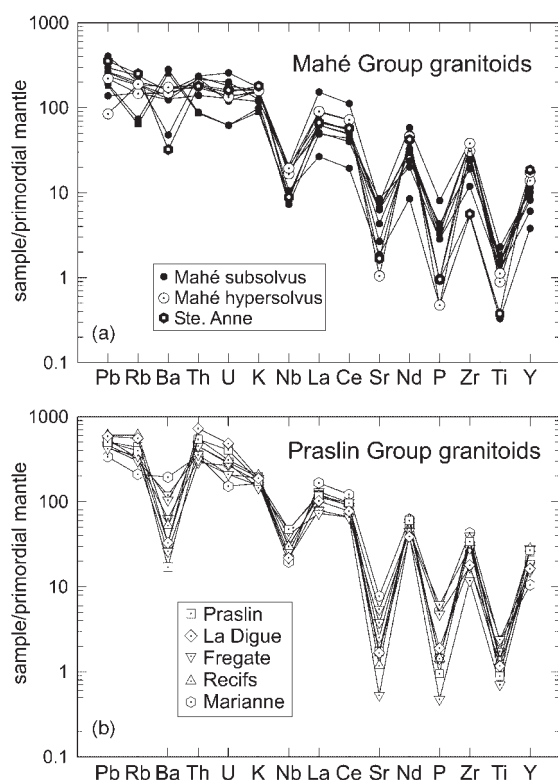
Fig. 8. Normalized multi-element (spider) diagrams comparing trace element concentrations of (a) Mahé Group and (b) Praslin Group granitoids. Data are normalized to 'primordial mantle' values of McDonough *et al.* (1992). In (a), subsolvus granitoids of the Mahé Group (filled symbols) are distinguished from hypersolvus granitoids (open symbols).

Fig. 9. Plots of (a) Rb vs Th and (b) U vs Pb for Seychelles granitoids and intermediate rocks, showing the enrichment in incompatible elements of Praslin Group granitoids relative to those of the Mahé Group.

samples extend to lower overall REE abundances, notably granodiorite LA99M-3A and aplite dyke LA97M-26D, both of which show concave-upward patterns (Fig. 10a). In general, Praslin Group granitoids show a tighter clustering of REE patterns in terms of abundance levels. A significant distinguishing feature in REE relates to the magnitude of Eu anomalies: Praslin Group granitoids have larger negative Eu anomalies ($[Eu/Eu^*]_N = 0.18$–0.58) than those for Mahé Group samples ($[Eu/Eu^*]_N = 0.41$–0.82) (Fig. 10a and b), and Eu anomalies tend to become larger with increasing SiO_2. Crude decreases of individual REE with increasing SiO_2 are apparent only for LREE (La, Ce); HREE show no such correlations. The pink to grey Marianne granite (LA97M-9) has a slightly steeper overall REE pattern than most other granitoids (Fig. 10b), and although its isotopic composition (discussed below) indicates a Praslin Group signature, its REE pattern shape, $[Eu/Eu^*]_N$ value of 0.58, and some (Rb, Pb, U, Ba), but not all (Th, LREE) trace element concentrations (Figs 7 and 9) are similar to

Mahé Group features. Similarly, the Ste. Anne hypersolvus granite (LA97A-29), whose isotopic and trace element signature associate it with the Mahé Group, has a REE pattern and $[Eu/Eu^*]_N$ value (0.20) resembling Praslin Group samples (Fig. 10a). The significance of these exceptions is explained in our interpretative discussion.

Intermediate rocks

Intermediate rocks include those that occur as rounded to angular inclusions and enclaves in granitoid hosts (LA99M-3B; LA97M-24B, 25B) (Fig. 3c and d), and as irregular masses and patches of coeval magmatic rocks (LA97M-26A, 26B, 26C) (Fig. 3b). Lithologies (Table 1) range from granodiorite to quartz diorite to diorite and amphibolite (given its mineralogy, we consider the term 'amphibolite' as most appropriate for sample LA97M-25B, even though its origin involves purely magmatic, and not metamorphic processes), and their normative
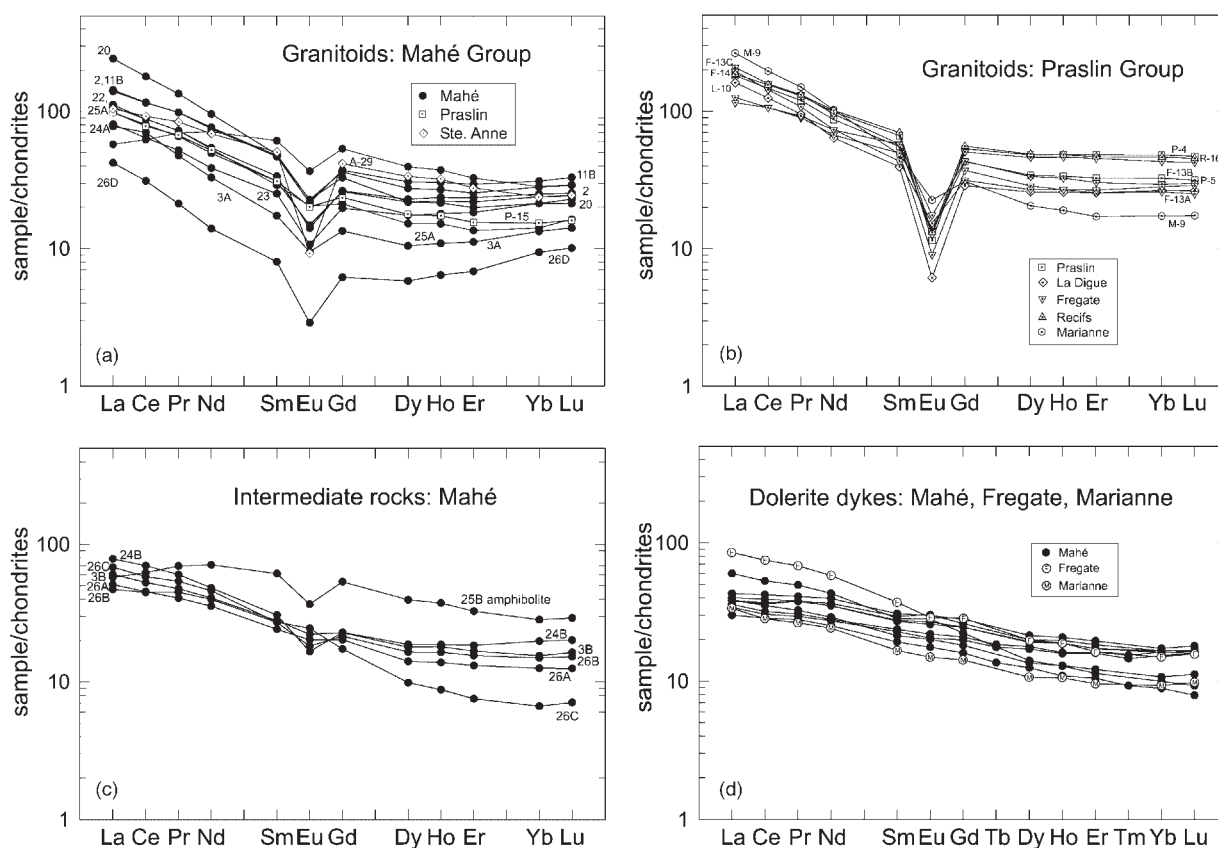
Fig. 10. Chondrite-normalized REE plots for (a) Mahé Group granitoids, (b) Praslin Group granitoids, (c) Mahé intermediate rocks and (d) dolerite dykes. Chondritic abundances used are from Anders & Grevesse (1989).

compositions extend from the field of Seychelles granitoids toward the plagioclase corner (Fig. 4). Silica content varies from 51·6 to 69·3 wt % (Table 1), although Suwa *et al.* (1983, 1994) reported an average of three 'gneissose tonalites + amphibolite' with $SiO_2 = 48·6$ wt %. Normative and modal colour index varies from ∼10 to 35; some of the more mafic samples are slightly olivine normative (Table 4). With very few exceptions, major, minor and trace element chemical compositions of intermediate rocks form an array between Mahé Group granitoids and Mahé dolerites (Figs 6 and 7).

Most intermediate rocks (four of six analysed samples) have similar REE patterns, with smoothly decreasing abundances from La at 45–80 times chondrites to Lu at 12–20 times chondrites, $[La/Lu]_N = 3·1–4·1$, and slight negative Eu anomalies ($[Eu/Eu^*]_N = 0·63–0·92$) (Fig. 10c). Amphibolite xenolith LA97M-25B shows higher REE abundances, with a concave-downward pattern for LREE, and a conspicuous negative Eu anomaly. The mafic hornblende quartz diorite (LA97M-26C), which occurs as an irregular mass in contact with other intermediate rocks, has a steeper REE pattern ($[La/Lu]_N =$

9·7), lower HREE, and a slight positive Eu anomaly relative to other analysed specimens (Fig. 10c). For the intermediate rocks as a group, there is a relationship between SiO_2 content and magnitude of Eu anomaly $[Eu/Eu^*]_N$, such that their compositions plot on an array between Mahé granitoids and dolerites.

Dolerites

Mahé dolerites are dominantly olivine tholeiites (nine of 14 analysed specimens, this study; Baker, 1963; Devey & Stephens, 1992); a few specimens (four of 14) are slightly nepheline normative, and one is slightly quartz normative. These dykes show a moderate range of SiO_2 (45·5–49·9 wt %, average 46·71 ± 1·28 wt %, $n = 14$), and with increasing silica, there are regular decreases in $Fe_2O_3^T$, TiO_2, P_2O_5, Sc and V, and increases in MgO (Figs 6 and 7). Single dolerite specimens from Fregate and Marianne have slightly higher silica (to 52·3 wt % SiO_2), but are otherwise chemically similar to Mahé dolerites (Figs 6 and 7). The large range in LOI values (0·2–3·2 wt %, average 1·73 ± 0·88 wt %, $n = 20$) demonstrates the variably altered character of Seychelles

dolerites. Harris & Ashwal (2002) have observed that increases in LOI amongst Mahé dolerites are correlated with decreases in whole-rock $\delta^{18}O$ values.

REE patterns for Mahé dolerites are similar, showing smoothly decreasing abundances from La at 30–60 times chondrites to Lu at 8–20 times chondrites, slight REE enrichment ([La/Lu]$_N$ = 2·2–6·5), and no appreciable Eu anomalies (Fig. 10d). Specimens from Marianne and Fregate are comparable, although the Fregate sample has slightly higher LREE (Fig. 10d).

Rb–Sr and Sm–Nd isotopic compositions

Rb–Sr and Sm–Nd isotopic and concentration data for 34 whole-rock samples, representing Seychelles granitoids, intermediate rocks and dolerites, are given in Table 3, and plotted in a series of diagrams in Figs 11–13. These data are not used here for magmatic geochronology because precise ages of our samples are provided by U–Pb zircon determinations (Tucker *et al.*, 2001). However, the following relationships are noteworthy. Sm–Nd isotopic data for eight of 10 Mahé Group granitoids (including Praslin and Ste. Anne samples LA97P-15 and LA97A-29) plot on or near a 750 Ma reference line (Fig. 11a); a regression of these data yields an age of 800 ± 90 Ma [mean square weighted deviation (MSWD) = 1·8]. Hypersolvus granitoid LA99M-2 and aplitic dyke LA97M-26D plot below this reference line. Sm–Nd data do not yield isochron relationships for any other combination or subset of Seychelles samples (granitoids, intermediate rocks, and/or dolerites), using our new data alone or in combination with previously published results (Weis & Deutsch, 1984; Dickin *et al.*, 1986).

There is evidence that the Rb–Sr isotopic system has been disturbed, especially for samples with high Rb/Sr, which yield impossibly low initial Sr ratios calculated at 750 Ma ($I_{Sr\,750}$) of <0·700 (Table 3). Although a large database of Rb–Sr isotopic measurements exists for Mahé Group granitoids (n = 38: data from this study, n = 9; Yanagi *et al.*, 1983, n = 23; Michot & Deutsch, 1977, n = 6), regressions using the complete or partial dataset yield ages (684–714 Ma) that are significantly younger than their known crystallization ages of $\sim$750 Ma. Insufficient Rb–Sr isotopic data exist for Praslin Group granitoids to meaningfully assess isochron relationships, although amongst those samples with U–Pb zircon ages of $\sim$750 Ma (Praslin, La Digue and Fregate), a seven-point errorchron of 763 ± 32 Ma can be regressed, with I_{Sr} = 0·703 ± 12, and MSWD = 55 (Fig. 11b).

The ε_{Nd} values calculated at 750 Ma ($\varepsilon_{Nd\,750}$) for Mahé Group granitoids vary from +0·74 to +3·12, but excluding aplite dyke sample LA97M-26D ($\varepsilon_{Nd\,750}$ = +0·74) and hypersolvus granite sample LA99M-2 ($\varepsilon_{Nd\,750}$ = +1·68), there is a clustering of $\varepsilon_{Nd\,750}$ values between

+2·70 and +3·12 (average 2·85 ± 0·17, n = 8, including sample LA97P-15). $I_{Sr\,750}$ values for Mahé Group granitoids vary widely between 0·6901 and 0·7047 (average 0·6962 ± 0·0155, n = 38, references as above), but for samples with $^{87}Rb/^{86}Sr$ <4, $I_{Sr\,750}$ = 0·7017–0·7047 (average 0·7031 ± 0·0008, n = 17). The hypersolvus granite from Ste. Anne (LA97A-29) has an ε_{Nd} value within the main group of Mahé granitoids, even if recalculated at its slightly older crystallization age ($\varepsilon_{Nd\,750}$ = +3·19, $\varepsilon_{Nd\,764}$ = +3·29). However, its I_{Sr} is distinctly higher than that of other Mahé Group granitoids ($I_{Sr\,750}$ = 0·7113, $I_{Sr\,764}$ = 0·7086, Fig. 12).

Initial isotopic compositions of Praslin Group granitoids show far more variability than those for Mahé Group samples, with consistently lower $\varepsilon_{Nd\,750}$ values and generally higher $I_{Sr\,750}$ values (Fig. 12). Results for individual islands are as follows: Praslin ($I_{Sr\,750}$ = 0·7072–0·7147; $\varepsilon_{Nd\,750}$ = −1·10 to −1·18, n = 2); La Digue ($I_{Sr\,750}$ = 0·7163; $\varepsilon_{Nd\,750}$ = −3·34, n = 1); Marianne ($I_{Sr\,750}$ = 0·7069; $\varepsilon_{Nd\,750}$ = −3·83, n = 1); Fregate ($I_{Sr\,750}$ = 0·6938–0·7070; $\varepsilon_{Nd\,750}$ = −1·86 to −2·96, n = 4). An individual sample of the oldest known Seychelles granitoid from Recifs (sample LA97R-16, 808·8 ± 1·9 Ma, Tucker *et al.*, 2001) has $\varepsilon_{Nd\,809}$ = +0·80, which is intermediate between the Nd isotopic compositions of Mahé and Praslin Group granitoids, but with $I_{Sr\,808}$ = 0·7263, far higher than all other known Neoproterozoic Seychelles rocks.

Dolerite dykes from Mahé, Marianne and Fregate show a correlation of increased $I_{Sr\,750}$ with decreased $\varepsilon_{Nd\,750}$, and plot on a steep array between Praslin Group granitoids and the estimated isotopic composition of depleted mantle at 750 Ma (Fig. 12). The total range in initial isotopic ratios for measured dolerites (n = 11: data from this study, n = 8; from Dickin *et al.*, 1986, n = 3) is $I_{Sr\,750}$ = 0·7021–0·7061 and $\varepsilon_{Nd\,750}$ = +5·45 to −0·87. Some of the Mahé dolerites show primitive isotopic compositions that approach depleted mantle; the most evolved dolerite measured is an individual specimen from Fregate with $I_{Sr\,750}$ = 0·7054 and $\varepsilon_{Nd\,750}$ = −0·87 (Fig. 12).

Intermediate rocks from Mahé plot along an array similar in slope to that for Seychelles dolerites, although very slightly displaced to lower $I_{Sr\,750}$ values, and with lesser total variation in both $I_{Sr\,750}$ (0·7027–0·7041) and $\varepsilon_{Nd\,750}$ (+0·40 to +4·33) (Fig. 12). Most intermediate rocks are slightly more isotopically evolved than host Mahé granitoids, although one sample (LA97M-26C) has higher $\varepsilon_{Nd\,750}$, and plots within the array of Seychelles dolerites (Fig. 12).

Depleted mantle model ages [T_{DM}, calculated using the model of DePaolo *et al.* (1991)] for Mahé Group granitoids range between 1035 and 1228 Ma, with a clustering of model ages at 1076 ± 29 Ma for eight of 11 samples (Table 3). Praslin Group granitoids have
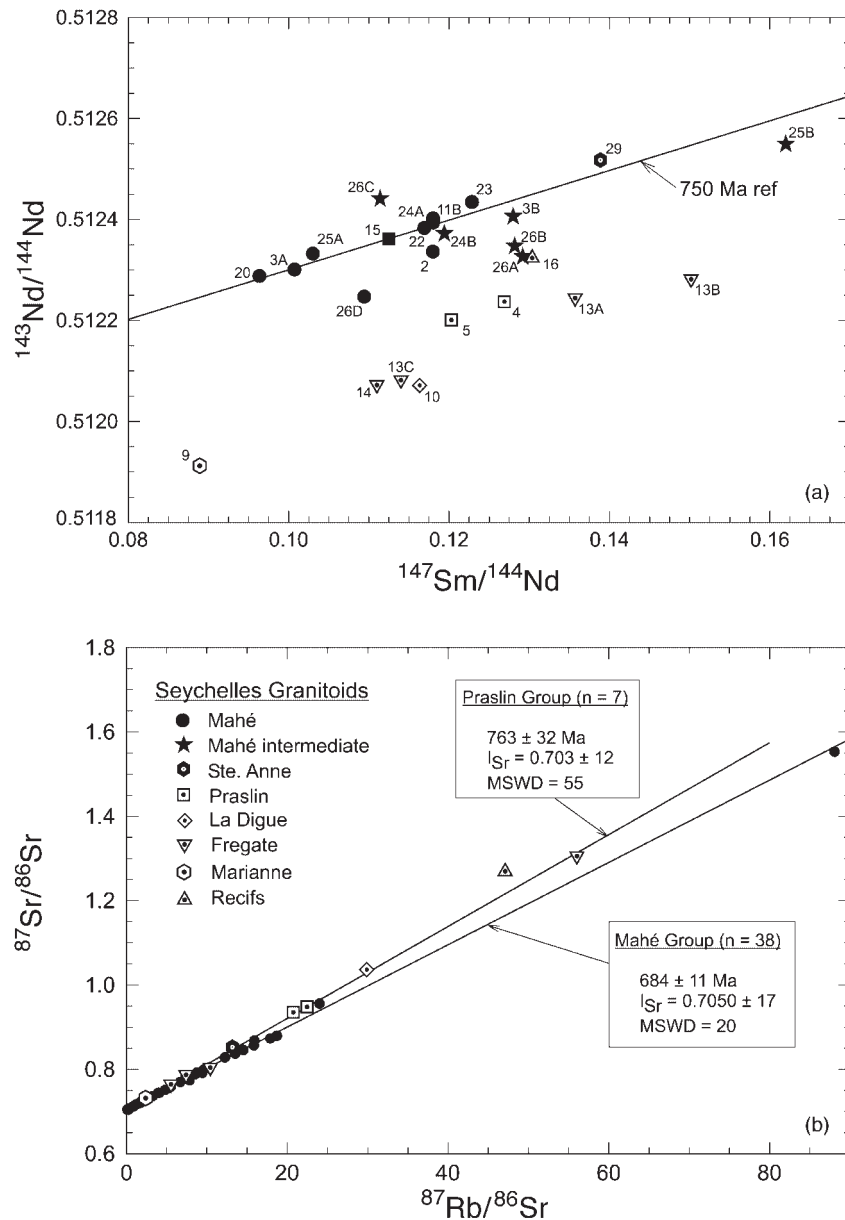
Fig. 11. Sm–Nd and Rb–Sr isochron diagrams for Seychelles granitoids and intermediate rocks. Maximum analytical uncertainties in measured $^{87}Sr/^{86}Sr$ and $^{143}Nd/^{144}Nd$ are smaller than symbol sizes. Mahé Group samples are shown as filled symbols, Praslin Group samples as open symbols. (a) Sm–Nd isotopic systematics. Mahé Group granitoids and intermediate rocks have distinctly higher $^{143}Nd/^{144}Nd$ than Praslin Group samples. Most Mahé Group granitoids (eight of 10 samples) plot near a 750 Ma reference line; exceptions include hypersolvus granite LA99M-2 and aplitic dyke LA97M-26D, both of which have distinctly lower $^{143}Nd/^{144}Nd$ than the bulk of Mahé Group rocks. Mahé intermediate rocks have variable isotopic compositions, reflecting their proposed origin as hybrids between granitoid and doleritic magmas. (b) Rb–Sr isotopic systematics. Mahé intermediate rocks are omitted for clarity. Regression for Mahé Group granitoids ($n = 38$) includes data from this study ($n = 9$), Yanagi *et al.* (1983) ($n = 23$) and Michot & Deutsch (1977) ($n = 6$). Regression for Praslin Group granitoids ($n = 7$) includes data for samples from Praslin, La Digue and Fregate; samples with crystallization ages >750 Ma (Recifs, Marianne) are excluded from the regression.

older T_{DM} model ages (1394–1958 Ma), whereas dolerites ($T_{DM} = 939$–1427 Ma) and Mahé intermediate rocks ($T_{DM} = 960$–1609 Ma) show overlapping model ages that are younger than those of Praslin Group granitoids (Table 3).

INTERPRETATION
Dolerites

We interpret the dolerite dykes of Mahé to have been emplaced approximately coevally with the main period
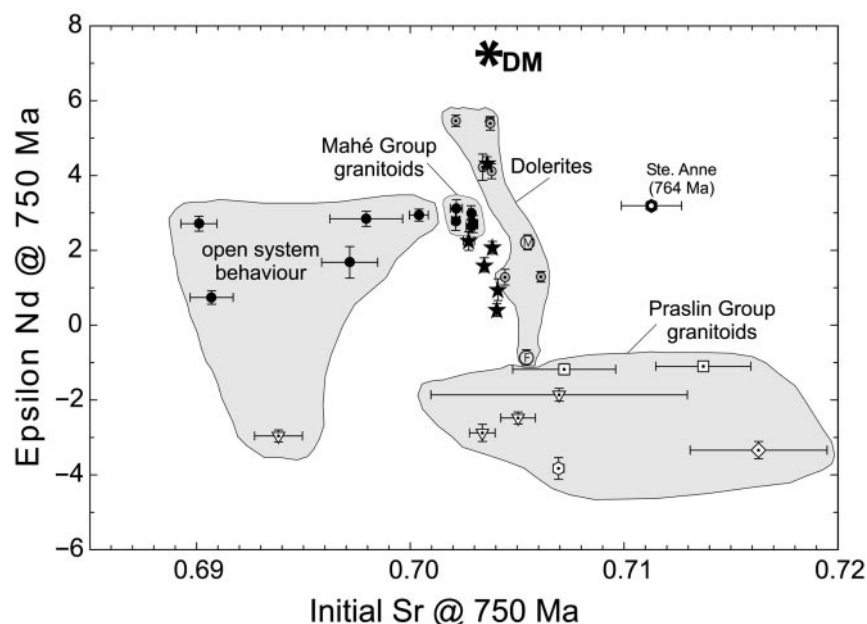
Fig. 12. Plot of initial Sr vs ε_{Nd} (both calculated at 750 Ma), showing initial isotopic compositions of Seychelles magmatic rocks. Data for Recifs biotite granophyre ($I_{Sr\ 808} = 0.7263$, $\varepsilon_{Nd\ 808} = +0.80$) are omitted for clarity. Uncertainties in initial isotopic compositions are calculated using analytical errors in $^{87}Rb/^{86}Sr$, $^{87}Sr/^{86}Sr$, $^{147}Sm/^{144}Nd$ and $^{143}Nd/^{144}Nd$, as given in Table 3; age uncertainties are not included. Large uncertainties in I_{Sr}, especially for Praslin Group granitoids, relate to their high Rb/Sr. Field labelled 'open system behaviour' includes samples with impossibly low I_{Sr} <0.700. Symbols as in Figs 7 and 11. Approximate composition of depleted mantle at 750 Ma (DM) is calculated from estimates given by DePaolo *et al.* (1991) and DePaolo & Wasserburg (1976).

of granitoid magmatism, at ∼750 Ma. The most compelling evidence comes from the precise U–Pb zircon age of 750·2 ± 2·5 Ma for a single Mahé dolerite specimen (LA97M-28C), which is equivalent to the magmatic crystallization ages of the vast majority of Seychelles granitoids. In addition, arguments are presented below for the existence of complex magma mingling effects between dolerites and granitoids, which gave rise to a volumetrically minor, but chemically diverse suite of intermediate rocks on Mahé. This suggests the contemporaneity of dolerite and granitoid magmas, at least for Mahé, and possibly for other Seychelles islands. In this regard, it is important to note that petrographically, all Mahé doleritic rocks show varying degrees of low-grade alteration, in which plagioclase has been partly to totally replaced by sericite and epidote, and mafic silicates (dominantly clinopyroxene) by actinolite, other amphiboles and chlorite (Table 5). By inference, we speculate that the dolerite dykes we sampled from Fregate and Marianne, which are also variably altered, were also probably emplaced at ∼750 Ma.

Mahé dolerites show a limited, but distinct chemical and isotopic variation, in which $\varepsilon_{Nd\ 750}$ values correlate negatively with $I_{Sr\ 750}$, and with wt % SiO_2 (Figs 12 and 13). These arrays suggest that dolerite compositions might be controlled, in part, by mixing between a depleted mantle component (represented, for example, by LA97M-28B, with $\varepsilon_{Nd\ 750} = +5.46$, $I_{Sr\ 750} = 0.702127$ and SiO_2 45·77 wt %; Tables 2 and 3), and an older silicic crustal component, variably introduced as a contaminant. The currently exposed granitoid host rocks (either Mahé or Praslin Groups) of these dolerites are unsuitable as potential contaminants, because their relatively unradiogenic Nd and Sr isotopic compositions (Fig. 13) would require their addition in unreasonably high proportions to account for the small observed variation in dolerite chemistry (e.g. SiO_2 45·77–49·94 wt %). A significantly older silicic contaminant, therefore, seems to be required. Isotopic and chemical data for suitable potential crustal contaminants are sparse, but limited isotopic and chemical studies have been made on Archaean to Proterozoic basement rocks of Rajasthan (northwestern India) and central to northern Madagascar (Gopalan *et al.*, 1990; Tobisch *et al.*, 1994; Tucker *et al.*, 1999a); these regions are argued on the basis of palaeomagnetic data to have been contiguous with the Seychelles at 750 Ma (Torsvik *et al.*, 2001a, 2001b). The most suitable candidate for a dolerite contaminant, amongst the limited choices, is represented by Archaean gneisses of NW India [Banded Gneiss Complex (BGC), Rajasthan, 2·8–3·3 Ga, Gopalan *et al.*, 1990; Tobisch *et al.*, 1994] and/or of central–northern Madagascar (2·5–
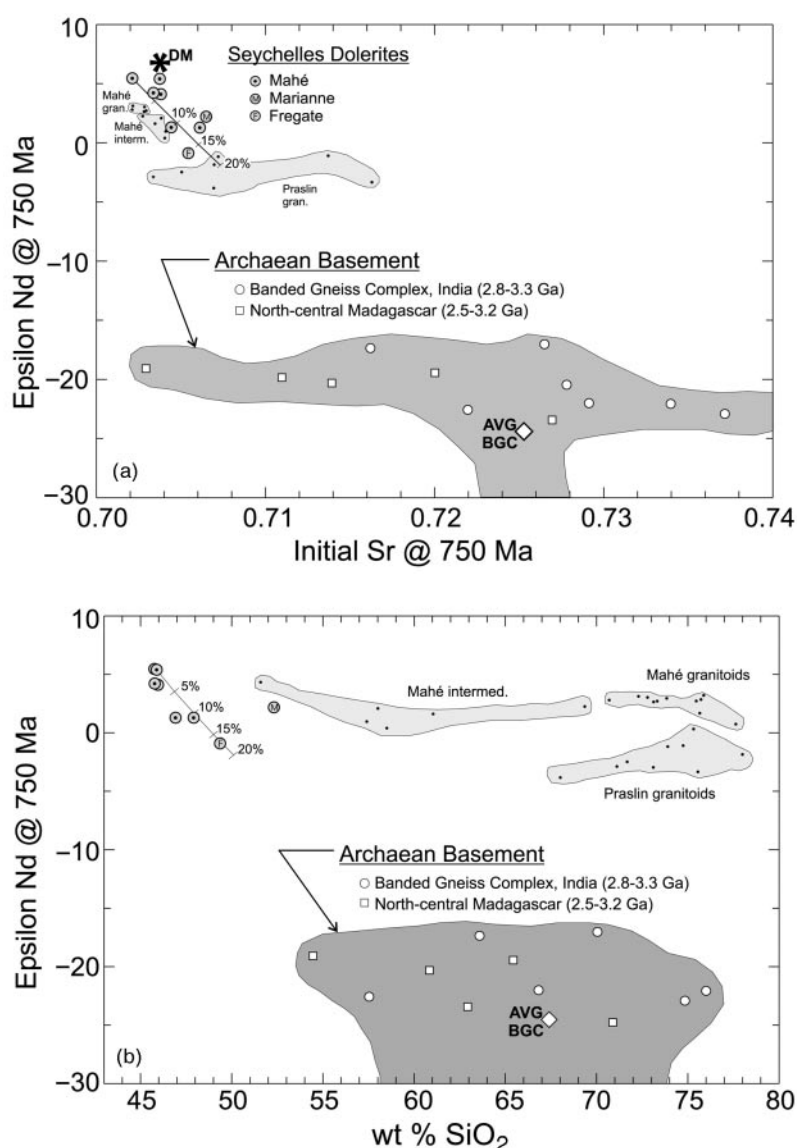
Fig. 13. Plots of $\varepsilon_{Nd\ 750}$ vs (a) $I_{Sr\ 750}$ and (b) wt % SiO_2 showing the results of mixing calculations to account for the isotopic variability of Seychelles dolerite dykes. Tick marks on mixing lines show percentages of average Archaean Banded Gneiss Complex composition (BGC) in mixtures with Seychelles dolerite LA97M-28B. Fields for Archaean basement represent potential contaminants, and show compositions of individual samples from BGC, Rajasthan, India (Gopalan *et al.*, 1990; Tobisch *et al.*, 1994) and north–central Madagascar (Tucker *et al.*, 1999*a*). Fields for Seychelles granitoids (Mahé and Praslin Groups) and intermediate rocks are also shown; these rocks are unsuitable as viable contaminating components for Seychelles dolerite dykes, as discussed in text. Approximate composition of depleted mantle at 750 Ma (DM) is calculated from estimates given by DePaolo *et al.* (1991) and DePaolo & Wasserburg (1976).

3·2 Ga, Tucker *et al.*, 1999*a*). Although in both cases, Archaean gneisses ranging in composition from granitic to gabbroic are present, those of broadly granitic composition would be most suitable chemically and isotopically, as a contaminating component.

Accordingly, we modelled chemical and isotopic compositions of mixtures of the most isotopically primitive dolerite (LA97M-28B) and an average of eight biotite

granite gneisses from the BGC of Rajasthan (Gopalan *et al.*, 1990), using the mixing equation of Langmuir *et al.* (1978). The observed ranges in $\varepsilon_{Nd\ 750}$, $I_{Sr\ 750}$ and wt % SiO_2 in Mahé dolerites can be accounted for with 0–13% bulk assimilation of average BGC (Fig. 13). A single dolerite specimen from Fregate can be similarly modelled with ∼15–16% assimilation, but the Marianne dolerite requires a more silicic contaminant than average BGC

to account for its higher SiO_2 content (52·30 wt %) (Fig. 13).

Although simple crustal assimilation can reasonably account for the observed range in Sr and Nd isotopic compositions and SiO_2 content of Mahé dolerites, their variations in other major and trace elements suggest the additional involvement of other processes, such as crystal fractionation and/or accumulation. For example, removal of <3% ilmenite from chemically and isotopically primitive dolerite compositions, in addition to crustal assimilation, could account for the decreases in TiO_2, MnO and other transition metals such as Zr, with increasing SiO_2 in Mahé dolerites (Figs 6 and 7). However, no reasonable amount of ilmenite fractionation, with or without crustal assimilation, can successfully explain the unusual enrichment in Mahé dolerites of MgO (Fig. 6), Ni and Cr with increasing SiO_2. One possibility involves a coupling of crustal assimilation with accumulation of Mg-rich orthopyroxene; 5–10% addition of En_{90-95} to chemically primitive dolerite could account for the positively correlated arrays of SiO_2 with MgO, Ni and Cr. The absence of Eu anomalies (Fig. 10d), and the negative correlations of Al_2O_3 with individual REE concentrations (Table 2), rule out plagioclase fractionation as a controlling factor in Mahé dolerite petrogenesis.

We recognize that bulk assimilation of solid crustal rocks might represent an oversimplification, as crustal contamination of basaltic magmas commonly involves incorporation of partial melts and/or diffusion-controlled selective assimilation (e.g. Baker *et al.*, 1991). However, given the uncertainties in possible contaminants, the absence of reasonably clear partial melts derived from such sources, and the small sample set of analysed dolerites, we hesitate to undertake more elaborate modelling. Furthermore, there is evidence for element mobility resulting from the variable secondary alteration processes that have affected these dolerites. For example, those dolerites in which plagioclase is most heavily sericitized (e.g. LA97M-21 and LA97M-27, Table 5) show elevated Rb and K_2O contents (Rb 78–99 ppm, K_2O 1·37–1·53 wt %; Table 2), beyond what can be reasonably attributed to crustal contamination or crystal fractionation effects. On the basis of stable isotope measurements of Mahé dolerites and granitoids, Harris & Ashwal (2002) argued that the fluids responsible for variable dolerite alteration could not have been derived from adjacent, coeval granitoids. Rather, the dolerites acted as effective channelways for externally derived aqueous fluids with $\delta^{18}O \leq 0‰$.

Mahé enclaves and intermediate rocks

Inclusions, or 'enclaves' of mafic to intermediate composition are common in nearly all types of granitoids

(Didier, 1973; Vernon, 1983; Didier & Barbarin, 1991), and may form by a variety of processes, including incorporation of country rock fragments (e.g. Grout, 1937) or restite materials from the granitoid source regions (e.g. Bateman *et al.*, 1963; Chen *et al.*, 1990), material accumulation or segregation from host magmas ('autoliths' or 'cognate inclusions', e.g. Didier, 1973, pp. 295–297; Maury *et al.*, 1978), liquid immiscibility (e.g. Bender *et al.*, 1982), and magma mixing and/or mingling (e.g. Barbarin, 1988; Wiebe *et al.*, 1997). Inclusion suites in some granitic bodies may have formed by more than one of these processes, and detailed field, petrographic, geochemical and isotopic data are usually needed to distinguish their origin (e.g. Larsen & Smith, 1990); evidence is often equivocal (Pin *et al.*, 1990).

In the case of the intermediate inclusions, enclaves and irregular masses present in Mahé granitoids, their wide ranges in major and trace element compositions (Figs 6 and 7) are inappropriate to consider an origin by liquid immiscibility, and there is no field or petrographic evidence for mineral accumulation processes in the host granitoids, suggesting that the intermediate rocks do not represent autoliths or cognate inclusions. U–Pb zircon ages of two intermediate rocks (LA97M-26A and 26B) are within error of the vast majority of ages of Seychelles granitoid magmatism (Tucker *et al.*, 2001). This, coupled with the paucity of older, inherited zircon components in the intermediate rocks, argues against their origin as fragments of country rock or restitic source materials. We believe, therefore, that the most likely origin for Mahé intermediate rocks involves processes of magma mixing, mingling and hybridization, evidence for which is becoming widely recognized in many granitic terranes of diverse tectonic setting (e.g. Wiebe, 1980, 1993*a*, 1993*b*, 1996; Reid *et al.*, 1983; Michael, 1991; and references therein). The most impressive field evidence for this on Mahé consists of irregular masses of mafic quartz diorite that have lobate to crenulate margins in contact with host granitoids (Fig. 3b); these features resemble those in well-documented examples of silicic magma chambers into which coeval mafic melts have been injected (e.g. Channel Islands, UK, Wiebe & Collins, 1998, fig. 2; coastal Maine, Wiebe, 1993*b*, fig. 4). The well-preserved igneous textures in most Mahé intermediate rocks (electronic Appendix) and the presence of complex zoning features in feldspars, suggestive of magmatic disequilibrium effects (Vernon, 1984, 1990), support an origin by magma mixing processes.

The compositional patterns in which intermediate rocks plot as arrays between Mahé granitoids and Mahé dolerites on a wide variety of bivariate chemical and isotopic diagrams (Figs 6, 7 and 12) strongly suggest the possibility of magmatic hybridization. Although some have argued that such chemical trends can represent variable degrees of separation of restite from granitoid

melt components (White & Chappell, 1977; Chappell *et al.*, 1987), this hypothesis has been strongly criticized (Wall *et al.*, 1987; Clemens, 1989). In any case, the slight negative Eu anomalies of most Mahé intermediate rocks (Fig. 10c) are inappropriate for restitic compositions in which plagioclase retention results in the large negative Eu anomalies of derivative granitoid magmas.

To evaluate the possibility of magma hybridization as a first approximation, least-squares mixing calculations for major elements were made using average Mahé granitoid ($n = 17$) and dolerite ($n = 14$) compositions; the results indicate that intermediate rocks could represent blends ranging from 85% granitoid + 15% dolerite (porphyritic hornblende–biotite granodiorite LA97M-24B) to 21% granitoid + 79% dolerite (mafic hornblende quartz diorite LA97M-26C). However, residuals for Al_2O_3 and Na_2O are unacceptably high because many of the intermediate rocks are enriched in these components above that expected for simple granitoid–dolerite mixtures. This, coupled with the elevated Sr concentrations of intermediate rocks (160–1072 ppm, average 475 ppm) relative to both Mahé granitoids (Sr 100 ± 61 ppm) and dolerites (Sr 413 ± 130 ppm), suggests that variable accumulation of plagioclase may have taken place in addition to magma mixing. Accordingly, the least-squares mixing calculations were redone, including end-member plagioclase compositions as variables. Acceptable fits (residuals generally <0·5 wt %) are obtained for most intermediate rocks, and yield the following results: granodiorite 24B = 76% granitoid + 12% dolerite + 12% An_{27}; mafic quartz diorite 26B = 32% granitoid + 55% dolerite + 13% An_{48}; quartz diorite 3B = 29% granitoid + 48% dolerite + 23% An_{37}; quartz diorite 26A = 27% granitoid + 40% dolerite + 33% An_{40}; mafic quartz diorite 26C = 18% granitoid + 67% dolerite + 15% An_{74}; amphibolite 25B = 17% granitoid + 33% dolerite + 50% An_{06}. These results are reasonable for the first four samples; for example, REE patterns calculated using data for average Mahé granitoid and dolerite, and estimated REE abundances for plagioclase (which has a negligible effect) in the proportions given by the mixing calculations give excellent matches to the observed REE patterns of these intermediate rocks, both in terms of pattern shape and REE abundance levels. For the remaining two samples, modelled plagioclase compositions are inappropriate; however, mafic quartz diorite 26C can be successfully modelled as a hybrid liquid with cumulus plagioclase and hornblende. Amphibolite 25B could be a fractionated hybrid liquid, similar to those proposed by Wiebe *et al.* (1997) for enclaves in Silurian granitoids of coastal Maine.

Although these calculations support an origin for the intermediate rocks as variable mixtures of granitoids and dolerites, simple binary mixing between average Mahé granitoid and dolerite cannot account in detail for the compositional dispersion of intermediate rocks in many bivariate diagrams (Figs 6, 7 and 12), which trend toward the entire observed spectrum of dolerite compositions. This suggests that the intermediate rocks represent blends of Mahé granitoid with dolerites that were variably contaminated (probably by Archaean crustal components, as discussed above) before their emplacement into high-level granitic magma chambers. The similarity in variability of initial Sr and Nd isotopic compositions between Mahé dolerites and intermediate rocks (Fig. 12) supports this interpretation. Interestingly, with one exception, all intermediate rocks show lower $\varepsilon_{Nd\ 750}$, and higher $I_{Sr\ 750}$ than host Mahé granitoids (Fig. 12), indicating that if magma mixing is the operative process, then crustally contaminated dolerite is a more abundant component than more primitive dolerite. The isotopic composition of sample LA97M-26C ($\varepsilon_{Nd\ 750} = +4\cdot3$; $I_{Sr\ 750} = 0\cdot70359$), however, resembles those of some of the more primitive dolerites (Fig. 12). As discussed above, the major and trace element chemistry of this sample indicates that it has the highest dolerite component of all intermediate rocks, and may also contain some cumulus plagioclase, probably originally of dolerite parentage.

Granitoids

Features of Seychelles granitoids that require explanation include their broadly granodioritic to monzogranitic compositions, the striking chemical and isotopic differences between Mahé and Praslin Group granitoids, the occurrence of subsolvus granitoids with an uncertain (but probably lesser) volume of hypersolvus granitoids, and a 100 my range in crystallization age, with a dominant peak at ∼750 Ma. In this section we discuss and interpret the conditions of melting and crystallization, the nature and compositions of source materials, and the relative roles of fractional crystallization, crustal assimilation and magma mixing for Seychelles granitoids.

Conditions of melting, emplacement and crystallization

Compositions of most Seychelles granitoids plot between the 500 bar and 5 kbar ternary invariant points in the water-saturated haplogranite system Q–Ab–Or (Tuttle & Bowen, 1958; Holtz *et al.*, 1992). These pressures could approximate either the depth of magma generation, assuming that the rock compositions represent those of unmodified primary melts, or the depth of crystallization, if the granitoids represent residual liquids after fractional crystallization from more primitive magmas. The ubiquitous presence of negative Eu anomalies indicates retention of plagioclase in source materials during partial melting; this is consistent with possible source materials discussed below. A relatively shallow level of emplacement

is indicated by the presence of porphyritic and granophyric textures in some samples. Textural evidence for the late crystallization of biotite, and/or minor amphibole suggests that the initial magmas were H_2O undersaturated, as would be required for magmatic ascent. Hoshino (1986) estimated late-magmatic crystallization temperatures of 650–700°C and oxygen fugacities slightly above the QFM (quartz–fayalite–magnetite) buffer, based on the compositions of richteritic amphiboles in some Mahé granitoids. Most Seychelles granitoids lack the appropriate equilibrium mineral assemblages needed for amphibole geobarometry (Hammarstrom & Zen, 1986; Johnson & Rutherford, 1989). The hypersolvus granitoids of Mahé and Ste. Anne probably crystallized at lower a_{H_2O} than the typical subsolvus varieties, consistent with the presence of Fe-rich augites in some specimens (Suwa *et al.*, 1994); ternary feldspars imply crystallization temperatures >825°C at pressures of ~ 1 kbar (Fuhrman & Lindsley, 1988).

Mahé granitoids show a limited, but distinct range in chemical composition (Figs 6 and 7) that could be attributed to fractional crystallization processes. Assuming that SiO_2 increases during fractionation, the major and trace element variability of Mahé granitoids can be explained by removal of mainly sodic plagioclase, with lesser K-feldspar, ilmenite and apatite. Silica enrichment is accompanied by decreases in Sr, increases in Pb (Fig. 7), and the enhancement of negative Eu anomalies, all of which support the dominant role of plagioclase fractionation. However, the absence of obvious cumulate rocks or magmatic layering amongst exposed Mahé granitoids raises some doubts about the importance of fractional crystallization processes. The chemical diversity observed here is typical of many granitic complexes for which crystal fractionation is often proposed; in cases where the requisite small volumes of complementary cumulate materials are absent, these are assumed to lie below present exposure level, or otherwise sequestered from view. Alternatively, or in addition to fractional crystallization, the chemical variability of these granitoids could result from blending with coeval dolerite magmas, as discussed above for Mahé intermediate rocks. However, this would imply an originally very SiO_2-rich granitic magma composition, and would be inconsistent with the occurrence of the most silicic of Mahé granitoids as aplitic dykes (e.g. LA97M-26D). In any case, Mahé and Praslin Group granitoids cannot be related solely by fractionation processes because of their distinctly different isotopic compositions, as discussed below.

Ages and initial isotopic compositions
The observed relationship in which the initial Sr ratios ($I_{Sr\ 750}$) of Mahé granitoids decline regularly (to impossibly low values) with increasing $^{87}Rb/^{86}Sr$ is suggestive of open-system behaviour in the Rb–Sr isotopic system, which also probably accounts for the Rb–Sr age regressions that are significantly younger than U–Pb zircon ages (Fig. 11b). Similar effects have been documented in other granitoid suites, and have been interpreted in terms of partial resetting of the Rb–Sr isotopic system during a later heating event (e.g. Cameron *et al.*, 1981), or variable introduction of fluids enriched in Rb and/or depleted in radiogenic Sr (e.g. Gerstenberger, 1989). In the case of Mahé granitoids, it is unclear whether Sr isotopic exchange took place continuously over a protracted time period between ~ 750 and ~ 700 Ma, or in response to a singular heating event at 700 Ma or slightly later. There is a gap in U–Pb age determinations between $748 \cdot 2 \pm 1 \cdot 2$ Ma and 703 ± 3 Ma (Stephens *et al.*, 1997; Tucker *et al.*, 2001), suggesting that if Seychelles magmatism was continuous during this interval, its products are either unexposed or have been overlooked.

The Sm–Nd isotopic system is far more coherent for Mahé Group granitoids (Fig. 11a), and we interpret the clustering of initial Nd values for eight of 10 samples at $\varepsilon_{Nd\ 750} = +2 \cdot 85 \pm 0 \cdot 17$ (Fig. 12) to represent primary magmatic values. Exceptions include hypersolvus granite LA97M-2 ($\varepsilon_{Nd\ 750} = +1 \cdot 68 \pm 0 \cdot 42$) and aplite dyke LA97M-26D ($\varepsilon_{Nd\ 750} = +0 \cdot 74 \pm 0 \cdot 18$), which may have slightly different isotopic signatures and/or different crystallization ages (no U–Pb age data are available for these samples). We estimate the initial Sr isotopic composition of the Mahé Group magma at $0 \cdot 7031 \pm 8$, based on a clustering of $I_{Sr\ 750}$ values for 17 samples with low Rb/Sr. Mahé Group granitoids, therefore, appear to have formed from rather isotopically homogeneous magmas, which had a substantial primitive component resembling depleted mantle.

In comparison, Praslin Group granitoids are isotopically less primitive and more variable, with $\varepsilon_{Nd,T} = +0 \cdot 80$ to $-3 \cdot 71$ and $I_{Sr,T} = 0 \cdot 7032 – 0 \cdot 7263$ (Fig. 12), although we cannot assess the extent to which their initial Sr ratios have been lowered by open-system behaviour. These effects are apparent for at least one sample (LA97F-13C), which has unreasonably low $I_{Sr\ 750} = 0 \cdot 6938$, but generally, Praslin Group granitoids have initial Sr ratios that are markedly higher, and initial Nd ratios lower, than those of the Mahé Group, as noted by Weis & Deutsch (1984). Mahé and Praslin Group granitoids, therefore, cannot be related solely by closed-system magma chamber processes such as fractional crystallization; their differences are discussed below in terms of possible source components. Our data do not support the suggestion of Weis & Deutsch (1984) that the Praslin Group granitoids acquired their chemical and isotopic signatures by hydrothermal alteration of rocks originally similar to Mahé Group materials, involving fluids that interacted with old continental crustal basement. If this

were so, then compositions of Praslin granitoids should plot along a mixing array between Mahé granitoids and a hypothetical fluid composition that is enriched in incompatible elements and $^{87}Sr/^{86}Sr$, and depleted in $^{143}Nd/^{144}Nd$. That this is not the case can be shown on a variety of chemical and isotopic plots, such as $\varepsilon_{Nd\ 750}$ vs Rb.

Granitoid petrogenesis

Petrogenesis of silicic magmas (granitoids and volcanic equivalents) has been discussed in terms of: (1) fractional crystallization from primitive (mantle-derived) mafic to intermediate magmas; (2) fractionation of such magmas combined with processes of crustal assimilation (of wall rock and/or silicic melts derived therefrom), magma replenishment and magma mixing; (3) intracrustal partial melting of a diverse spectrum of rock compositions, with or without assimilation, magma replenishment and magma mixing. These possibilities are obviously easier to sort out for well-exposed volcanic terranes, where rocks can more confidently be presumed to represent liquid compositions.

There are arguably very few well-documented examples of silicic magmas having formed purely by direct fractional crystallization from basalt, the most convincing of which come from oceanic islands such as the Galapagos (Byerly, 1980; Juster *et al.*, 1989), or oceanic arcs such as the Aleutians (Singer *et al.*, 1992), where lava compositions of constant isotopic composition show a continuum from voluminous basalt to minor rhyodacites. In rare cases where plutonic granitoids have been proposed to represent basaltic differentiates unaccompanied by other processes, such plutons are commonly zoned, for example, from gabbroic margins to granodioritic interiors (e.g. Captains Bay pluton, Unalaska Island, Alaska, Perfit *et al.*, 1980). Although the clustering of relatively primitive isotopic compositions of Mahé granitoids allows an origin solely by extensive fractionation of basaltic magmas similar to those represented by some Mahé dolerites, there is no spectrum of rock compositions that could represent a fractionation sequence from basalt to granodiorite or granite. Rather, the observed array of Mahé intermediate rock compositions can confidently be attributed to mixing between coeval basaltic and granitoid magmas, as discussed above. We note further that the rhyodacite differentiates of the Galapagos and Aleutians are far less enriched in incompatible trace elements, including REE (at equivalent SiO_2), than are Mahé granitoids. The more evolved and variable isotopic compositions of Praslin Group granitoids (Figs 12–13) cannot be accounted for by simple basalt fractionation without involvement of a crustal component. We conclude that Seychelles granitoids are unlikely to have originated solely by fractional crystallization of mantle-derived magmas.

A more pertinent analogy, perhaps, are rhyolitic lavas in some continental arcs that have been explained by the combined effects of fractional crystallization (from mantle-derived basalt or andesite), crustal assimilation (of wall-rocks or granitic melts), magma replenishment and mixing (e.g. Grove *et al.*, 1997), the so-called FARM process (fractionation, assimilation, replenishment, mixing; Baker *et al.*, 1991) or MASH process (melting, assimilation, storage, homogenization, Hildreth & Moorbath, 1988). Such models generally require a substantial crustal component, estimated at 55–60% or more for rhyolites at Medicine Lake, California (Grove *et al.*, 1997); likewise, DePaolo (1981) estimated ∼50% each of crustal and mantle components for the huge Sierra Nevada and Peninsular Ranges calc-alkaline batholiths of California. Identifying the role of primitive melt fractionation and recognizing its products often requires the presence of a diverse compositional spectrum of rocks that match or approach liquid compositions, as well as possible complementary cumulate materials. The best-documented cases are supported by compositional data for known liquidus mineral assemblages, experimental phase equilibria, and isotopic data (e.g. Baker *et al.*, 1991; Grove *et al.*, 1997).

Lacking many of these clues, it is difficult to assess the applicability of FARM- or MASH-type models for Seychelles granitoids. Presumably, Praslin Group granitoids, with their slightly more 'granitic' compositions, enrichments in incompatible trace elements and more evolved isotopic compositions could reflect larger amounts of, and/or different compositions or ages of assimilated crustal components relative to Mahé granitoids; this basic model was endorsed for Seychelles granitoids by Weis & Deutsch (1984). If Mahé granitoids also acquired their chemical and isotopic compositions by substantial (but perhaps lesser) assimilation of crustal materials, then these assimilants must be juvenile rocks whose mantle-extraction ages only slightly pre-date granitoid emplacement. Given the broad petrologic similarity between Mahé and Praslin Group granitoids, it seems likely that their differences in detail can be attributed to their 'crustal' component, regardless of whether this component was assimilated by putative parental mantle-derived magmas, or by fractionated residua. These components, which are probably substantially different at least in age, must have been in close spatial proximity, to account for the occurrence of coeval, adjacent granitoid plutons of the Mahé and Praslin Groups (as exposed at present on western Praslin, Fig. 2). In any case, it is difficult to recognize the chemical or mineralogical imprint of the mantle-derived component (or its putative fractionation products) in Seychelles granitoids. As stated above, the compositional variability and mineralogical attributes expected for fractionation of mantle-derived magmas are lacking amongst Seychelles granitoids. Of

course, these complementary products could possibly be sequestered below present exposure level, or have been eroded or tectonically transported.

Although we cannot exclude FARM- or MASH-type processes for Seychelles granitoids, we propose that the available data are most consistent with a model fundamentally involving intracrustal melting, the heat source for which was basaltic magmatism. Similar models have been frequently proposed for silicic volcanic rocks and granitoids of diverse ages and tectonic settings, with varying degrees of confidence, source compositions, and involvement of other processes. The metaluminous 'I-type' (Chappell & White, 1974, 1992) chemistry of Seychelles granitoids (Fig. 5) effectively eliminates pelitic metasediments as suitable source materials, and implies dominantly or entirely meta-igneous sources. Considerable divergence of opinion exists, however, as to possible and impossible source compositions that could yield substantial volumes of granitic magma upon partial melting. There is abundant experimental evidence that hydrous melting of basalt (or amphibolite) could yield tonalitic–trondhjemitic magmas (e.g. Wyllie, 1984), which might evolve (by fractionation and/or crustal interaction) toward more 'granitic' compositions. Some studies, however, such as one concerning calc-alkaline plutons in the Cascades, favour direct melting of lower-crustal metabasalt (dominantly amphibolite) to yield a variety of granitoids, whose compositions were controlled by variations in f_{H_2O} (derived from crystallizing basaltic magmas) in melting reactions (Tepper *et al.*, 1993). Similarly, the small volumes of rhyolite at Iceland appear to have formed by remelting of hydrothermally altered basalt (Jónasson, 1994). On the other hand, Roberts & Clemens (1993), on the basis of a review of extant experimental results, argued that because of their low K_2O contents, metabasaltic rocks of all kinds are unsuitable as sources for high-K, calc-alkaline, I-type granitoid magmas. As a result of the lack of basement exposures, Seychelles granitoids are not likely to contribute toward resolution of these debates; nevertheless, below we discuss possible constraints on their sources.

Nature of possible source materials

The relatively primitive isotopic signatures of Mahé granitoids imply the involvement of a juvenile, mantle-derived source component. Depleted mantle model ages (T_{DM}) constrain the maximum age of this source to $\sim$1035–1100 Ma, although the timing for its mantle extraction could approach the $\sim$750 Ma granitoid emplacement ages, if an additional, isotopically evolved component such as ancient crust is involved. A small contribution, for example, of Archaean crust, either as a contaminant to magmas parental to the source, or as a constituent of the granitoid source itself, could account

for the slightly lower $\varepsilon_{Nd\ 750}$ values of Mahé granitoids than the most primitive of Mahé dolerites ($\varepsilon_{Nd\ 750} \sim +5{\cdot}4$) or of model depleted mantle at 750 Ma ($\varepsilon_{Nd\ 750} = +7{\cdot}2$, DePaolo *et al.*, 1991). The source for Mahé granitoids, therefore, could have been composed dominantly of basaltic to intermediate magmatic rocks with ages and isotopic compositions similar to currently exposed Mahé dolerites, with or without a contribution from ancient crust, depending on the extent to which the mantle-derived component approached model depleted mantle.

Although no potential source materials are exposed in the Seychelles, suitable candidates do occur in Madagascar and northwestern India (Fig. 1), both of which may have been adjacent to the Seychelles at 750 Ma, as discussed below. Suitable candidates for an ancient crustal component could be the 2·8–3·3 Ga granitoid gneisses of the BGC, Rajasthan, which were successfully modelled above as a contaminating component in Mahé dolerites, or the 2·5–3·2 Ga gneisses of central–northern Madagascar (Tucker *et al.*, 1999*a*). Isotopic compositions of Seychelles granitoids are compared with these potential contaminants in Fig. 13. The juvenile source component might be similar to the abundant intermediate to basaltic volcanic rocks and associated granodioritic plutons that occur in the Daraina region of northeastern Madagascar. Preliminary work (Tucker *et al.*, 1999*b*, 1999*c*) suggests that these rocks have appropriate ages (715–754 Ma) and isotopic compositions ($\varepsilon_{Nd\ 750} = +2{\cdot}4$ to $+2{\cdot}8$). Other possibilities include the Malani Igneous Suite of Rajasthan, NW India, which consists dominantly of $\sim$750 Ma silicic volcanic rocks and plutons (Pareek, 1981; Bhushan, 2000), although associated mafic to intermediate lavas and intrusive rocks are also present (Roy & Sharma, 1999).

The comparatively evolved and more variable isotopic signature of Praslin Group granitoids requires a larger ancient crustal component. Whether this component may have represented a larger part of a mixed source (e.g. juvenile magmatic rocks + Archaean basement) or of an assimilated magmatic component in mantle-derived source materials is difficult to determine. Seychelles basaltic magmas with $\varepsilon_{Nd\ 750}$ at least as low as $-0{\cdot}87$ and $I_{Sr\ 750}$ as high as 0·7054 are represented by a dolerite dyke at Fregate (Table 3), but these values only approach the isotopic compositions of Praslin Group granitoids (Fig. 13). Of course, mafic to intermediate magmatic rocks with more evolved isotopic compositions may have lain below. Alternatively, the source for Praslin Group granitoids could be entirely or dominantly represented by ancient crust whose isotopic compositions evolved to match the observed granitoid signatures at 750 Ma. We note that Archaean ($\sim$3·3 Ga) amphibolitic rocks of the BGC of Rajasthan (Gopalan *et al.*, 1990; Tobisch *et al.*, 1994) have initial Sr and Nd isotopic compositions

at 750 Ma that overlap or approach those of Praslin Group granitoids, and therefore could be suitable source candidates. However, we share the concerns of Roberts & Clemens (1993) that such mafic rocks contain insufficiently high incompatible elements to allow segregation and emplacement of appreciable volumes of granitoid melt, especially for the incompatible-enriched Praslin Group materials. Average incompatible concentrations for BGC amphibolites (K_2O 0·39 wt %, Rb 6·9 ppm, Nd 15·3 ppm) are typical of tholeiitic basalts, and we surmise that such compositions are unlikely as dominant sources for even the least incompatible-enriched of Praslin granitoids (K_2O 4·2–5·9 wt %, Rb 134–384 ppm, Nd 53–85 ppm).

Given the available constraints, we feel that the most reasonable model for the origin of Seychelles granitoids involves partial melting of a mixed source, the dominant components of which include juvenile, mantle-derived mafic to intermediate rocks, and ancient crustal basement, possibly similar to Archaean tonalitic gneisses of the BGC. Mahé granitoids were derived dominantly from the juvenile source component, whereas the sources for Praslin Group granitoids included a larger, but variable proportion of ancient crustal material. It is difficult to determine the relative proportions of juvenile and ancient source components for either Mahé or Praslin Group granitoids without isotopic and concentration data for reasonably well-constrained estimates of both source components, and for hypothetical partial melts derived therefrom.

Hypersolvus vs subsolvus granitoids

The presence of coeval hypersolvus and subsolvus granitoids is an interesting and important feature of Seychelles magmatism. It is difficult to constrain the relative abundances of the two types, but our sampling suggests that hypersolvus varieties are volumetrically subordinate, and restricted to parts of Mahé and Ste. Anne. Hypersolvus granitoids are generally thought to have crystallized at higher temperatures and lower a_{H_2O} than subsolvus granitoids (e.g. Tuttle & Bowen, 1958; Clemens *et al.*, 1986), and are commonly linked to so-called A-type granites (e.g. Whalen *et al.*, 1987). Coexisting hypersolvus and subsolvus granitoids have been described from many terranes of varying tectonic setting (e.g. Turner *et al.*, 1992), and the origin of hypersolvus granites has been discussed in terms of a variety of magmatic and metasomatic processes (e.g. Martin & Bonin, 1976; Küster & Harms, 1998).

That hypersolvus and subsolvus granitoids of Mahé were coeval is supported by the U–Pb zircon age of 750·9 ± 2 Ma for sample LA97M-11B, although the hypersolvus material at Ste. Anne is slightly older, at 764·2 ± 1·4 Ma (Tucker *et al.*, 2001). Trace element

concentrations, including incompatibles, of our three hypersolvus granitoid samples are within the ranges for Mahé Group subsolvus granitoids (Fig. 8), as are their initial Nd isotopic compositions ($\varepsilon_{Nd, T} =$ +1·68 to +3·29, Fig. 12). However, the hypersolvus samples have consistently lower Sr, Al_2O_3, CaO and MgO, and higher Ga and Y compared with Mahé subsolvus granitoids. REE patterns for the two Mahé hypersolvus samples resemble those of Mahé subsolidus granitoids, although the specimen from Ste. Anne shares some similarities with Praslin Group granitoids (Fig. 10a). Overall, the chemical and isotopic properties of hypersolvus granitoids clearly identify them as members of the Mahé Group.

There is no petrographic, chemical or isotopic evidence that Seychelles hypersolvus granitoids were affected by metasomatic or hydrothermal alteration processes. The observed depletions in Sr, Al_2O_3 and CaO reflect the absence of modal plagioclase. These and other trace element abundances are possibly explicable in terms of plagioclase fractionation from a low-Ca granitoid parental magma, as suggested by Clemens *et al.* (1986), although if the Seychelles hypersolvus granitoids formed at higher temperatures and lower a_{H_2O} than subsolvus varieties, as would be consistent with the presence of minor pyroxene in some specimens (Hoshino, 1986), then an origin as late-stage fractionates seems implausible. Wiebe *et al.* (1997) proposed an intriguing and attractive model for the origin of hypersolvus granitoids that occur specifically in plutonic complexes where there is evidence for interaction between coexisting granitic and basaltic magmas. In their model, a substantial body of hypersolvus granite could form by infusions of basaltic magma into a chamber that was crystallizing subsolvus granite. Ponded basaltic magma effectively raises the temperature and lowers a_{H_2O} in the resident silicic magma chamber, and induces the crystallization of hypersolvus granite. In the example studied by Wiebe *et al.* (1997), the Silurian Cadillac Mountain complex of coastal Maine, the observed incompatible element enrichments in hypersolvus granites relative to subsolvus varieties are attributed to gradual contamination of silicic magmas by trapped basaltic intrusions that were undergoing replenishment, mixing and fractional crystallization (RFC) processes. The Seychelles hypersolvus granitoids do not show such dramatic incompatible element enrichments, and so the chemical interactions between basaltic and granitic magmas there may have been relatively minor. If this model is applicable to the Seychelles, it implies that a significant mafic–silicic layered intrusion (Wiebe, 1993a, 1993b) might underlie the exposed granitoids, especially on Mahé and nearby islands such as Ste. Anne, where hypersolvus granitoids occur.

DISCUSSION AND IMPLICATIONS

Regional correlations with possibly related magmatic rocks in Rodinia

New field work coupled with precise geochronology and palaeomagnetic studies are providing accumulating evidence for the existence of several terranes that may be temporally, spatially, petrologically and tectonically related to the 750 Ma magmatic rocks of the Seychelles. For example, the Malani Igneous Suite (MIS) of Rajasthan in northwestern India consists of subequal volumes of contemporaneous rhyolitic and granitoid magmatic rocks, and is evidently the world's third largest felsic magmatic province (Pareek, 1981; Bhushan, 2000). New U–Pb zircon ages from the MIS of 751–771 Ma [unpublished data of Tucker *et al.*, cited by Torsvik *et al.* (2001*b*)] support Rb–Sr whole-rock ages of 730 ± 10 Ma [recalculated from Crawford & Compston (1970) using new decay constants] and 779 ± 10 Ma (Rathore *et al.*, 1996), and are equivalent to the range of U–Pb zircon ages of Seychelles magmatic rocks. Palaeomagnetic data place the MIS at 41°N (Torsvik *et al.*, 2001*b*) and the Seychelles at 30°N (Torsvik *et al.*, 2001*a*) at 750 Ma, only ∼600 km apart at this time (Fig. 14). Two petrologically and geochemically distinct groups of silicic igneous rocks have been recognized in the MIS, and include the dominantly peraluminous Jalore type and the more alkaline Siwana type (Eby & Kochhar, 1990). Isotopic data for these two groups (Dhar *et al.*, 1996; unpublished data, R. D. Tucker & L. M. Carter, 2001) show remarkable correspondence to Seychelles granitoids, especially for Nd; the Jalore and Siwana types of the MIS are possible counterparts of the Mahé and Praslin Groups of the Seychelles, respectively.

In northeastern Madagascar, Tucker *et al.* (1999*b*, 1999*c*) have recognized felsic and intermediate volcanic and intrusive rocks as part of the Daraina Complex, which yield U–Pb zircon ages of 715–754 Ma. Unlike the relatively pristine magmatic rocks of the Seychelles and MIS, the Daraina Complex has been variably deformed and metamorphosed at 500–550 Ma (Tucker *et al.*, 1999*b*, 1999*c*), thus compromising possible palaeomagnetic studies. Magmatic ages, however, are equivalent to those of the Seychelles and MIS igneous rocks, and Nd isotopic compositions of Daraina samples ($\varepsilon_{Nd, T}$ = +2·4 to +2·8) closely resemble Mahé Group granitoids as well as Jalore type granitic and rhyolitic rocks. Based on these and other data, spatial contiguity at ∼750 Ma of northeastern Madagascar, the Seychelles and northwestern India has been proposed (Tucker *et al.*, 1999*b*, 1999*c*; Torsvik *et al.*, 2001*a*, 2001*b*). Other possible correlatives of Seychelles magmatic rocks include granitic and gabbroic intrusive rocks of similar age (779–814 Ma), which form a linear belt 450 km long in west–central Madagascar (Handke *et al.*, 1999). Still others have been
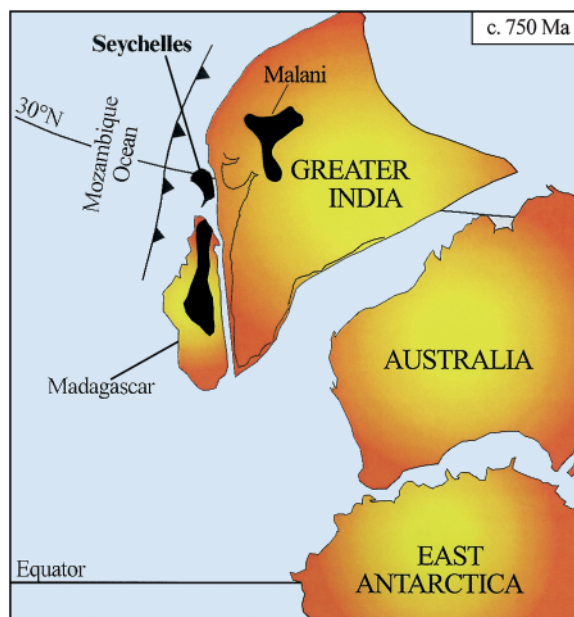

Fig. 14. Palaeogeographic reconstruction of Greater India, the Seychelles microcontinent and Madagascar [modified from Torsvik *et al.* (2001*b*)]. This tectonic trio was located along the western margin of Rodinia remnants (near Australia and East Antarctica). Black patches represent inferred extent of 700–800 Ma igneous rocks.

discussed by Kröner *et al.* (2000), who referred to a 'massive and widespread magmatic event that produced granitoid rocks during the period ∼824 to ∼720 Ma', of which the Seychelles rocks would obviously be a part.

Tectonic setting: evidence for a continental arc origin

The Neoproterozoic magmatic rocks of the Seychelles have classically been interpreted by almost all workers as having formed in an extensional, hotspot- or rift-related tectonic environment (Weis & Deutsch, 1984; Plummer, 1995; Stephens *et al.*, 1995, 1997; Bowden *et al.*, 2001). The main evidence includes the perceived alkaline character of the granitoids, and the well-known magmatic depletions of Mahé granitoids in $\delta^{18}O$, which are observed mainly in hotspot and extensional environments (e.g. Taylor, 1986). We find these arguments unconvincing, and consider another alternative here.

Seychelles granitoids are almost entirely metaluminous granodiorites and monzogranites (Fig. 5), typical of so-called I-type granites (e.g. Chappell & White, 1974; Chappell & Stephens, 1988). Peralkaline granitoids are absent, and it is inappropriate to consider these rocks 'alkaline' or even 'mildly alkaline'. Even the hypersolvus varieties from Mahé and Ste. Anne are monzogranites on a normative basis. Some Praslin Group granitoids are slightly more potassic than the overall range of Mahé

Group samples, but there is considerable overlap (Figs 3 and 6). There is nothing about the alkalinity of Seychelles granitoids that independently demands or suggests an extensional tectonic setting.

Granitoids from the Seychelles were some of the first identified examples of low-^{18}O silicic magmas, with $\delta^{18}O = +3$ to $+4$‰ (Taylor, 1968, 1974, 1977), considerably lower than the $\delta^{18}O$ values of $+5\cdot5$ to $+11$‰ for most terrestrial igneous rocks (e.g. Taylor & Sheppard, 1986). These low $\delta^{18}O$ values, coupled with the magmatic ^{18}O fractionation observed between quartz and feldspars ($\Delta^{18}O_{quartz\text{-}feldspar} = 1\cdot25\text{--}1\cdot5$; Taylor, 1977) have been interpreted as evidence for granite formation in an intra-plate plume or rift (Stephens et al., 1995, 1997). The connection to regional extensional environments comes from analogy with known hotspot- or rift-related magmatic provinces such as Yellowstone and Iceland, where similar $\delta^{18}O$ depletions are observed and are thought to originate by large-scale extensional fracture systems that allow penetration of surface waters to depths where they can interact with magma chambers (Taylor, 1968). Of course, as pointed out by Taylor (1977, 1986), such oxygen isotope features can also be explained if the granitoid source(s) were themselves depleted in ^{18}O, by interaction with meteoric and/or hydrothermal waters in a variety of possible settings. Harris & Ashwal (2002) have reanalysed the oxygen and hydrogen isotope compositions of Seychelles granitoids, and concluded that meteoric water with sufficiently low $\delta^{18}O$ and δD values could not have been present at a palaeolatitude of $\sim30°N$ (constrained palaeomagnetically, Torsvik et al., 2001a) during granitoid formation. Instead, their data can be modelled in terms of mixed source components similar to those proposed in this paper.

In our view, the available geological, geochronological, geochemical and isotopic data for Neoproterozoic magmatism in the Seychelles are far more compatible with a compressional tectonic setting, possibly a continental or Andean-type arc. If this is the case, then the Seychelles 'microcontinent' probably represents only a very small fraction of a larger magmatic entity that has been fragmented by Phanerozoic plate motion processes, and much of the geology contiguous with the Seychelles islands now lies submerged below the Indian Ocean. In this sense, the exposures of the Seychelles can be perceived as a 'drowned' fragment of continental crust, with only some of the former granitic peaks now standing above sea level. Below we discuss features consistent with a continental arc setting for Seychelles magmatic rocks.

Ages

The total age span of ~100 my for magmatic emplacement of Seychelles granitoids, as constrained by U–Pb zircon geochronology (703 ± 3 to 809 ± 2 Ma),

is difficult to reconcile with plume- or rift-related models, which do not result in such spatially restricted (i.e. self-intrusive) magmatic products over this long a time interval. In contrast, in Andean-type continental arcs, there is good evidence for near-continuous, subduction-related magmatism over a time span of 100–150 my or more, in both young (e.g. Peruvian Andes, Pitcher et al., 1985) and ancient examples (e.g. Flin Flon Belt, Palaeoproterozoic Trans-Hudson Orogen, Canada, Whalen et al., 1999). The Coastal Batholith of Peru consists of hundreds of intersecting plutons over an area ~2000 km $\times$ 65 km that were emplaced between 102 and 34 Ma, an interval of ~70 my (Atherton, 1984). Likewise, the North Patagonian Batholith of southern Chile includes granitoid plutons emplaced over ~125 my, from 130 Ma to 10 Ma (Pankhurst et al., 1999). The dominant clustering of Seychelles granitoid ages at 752 ± 4 Ma may, therefore, be more apparent than real, especially considering the enormous difference in scale between the extent of the Peruvian Batholith ($\sim130\,000$ km^2) and the exposed granitoids of the Seychelles (total of ~230 km^2 over an area of ~2100 km^2).

Lithologies and rock chemistry

Plutonic rocks in continental arcs show enormous variations in lithology, from gabbro to leucogranite, and although intermediate compositions (tonalites and granodiorites) dominate overall, relative lithological proportions depend on the size and location of the area considered (e.g. Pitcher, 1978). Granitoids are typically subsolvus, metaluminous, so-called 'I-type', biotite- and/or hornblende-bearing tonalites, diorites, granodiorites and monzogranites (e.g. McCourt, 1981) that mineralogically and texturally resemble those of the Seychelles. Hypersolvus granitoids are not common, but occurrences that are chemically similar to those from Mahé and Ste. Anne have been documented, for example, in the Chilean Andes (Parada, 1984). The presence of hypersolvus granitoids, therefore, cannot be taken as definitive evidence for regional extensional or 'within-plate' tectonic settings, as is commonly perceived.

Plutonic rocks in continental arcs show abundant field and petrographic evidence for interaction, mingling and hybridization between coeval granitic and basaltic magmas, and features very similar to those observed on Mahé (Fig. 3) can be found in the great Mesozoic–Cainozoic batholiths of both North and South America, including the Sierra Nevada of California (Reid et al., 1983; Barbarin, 1990), the Coastal Batholith of Peru (Cobbing & Pitcher, 1972; Bussell, 1985), and related intrusive rocks in southern Chile (Michael, 1991). Commingled mafic and felsic rocks, enclaves and inclusions, and syn-plutonic basaltic to intermediate dykes are extremely common in continental arc granitoids, and very

many studies have documented evidence for chemical hybridization processes, similar to those proposed here for Seychelles intermediate rocks, on a variety of scales (e.g. Bussell, 1985; Barbarin & Didier, 1992; Miller & Wooden, 1994).

In terms of major element chemistry, the spectrum of Seychelles magmatic rocks (granitoids, intermediate rocks and dolerites) closely resembles the diverse array of rock compositions in the composite batholiths of Mesozoic–Tertiary age in the Cordillera of North (e.g. Tepper *et al.*, 1993; Miller & Wooden, 1994) and South America (e.g. McCourt, 1981; Pitcher *et al.*, 1985), where plutonic components from gabbroic to granitic have been well documented. In such analogies, however, the relatively minor intermediate rocks of the Seychelles would correspond to the volumetrically dominant tonalitic to granodioritic compositions in the Cordilleran examples, and the gabbroic plutons to the Seychelles dolerite dykes. Granitoids akin to those of the Mahé Group are plentiful in Cordilleran plutonic complexes, but it would be perhaps misleading to overstate the significance of compositional analogies, because similar major element chemical trends that accompany modest variations in silica, resulting largely from colour index variation, are present in most granitoid complexes regardless of tectonic setting. In general, therefore, compositions of Seychelles magmatic rocks are compatible with a continental arc setting, although a direct analogy is somewhat compromised by imbalances in relative lithological abundances and their modes of occurrence. This may be reconciled, in part by the size and exposure level of the Seychelles, as mentioned above. What is evidently lacking in the Neoproterozoic rocks of the Seychelles is any evidence for the presence of peralkaline granites or syenites, which are commonly associated with rifts (e.g. Oslo Graben, Neumann, 1979) or continental hotspots (e.g. Niger–Nigeria Province, Bowden & Turner, 1974).

Isotopic compositions

Isotopic signatures have been well documented for plutonic rocks in many continental arcs, and typically show a correlated trend of ε_{Nd} and I_{Sr} values extending from the 'mantle array' toward a variety of older continental crustal components (e.g. Farmer & DePaolo, 1983; Liew & McCulloch, 1985). The continuity, extent and curvature of these Sr–Nd arrays depend, amongst other things, on the ages of crustal basement rocks, and on exposure level and state of preservation, both of which decline in older terranes. In well-preserved magmatic arc terranes, the isotopic variations may be geographically correlated, such that near continental margins, granitoids are dominated by juvenile, mantle components, whereas toward continental interiors, the granitoids exhibit a progressive increase in ancient, evolved, continental basement signatures (DePaolo, 1981). Controlling parameters include crustal thickness and structure, as well as temperature distributions and volumes of generated magmas (DePaolo, 1988). Still under debate, in many cases, are the relative roles of fractional crystallization of mantle-derived magmas (with or without combined crustal assimilation), and intracrustal melting, in controlling the isotopic and petrologic characteristics of resultant granitoids, especially those with juvenile isotopic signatures (see McCulloch & Chappell, 1982; DePaolo, 1988). In some cases, temporal variations in juvenile or evolved isotopic signatures amongst magmatic arc granitoids have been documented; these may be correlated with geochemistry, and have been interpreted in terms of arc maturity (Brown *et al.*, 1984; Whalen *et al.*, 1999).

For Seychelles granitoid rocks, the initial Sr and Nd isotopic relations are somewhat compromised by open-system behaviour (dominantly for I_{Sr} in Mahé Group granitoids, Fig. 12). Despite these effects, the primary magmatic isotopic compositions of Seychelles granitoids can be inferred, as discussed above, to reflect variable proportions of juvenile and evolved source components, with Mahé Group granitoids having been derived from sources with a higher juvenile or evolved signature relative to those of the Praslin Group. A more continuous array between possible source components is shown by Sr–Nd isotopic compositions of Seychelles dolerites, although this array is interpreted to reflect variable contamination of mantle-derived magmas with ancient crustal basement, or partial melts derived therefrom. The total range in Sr and Nd initial isotopic composition for Seychelles Neoproterozoic magmatic rocks is smaller than that observed for plutonic rocks in younger and better exposed magmatic arc terranes such as the Mesozoic Sierra Nevada and Peninsular Ranges batholiths of the western USA (DePaolo, 1981; Farmer & DePaolo, 1983). Such limited variability in I_{Sr} and ε_{Nd} in the Seychelles is not surprising, given the small area over which these dominantly coeval, multiply intrusive granitoid plutons were emplaced, and suggests that if a continental magmatic arc model is to be entertained here, then the Seychelles plutons represent a limited structural position in a Neoproterozoic arc, intermediate between the continental margin and continental interior. A comparable range in initial Sr and Nd initial isotopic compositions to that of the Seychelles is observed in spatially restricted subsets of larger magmatic arcs, such as Chilliwack batholith of the North Cascades, Washington (Tepper *et al.*, 1993). This component of the vast Cordilleran magmatic system of western North and South America also shows a similar overlap in Sr and Nd initial isotopic compositions between mafic and granitoid plutonic components, as observed for Mahé granitoids and dolerites (Fig. 12). Seychelles Nd and Sr isotopic data, therefore, are consistent with a continental magmatic arc setting, although limited exposures preclude detailed study of the temporal

and spatial variations that can often be observed in modern arcs.

Palaeomagnetic reconstructions

An important constraint on the tectonic setting of Seychelles magmatism comes from palaeomagnetic studies and reconstructions, which place the Seychelles microcontinent, and inferred regional correlatives (e.g. Malani Igneous Province, NW India; Daraina Complex, NE Madagascar) at a marginal position to what has been called the Rodinia supercontinent, during the period 725–750 Ma (e.g. Karlstrom *et al.*, 2000; Torsvik *et al.*, 2001*a*). Torsvik *et al.* proposed eastward-directed (present-day coordinates) subduction beneath, and associated magmatism into and onto, the western margin of Rodinia at ~750 Ma, with the products of this magmatism now represented in NW India, the Seychelles and NE Madagascar (Fig. 14). A similar model was deemed allowable by Kröner *et al.* (2000), although they also considered that the Late Neoproterozoic granitoids of central Madagascar might alternatively have originated by plume-related magmatic underplating, or sub-crustal mantle delamination during Rodinia break-up.

An Andean arc on the western margin of Rodinia would have been active concurrently with rifting events elsewhere in the supercontinent, which have been proposed to mark its initial break-up (Hoffman, 1991; Dalziel, 1992; Weil *et al.*, 1998). These events are believed to have eventually resulted in collisional events at ~550 Ma, related to the assembly of Gondwana (e.g. Powell *et al.*, 1993; Meert & Van der Voo, 1997). Although the details of Rodinia's configuration and its break-up history are currently under great debate (e.g. Hoffman, 1999; Torsvik *et al.*, 2001*a*), a marginal position for NE Madagascar–Seychelles–NW India is seemingly on solid ground, and the proposed collisional events involved in the assembly of Gondwana would account for the deformation and metamorphism of proposed arc-related magmatic rocks in NE Madagascar (Tucker *et al.*, 1999*b*, 1999*c*; Kröner *et al.*, 2000; Torsvik *et al.*, 2001*a*). In any case, a marginal rather than continental interior position for the Seychelles represents a serious weakness to rift- or plume-related tectonic models, as noted by some proponents of extensional settings for Seychelles magmatism (Stephens *et al.*, 1997). The full extent and timing of arc rocks related to those of the Seychelles awaits further geologic, geochronological, palaeomagnetic and isotopic studies.

SUMMARY AND CONCLUSIONS

The Neoproterozoic (703–809 Ma, dominantly 752 ± 4 Ma) granitoids of the Seychelles are undeformed and unmetamorphosed granodiorites and monzogranites, with metaluminous, I-type chemistry. Subsolvus varieties

appear to predominate, although a significant but uncertain volume of hypersolvus granitoids is also present; in both types, however, normative plagioclase exceeds normative K-feldspar. These granitoids, therefore, cannot be considered alkaline, or even 'mildly' alkaline, as previously alleged.

Two groups of coeval granitoids can be distinguished on the basis of colour, trace element geochemistry and isotopic characteristics, as recognized earlier by Weis & Deutsch (1984). Dominantly grey granitoids of the Mahé Group, exposed on Mahé, Ste. Anne and a small part of Praslin, have relatively low incompatible element concentrations and relatively primitive initial isotopic signatures that cluster at $\varepsilon_{Nd\ 750} = +2\cdot85 \pm 0\cdot17$ and $I_{Sr\ 750} = 0\cdot7031 \pm 0\cdot0008$. Praslin Group granitoids, exposed on Praslin, La Digue, Fregate and numerous smaller islands, are characterized by red to pink colour, variable relative enrichments in incompatible elements (Rb 192–384 ppm, U 4·4–10·2 ppm, Th 24–61 ppm, Pb 30–43 ppm), and variable, but relatively evolved isotopic signatures ($\varepsilon_{Nd,T} = +0\cdot80$ to $-3\cdot71$, $I_{Sr,T} = 0\cdot7032$–$0\cdot7263$). Representatives of both groups are present on Praslin, suggesting that magmatic, rather than tectonic processes controlled their juxtaposition.

Dolerite and granitoid magmatism were coeval in the Seychelles, as indicated by U–Pb geochronology, and by field evidence for complex magmatic intermingling processes that produced a wide variety of intermediate rocks that occur as irregular, lobate masses, enclaves and xenoliths. Major, minor, trace element and isotopic compositions of the intermediate rocks form linear arrays between granitoids and dolerites, suggesting simple two-component mixing, but trace element modelling, especially for REE, indicates that plagioclase (and, in a few cases, hornblende) fractionation played an important role.

Seychelles dolerite dykes are mainly olivine tholeiites, with lesser nepheline-normative compositions, and show variable secondary replacement of magmatic feldspar and pyroxene by sericite, epidote, amphibole, chlorite and biotite, indicating that the dykes may have acted as channelways for the passage of hydrothermal fluids. Initial Nd and Sr isotopic compositions of dolerites approach that of 750 Ma depleted mantle, but show a steep array of correlated ε_{Nd} and I_{Sr} values that can be modelled in terms of up to ~15% crustal contamination with an Archaean granitoid component.

Likewise, the isotopic signatures of Mahé and Praslin Group granitoids indicate derivation from a mixed source that included a dominant juvenile mantle-derived component, with variable amounts of isotopically evolved Archaean silicic basement. Parental melts of Praslin Group granitoids included a larger component of ancient basement relative to Mahé Group rocks, as either a source contribution or an assimilant. The dominant

juvenile source component may resemble the 715–754 Ma mafic to intermediate volcanic rocks and related intrusive rocks in northeastern Madagascar, or the ~750 Ma silicic to intermediate lavas and plutons of the Malani Igneous Suite of Rajasthan in northwestern India; both of these terranes were spatially contiguous with the Seychelles at ~750 Ma. The evolved crustal component could be represented by Archaean (2·5–3·2 Ga) granitoid gneisses of central–northern Madagascar or the Banded Gneiss Complex of Rajasthan. Potential source materials are absent from view in the Seychelles, but our data suggest that Archaean basement was present in the Seychelles microcontinent at 750 Ma, and may be present still.

The limited extent of Seychelles exposures, their possibly unrepresentative nature, and the absence of country rocks, associated volcanic or sedimentary materials and potential source materials, renders tectonic interpretation difficult. Nevertheless, we feel that the properties of Seychelles magmatic rocks summarized above are most consistent with an Andean-type arc setting. These include: a magmatic age span of ~100 my; the presence of biotite- and hornblende-bearing, metaluminous, I-type granitoids and coeval basaltic and intermediate magmas; and the isotopic arrays between depleted mantle and ancient crustal components. These, coupled with palaeomagnetic reconstructions that place the Seychelles at the margins, rather than in the interior of the Rodinia supercontinent, represent a strong case for a continental arc interpretation. Previous assertions of a regional extensional setting (i.e. rift or plume) for Seychelles magmatism were based on a perception of the granitoids as chemically alkaline, and on the magmatic depletions of Mahé granitoids in $\delta^{18}O$. We have shown that the former is erroneous, and stress the likelihood that the observed ^{18}O depletions are a source feature rather than specifically indicative of magma chamber interactions with meteoric or hydrothermal waters in a rift or plume setting. We conclude that the Neoproterozoic magmatic rocks of the Seychelles may represent a small part of a much larger Andean-type arc system, whose extent and significance is just beginning to be realized.

ACKNOWLEDGEMENTS

REFERENCES

Agata, T. & Suwa, K. (1983). Opaque minerals from the Seychelles granitic rocks. *Eighth Preliminary Report on African Studies, Nagoya University*, pp. 63–74.

Anders, E. & Grevesse, N. (1989). Abundances of the elements: meteoritic and solar. *Geochimica et Cosmochimica Acta* **53**, 197–214.

André, L. & Ashchepkov, I. V. (1996). Acid leaching experiments on the mantle-derived Vitim clinopyroxenes: implications for the role of clinopyroxenes in the mantle processes. In: Demaiffe, D. (ed.) *Petrology and Geochemistry of Magmatic Suites of Rocks in the Continental and Oceanic Crusts*. Brussels: Université Libre de Bruxelles; Tervuren: Musée Royal de l'Afrique Centrale, pp. 321–336.

Atherton, M. P. (1984). The Coastal Batholith of Peru. In: Harmon, R. S. & Barreiro, B. A. (eds) *Andean Magmatism*. Nantwich, UK: Shiva, pp. 168–179.

Baker, B. H. (1963). Geology and mineral resources of the Seychelles archipelago. *Geological Survey of Kenya Memoir* **3**, 140 pp.

Baker, B. H. (1967). The Precambrian of the Seychelles Archipelago. In: Rankama, K. (ed.) *The Precambrian*, Vol. 3. New York: John Wiley, pp. 122–132.

Baker, B. H. & Miller, J. H. (1963). Geology and geochronology of the Seychelles Islands and the structure of the floor of the Arabian Sea. *Nature* **199**, 346–348.

Baker, M. B., Grove, T. L., Kinzler, R. J., Donnelly-Nolan, J. M. & Wandless, G. A. (1991). Origin of compositional zonation (high-alumina basalt to basaltic andesite) in the Giant Crater lava field: Medicine Lake volcano, northern California. *Journal of Geophysical Research* **96**, 21819–21842.

Barbarin, B. (1988). Field evidence for successive mixing and mingling between the Piolard Diorite and the Saint-Julien-la-Vêtre Monzogranite (Nord-Forez, Massif Central, France). *Canadian Journal of Earth Science* **25**, 49–59.

Barbarin, B. (1990). Plagioclase xenocrysts and mafic magmatic enclaves in some granitoids of the Sierra Nevada Batholith, California. *Journal of Geophysical Research* **95**, 17747–17756.

Barbarin, B. & Didier, J. (1992). Genesis and evolution of mafic microgranular enclaves through various types of interaction between coexisting felsic and mafic magmas. In: Brown, P. E. & Chappell, B. W. (eds) *The Second Hutton Symposium on the Origin of Granites and Related Rocks: Proceedings. Geological Society of America*, Special Paper **272**, 142–153.

Bateman, P. C., Clarke, L. D., Huber, N. K., Moore, J. G. & Rhinehart, C. D. (1963). The Sierra Nevada Batholith—a synthesis of recent work across the central part. *US Geological Survey Professional Paper* **414D**, 46 pp.

Bender, J. F., Hanson, G. N. & Bence, A. E. (1982). The Cortlandt Complex: evidence for large-scale liquid immiscibility involving granodiorite and diorite magmas. *Earth and Planetary Science Letters* **58**, 330–344.

Bhushan, S. K. (2000). Malani rhyolites—a review. *Gondwana Research* **3**, 65–77.

Bowden, P. & Turner, D. C. (1974). Peralkaline and associated ring-complexes in the Nigeria–Niger Province, West Africa. In: Sørensen, H. (ed.) *The Alkaline Rocks*. New York: John Wiley, pp. 330–351.

Bowden, P., Evans, D. A. D., Li, Z. X. & Powell, C. McA. (2001). Afro-Australasian Precambrian anorogenic magmatism as indicators of supercontinental fragmentation. European Union of Geosciences,

EUG 11, Strasbourg, France, 8–12 April 2001. *Journal of Conference Abstracts* **6**, 771.

Brown, G. C., Thorpe, R. S. & Webb, P. C. (1984). The geochemical characteristics of granitoids in contrasting arcs and comments on magma sources. *Journal of the Geological Society, London* **141**, 413–426.

Bussell, M. A. (1985). The centred complex of the Rio Huaura: a study of magma mixing and differentiation in high-level magma chambers. In: Pitcher, W. S., Atherton, M. P., Cobbing, E. J. & Beckinsale, R. D. (eds) *Magmatism at a Plate Edge: the Peruvian Andes*. Glasgow: Blackie, pp. 128–155.

Byerly, G. (1980). The nature of differentiation trends in some volcanic rocks from the Galapagos Spreading Center. *Journal of Geophysical Research* **85**, 3797–3810.

Cameron, M., Collerson, K. D., Compston, W. & Morton, R. (1981). The statistical analysis and interpretation of imperfectly-fitted Rb–Sr isochrons from polymetamorphic terrains. *Geochimica et Cosmochimica Acta* **45**, 1087–1097.

Chappell, B. W. & Stephens, W. E. (1988). Origin of infracrustal (I-type) granite magmas. *Transactions of the Royal Society of Edinburgh* **79**, 71–86.

Chappell, B. W. & White, A. J. R. (1974). Two contrasting granite types. *Pacific Geology* **8**, 173–174.

Chappell, B. W. & White, A. J. R. (1992). I- and S-type granites in the Lachlan fold belt. *Transactions of the Royal Society of Edinburgh, Earth Sciences* **83**, 1–26.

Chappell, B. W., White, A. J. R. & Wyborn, D. (1987). The importance of residual source material (restite) in granite petrogenesis. *Journal of Petrology* **28**, 1111–1138.

Chen, Y. D., Price, R. C., White, A. J. R. & Chappell, B. W. (1990). Mafic inclusions from the Glenborg and Blue Gum granite suites, southeastern Australia. *Journal of Geophysical Research* **95**, 17757–17785.

Clemens, J. D. (1989). The importance of residual source material (restite) in granite petrogenesis: a comment. *Journal of Petrology* **30**, 1313–1316.

Clemens, J. D., Holloway, J. R. & White, A. J. R. (1986). Origin of an A-type granite: experimental constraints. *American Mineralogist* **71**, 317–324.

Cobbing, E. J. & Pitcher, W. S. (1972). The Coastal Batholith of central Peru. *Journal of the Geological Society, London* **128**, 421–460.

Crawford, A. B. & Compston, W. (1970) The age of the Vindhyan System of Peninsular India. *Quarterly Journal of the Geological Society, London* **125**, 351–372.

Dalrymple, G. B. (1979). Critical tables for conversion of K–Ar ages from old to new constants. *Geology* **7**, 558–560.

Dalziel, I. W. D. (1992). On the organization of American plates in the Neoproterozoic and the breakout of Laurentia. *GSA Today* **2**, 237–241.

Davies, D. (1968). When did the Seychelles leave India? *Nature* **220**, 1225–1226.

Davies, D. & Francis, T. J. G. (1964). The crustal structure of the Seychelles Bank. *Deep-Sea Research* **11**, 921–927.

DePaolo, D. J. (1981). A neodymium and strontium isotopic study of the Mesozoic calc-alkaline batholiths of the Sierra Nevada and Peninsular Ranges, California. *Journal of Geophysical Research* **86**, 10470–10488.

DePaolo, D. J. (1988). *Neodymium Isotope Geochemistry*. Berlin: Springer-Verlag, 187 pp.

DePaolo, D. J. & Wasserburg, G. J. (1976). Inferences about magma sources and mantle structure from variations of $^{143}Nd/^{144}Nd$. *Geophysical Research Letters* **3**, 743–746.

DePaolo, D. J., Linn, A. M. & Schubert, G. (1991). The continental crustal age distribution: methods of determining mantle separation

ages from Sm–Nd isotopic data and application to the southwestern United States. *Journal of Geophysical Research* **96**, 2071–2088.

Devey, C. W. & Stephens, W. E. (1991). Tholeiitic dykes in the Seychelles and the original spatial extent of the Deccan. *Journal of the Geological Society, London* **148**, 979–983.

Devey, C. W. & Stephens, W. E. (1992). Deccan-related magmatism west of the Seychelles–India rift. In: Alabaster, B. C. & Pankhurst, R. J. (eds) *Magmatism and the Causes of Continental Break-up. Geological Society, London, Special Publications* **68**, 271–291.

Dhar, S., Frei, R., Kramers, J. D., Nägler, T. F. & Kochhar, N. (1996). Sr, Pb, and Nd isotope studies and their bearing on the petrogenesis of the Jalor and Siwana Complexes, Rajasthan, India. *Journal of the Geological Society of India* **48**, 151–160.

Dickin, A. P., Fallick, A. E., Halliday, A. N., Macintyre, R. M. & Stephens, W. E. (1986). An isotopic and geochronological investigation of the younger igneous rocks of the Seychelles microcontinent. *Earth and Planetary Science Letters* **81**, 46–56.

Didier, J. (1973). *Granites and their Enclaves. The Bearing of Enclaves on the Origin of Granites. Developments in Petrology 3*. Amsterdam: Elsevier, 393 pp.

Didier, J. & Barbarin, B. (eds) (1991). *Enclaves and Granite Petrology. Developments in Petrology 13*. Amsterdam: Elsevier, 625 pp.

Du Toit, A. L. (1937). *Our Wandering Continents*. London: Oliver & Boyd, 366 pp.

Eby, G. N. & Kochhar, N. (1990). Geochemistry and petrogenesis of the Malani Igneous Suite, Northern India. *Journal of the Geological Society of India* **36**, 109–130.

Farmer, G. L. & DePaolo, D. J. (1983). Origin of Mesozoic and Tertiary granite in the western U.S. and implications for pre-Mesozoic crustal structure. I. Nd and Sr isotopic studies in the geocline of the northern Great Basin. *Journal of Geophysical Research* **88**, 3379–3401.

Francis, T. J. G., Davies, D. & Nill, M. N. (1966). Crustal structure between Kenya and the Seychelles. *Philosophical Transactions of the Royal Society of London, Series A* **259**, 240–261.

Frankel, J. J. (1969). A mega-porphyritic dolerite on Long Island, Seychelles Archipelago. *Geological Magazine* **106**, 260–269.

Frankel, J. J. & Kent, L. E. (1964). On rocks from the Seychelles Islands. *22nd International Geological Congress, New Delhi, Part 10*. New Delhi: International Geological Congress, pp. 161–190.

Fuhrman, M. L. & Lindsley, D. H. (1988). Ternary-feldspar modeling and thermometry. *American Mineralogist* **73**, 201–215.

Gerstenberger, H. (1989). Autometasomatic Rb enrichments in highly evolved granites causing lowered Rb–Sr isochron intercepts. *Earth and Planetary Science Letters* **93**, 65–75.

Gopalan, K., Macdougall, J. D., Roy, A. B. & Murali, A. V. (1990). Sm–Nd evidence for 3·3 Ga old rocks in Rajasthan, northwestern India. *Precambrian Research* **48**, 287–297.

Grout, F. F. (1937). Criteria of origin of inclusions in plutonic rocks. *Geological Society of America Bulletin* **48**, 1521–1572.

Grove, T. L., Donnelly-Nolan, J. M. & Housh, T. (1997) Magmatic processes that generated the rhyolite of Glass Mountain, Medicine Lake volcano, N. California. *Contributions to Mineralogy and Petrology* **127**, 205–223.

Hammarstrom, J. M. & Zen, E-an (1986). Aluminum in hornblende: an empirical igneous geobarometer. *American Mineralogist* **71**, 1297–1313.

Handke, M. J., Tucker, R. D. & Ashwal, L. D. (1999). Neoproterozoic continental arc magmatism in west–central Madagascar. *Geology* **27**, 351–354.

Hargraves, R. B. & Duncan, R. A. (1990). Radiometric age and paleomagnetic results from Seychelles dikes. In: Duncan, R. A., Backman, J., Peterson, L. C. *et al.* (eds) *Proceedings of the Ocean Drilling*

Program, Scientific Results, 115. College Station, TX: Ocean Drilling Program, pp. 119–122.

Harris, C. & Ashwal, L. D. (2001). O and H isotope composition of granites and related rocks from the Seychelles. *Contributions to Mineralogy and Petrology* (submitted).

Hildreth, W. & Moorbath, S. (1988). Crustal contributions to arc magmatism in the Andes of Central Chile. *Contributions to Mineralogy and Petrology* **98**, 455–489.

Hoffman, P. F. (1991). Did the breakout of Laurentia turn Gondwanaland inside-out? *Science* **252**, 1409–1411.

Hoffman, P. F. (1999). The break-up of Rodinia, birth of Gondwana, true polar wander and the snowball Earth. *Journal of African Earth Sciences* **28**, 17–33.

Holtz, F., Pichavant, M., Barbey, P. & Johannes, W. (1992). Effects of H_2O on liquidus phase relations in the haplogranite system at 2 and 5 kbar. *American Mineralogist* **77**, 1223–1241.

Hoshino, M. (1986). Amphiboles and coexisting ferromagnesian silicates in granitic rocks in Mahé, Seychelles. *Lithos* **19**, 11–25.

Hoshino, M. & Suwa, K. (1983). Amphiboles in some granitic rocks from Mahe Island and Cerf Island, Seychelles. *Eighth Preliminary Report on African Studies, Nagoya University*, pp. 47–62.

Johnson, M. C. & Rutherford, M. J. (1989). Experimental calibration of the aluminum-in-hornblende geobarometer with application to the Long Valley caldera (California) volcanic rocks. *Geology* **17**, 837–841.

Jónasson, K. (1994). Rhyolite volcanism in the Krafla central volcano, north-east Iceland. *Bulletin of Volcanology* **56**, 516–528.

Juster, T. C., Grove, T. L. & Perfit, M. R. (1989). Experimental constraints on the generation of FeTi basalts, andesites, and rhyodacites at the Galapagos Spreading Center, 85°W and 95°W. *Journal of Geophysical Research* **94**, 9251–9274.

Karlstrom, K. E., Bowring, S. A., Dehler, C. M., Knoll, A. H., Porter, S. M., Des Marais, D. J., Weil, A. B., Sharp, Z. D., Geissman, J. W., Elrick, M. B., Timmons, J. M., Crossey, L. J. & Davidek, K. L. (2000). Chuar Group of the Grand Canyon: record of breakup of Rodinia, associated change in the global carbon cycle, and ecosystem expansion by 740 Ma. *Geology* **28**, 619–622.

Kröner, A., Hegner, E., Collins, A. S., Windley, B. F., Brewer, T. S., Razakamanana, T. & Pidgeon, R. T. (2000). Age and magmatic history of the Antananarivo Block, central Madagascar, as derived from zircon geochronology and Nd isotopic systematics. *American Journal of Science* **300**, 251–288.

Küster, D. & Harms, U. (1998) Post-collisional potassic granitoids from the southern and northwestern parts of the Late Neoproterozoic East African Orogen: a review. *Lithos* **45**, 177–195.

Langmuir, C. H., Vocke, R. D. & Hanson, G. N. (1978). A general mixing equation with application to Icelandic basalts. *Earth and Planetary Science Letters* **37**, 380–392.

Larsen, L. L. & Smith, E. I. (1990). Mafic enclaves in the Wilson Ridge pluton, northwestern Arizona: implications for the generation of a calc-alkaline intermediate pluton in an extensional environment. *Journal of Geophysical Research* **95**, 17693–17716.

Laughton, A. S., Matthews, D. H. & Fisher, R. L. (1970). The structure of the Indian Ocean. In: Maxwell, A. E., Hill, M. N. & Munk, W. H. (eds) *The Sea* 4. New York: Wiley, pp. 543–586.

Liew, T. C. & McCulloch, M. T. (1985). Genesis of granitoid batholiths of Peninsular Malaysia and implications for models of crustal evolution: evidence from a Nd–Sr isotopic and U–Pb zircon study. *Geochimica et Cosmochimica Acta* **49**, 587–600.

Ludwig, K. R. (1999). User's manual for Isoplot/Ex version 2·3. *Berkeley Geochronology Center Special Publication* **1a**, 53 pp.

Maniar, P. D. & Piccoli, P. M. (1989). Tectonic discrimination of granitoids. *Geological Society of America Bulletin* **101**, 635–643.

Martin, R. F. & Bonin, B. (1976). Water and magma genesis: the association hypersolvus granite–subsolvus granite. *Canadian Mineralogist* **14**, 228–237.

Matthews, D. H. & Davies, D. (1966). Geophysical studies of the Seychelles bank. *Philosophical Transactions of the Royal Society of London, Series A* **259**, 227–239.

Maury, R. C., Didier, J. & Lameyre, J. (1978). Comparative magma/xenolith relationships in some volcanic and plutonic rocks from French Massif Central. *Contributions to Mineralogy and Petrology* **66**, 401–408.

McCourt, W. J. (1981). The geochemistry and petrography of the Coastal Batholith of Peru, Lima segment. *Journal of the Geological Society, London* **138**, 407–420.

McCulloch, M. T. & Chappell, B. W. (1982). Nd isotopic characteristics of S- and I-type granites. *Earth and Planetary Science Letters* **58**, 51–64.

McDonough, W. F., Sun, S.-S., Ringwood, A. E., Jagoutz, E. & Hofmann, A. F. (1992). Potassium, rubidium, and cesium in the Earth and Moon and the evolution of the mantle of the Earth. *Geochimica et Cosmochimica Acta* **56**, 1001–1012.

Meert, J. G. & Van der Voo, R. (1997). The assembly of Gondwana 800–550 Ma. *Journal of Geodynamics* **23**, 223–235.

Michael, P. J. (1991). Intrusion of basaltic magma into a crystallizing granitic magma chamber: the Cordillera del Paine pluton in southern Chile. *Contributions to Mineralogy and Petrology* **108**, 396–418.

Michot, J. & Deutsch, S. (1977). Les Seychelles, un nucléus sialique. *Annales de la Société Géologique Belgique* **100**, 147–156.

Miller, C. F. & Wooden, J. L. (1994). Anatexis, hybridization and the modification of ancient crust: Mesozoic plutonism in the Old Woman Mountains area, California. *Lithos* **32**, 111–133.

Miller, J. A. & Mudie, J. D. (1961). Potassium–argon age determinations on granite from the islands of Mahé in the Seychelles archipelago. *Nature* **192**, 1174–1175.

Neumann, E.-R. (1979). Petrogenesis of the Oslo Region larvikites and associated rocks. *Journal of Petrology* **21**, 499–531.

Pankhurst, R. J., Weaver, S. D., Herve, F. & Larrondo, P. (1999). Mesozoic–Cenozoic evolution of the North Patagonian Batholith in Aysen, southern Chile. *Journal of the Geological Society, London* **156**, 673–694.

Parada, M. A. (1984). La asociation de granitos subsolvus e hipersolvus del pluton Monte Grande (Chile 30°S) y el desarrollo de sus pertitas. *Revista Geológica de Chile* **23**, 69–77.

Pareek, H. S. (1981). Petrochemistry and petrogenesis of the Malani Igneous Suite, India. *Geological Society of America Bulletin* **92**, 206–273.

Perfit, M. R., Brueckner, H., Lawrence, J. R. & Kay, R. W. (1980). Trace element and isotopic variations in a zoned pluton and associated volcanic rocks, Unalaska Island, Alaska: a model for fractionation in the Aleutian calcalkaline suite. *Contributions to Mineralogy and Petrology* **73**, 69–87.

Pin, C., Binon, M., Belin, J. M., Barbarin, B. & Clemens, J. D. (1990) Origin of microgranular enclaves in granitoids: equivocal Sr–Nd evidence from Hercynian rocks in the Massif Central (France). *Journal of Geophysical Research* **95**, 17821–17828.

Pitcher, W. S. (1978). The anatomy of a batholith. *Journal of the Geological Society, London* **135**, 157–182.

Pitcher, W. S., Atherton, M. P., Cobbing, E. J. & Beckinsale, R. D. (eds) (1985). *Magmatism at a Plate Edge: the Peruvian Andes*. Glasgow: Blackie, 328 pp.

Plummer, P. S. (1995). Ages and geological significance of the igneous rocks from Seychelles. *Journal of African Earth Sciences* **20**, 91–101.

Plummer, P. S. & Belle, E. R. (1995). Mesozoic tectono-stratigraphic evolution of the Seychelles microcontinent. *Sedimentary Geology* **96**, 73–91.

Powell, C. McA., Li, Z. X., McElhinney, M. W., Meert, J. G. & Park, J. K. (1993). Paleomagnetic constraints on timing the Neoproterozoic break-up of Rodinia and the Cambrian formation of Gondwana. *Geology* **21**, 889–892.

Rathore, S. S., Venkatesan, T. R. & Srivastava, R. K. (1996). Rb–Sr and Ar–Ar systematics of Malani volcanic rocks of southwest Rajasthan: evidence for a younger post-crystallization thermal event. *Proceedings of the Indian Academy of Sciences (Earth & Planetary Sciences)* **105**, 131–141.

Reid, J. B., Evans, O. C. & Fates, D. G. (1983). Magma mixing in granitic rocks of the central Sierra Nevada, California. *Earth and Planetary Science Letters* **66**, 243–261.

Roberts, M. P. & Clemens, J. D. (1993). Origin of high-potassium calc-alkaline, I-type granitoids. *Geology* **21**, 825–828.

Roy, A. B. & Sharma, K. K. (1999). Geology of the region around Sirohi town, western Rajasthan—story of Neoproterozoic evolution of the Trans-Aravalli crust. In: Paliwal, B. S. (ed.) *Geological Evolution of Northwestern India.* Jodhpur: Scientific Publishers, pp. 19–33.

Singer, B. S., Myers, J. S. & Frost, C. D. (1992). Mid-Pleistocene lavas from the Seguam volcanic center, central Aleutian arc: closed-system fractional crystallization of a basalt to rhyodacite eruptive suite. *Contributions to Mineralogy and Petrology* **110**, 87–112.

Smith, W. H. F. & Sandwell, D. T. (1997). Global seafloor topography from satellite altimetry and ship depth soundings. *Science* **277**(5334), 1956–1962.

Stephens, W. E. & Devey, C. M. (1992). Seychelles and the fragmentation of Gondwana: evidence from the igneous rocks. In: Plummer, P. S. (ed.) *Proceedings of the First Indian Ocean Regional Seminar on Petroleum Exploration, Seychelles.* Victoria, Seychelles: Seychelles National Oil Company, pp. 211–222.

Stephens, W. E., Fallick, A. E. & Ellam, R. M. (1995). ^{18}O depletion in granites as a signature of extensional tectonics: Seychelles basement granites and implications for Late Proterozoic Gondwana. European Union of Geosciences, EUG 8, Strasbourg, France, 9–13 April 1995. *Terra Nova* **7**, 145.

Stephens, W. E., Jemielita, R. A. & Davis, D. (1997). Evidence for *ca.* 750 Ma intra-plate extensional tectonics from granite magmatism on the Seychelles: new geochronological data and implications for Rodinia reconstructions and fragmentation. European Union of Geosciences, EUG 9, Strasbourg, France, 23–27 March 1997. *Terra Nova* **9**, 166.

Streckeisen, A. (1976). To each plutonic rock its proper name. *Earth-Science Reviews* **12**, 1–33.

Suwa, K., Yanagi, T., Tokieda, K., Umemura, H., Asami, M. & Hoshino, M. (1983). Geology and petrology of the Seychelles Islands. *Eighth Preliminary Report on African Studies, Nagoya University*, pp. 3–21.

Suwa, K., Tokieda, K. & Hoshino, M. (1994). Palaeomagnetic and petrological reconstruction of the Seychelles. *Precambrian Research* **69**, 281–292.

Taylor, H. P., Jr (1968). The oxygen isotope geochemistry of igneous rocks. *Contributions to Mineralogy and Petrology* **19**, 1–71.

Taylor, H. P., Jr (1974). A low-^{18}O, late Precambrian granite batholith in the Seychelles Islands, Indian Ocean: evidence for formation of ^{18}O-depleted magmas and interactions with meteoric groundwaters. *Geological Society of America, Abstracts with Programs* **6**(7), 981–982.

Taylor, H. P., Jr (1977). Water/rock interactions and the origin of H_2O in granitic batholiths. *Journal of the Geological Society, London* **133**, 509–558.

Taylor, H. P., Jr (1986) Igneous rocks: II. Isotopic case studies of Circumpacific magmatism. In: Valley, J. W., Taylor, H. P., Jr & O'Neil, J. R. (eds) *Stable Isotopes in High-Temperature Geological Processes. Mineralogical Society of America, Reviews in Mineralogy* **16**, 273–317.

Taylor, H. P., Jr & Sheppard, S. M. F. (1986). Igneous rocks: I. Processes of isotopic fractionation and isotope systematics. In: Valley, J. W., Taylor, H. P., Jr & O'Neil, J. R. (eds) *Stable Isotopes in High-Temperature Geological Processes. Mineralogical Society of America, Reviews in Mineralogy* **16**, 227–271.

Tepper, J. H., Nelson, B. K., Bergantz, G. W. & Irving, A. J. (1993). Petrology of the Chilliwack batholith, North Cascades, Washington: generation of calc-alkaline granitoids by melting of mafic lower crust with variable water fugacity. *Contributions to Mineralogy and Petrology* **113**, 333–351.

Tobisch, O. T., Collerson, K. D., Bhattacharyya, T. & Mukhopadhyay, D. (1994). Structural relationships and Sr–Nd isotope systematics of polymetamorphic granitic gneisses and granitic rocks from central Rajasthan, India: implications for the evolution of the Aravalli craton. *Precambrian Research* **65**, 319–339.

Torsvik, T. H., Ashwal, L. D., Tucker, R. D. & Eide, E. A. (2001*a*). Neoproterozoic geochronology and palaeogeography of the Seychelles microcontinent: the India link. *Precambrian Research* **110**, 47–59.

Torsvik, T. H., Carter, L. M., Ashwal, L. D., Bhushan, S. K., Pandit, M. K. & Jamtveit, B. (2001*b*). Rodinia refined or obscured: palaeo-magnetism of the Malani Igneous Suite (NW India). *Precambrian Research* **108**, 319–333.

Tucker, R. D., Ashwal, L. D., Handke, M. J., Hamilton, M. A., Le Grange, M. & Rambeloson, R. A. (1999*a*). U–Pb geochronology and isotope geochemistry of the Archean and Proterozoic rocks of north–central Madagascar. *Journal of Geology* **107**, 135–153.

Tucker, R. D., Ashwal, L. D. & Torsvik, T. H. (1999*b*). Neoproterozoic silicic magmatism in northern Madagascar, Seychelles and NW India: clues to Neoproterozoic supercontinent formation and dispersal. *EOS Transactions, American Geophysical Union* **80**, S372–S373.

Tucker, R. D., Ashwal, L. D., Hamilton, M. A., Torsvik, T. H. & Carter, L. M. (1999*c*). Neoproterozoic silicic magmatism of northern Madagascar, Seychelles and NW India: clues to Rodinia's assembly and dispersal. *Geological Society of America, Abstracts with Programs* **31**, A317.

Tucker, R. D., Ashwal, L. D. & Torsvik, T. H. (2001). U–Pb geochronology of Seychelles granitoids: a Neoproterozoic continental arc fragment. *Earth and Planetary Science Letters* **187**, 27–38.

Turner, S. P., Foden, J. D. & Morrison, R. S. (1992). Derivation of some A-type magmas by fractionation of basaltic magma: an example from the Padthaway Ridge, South Australia. *Lithos* **28**, 151–179.

Tuttle, O. F. & Bowen, N. L. (1958). Origin of granite in the light of experimental studies in the system $NaAlSi_3O_8$–$KAlSi_3O_8$–SiO_2–H_2O. *Geological Society of America, Memoir* **74**, 153 pp.

Vernon, R. H. (1983). Restite, xenoliths and microgranitoid enclaves in granites. *Journal and Proceedings, Royal Society of New South Wales* **116**, 77–103.

Vernon, R. H. (1984). Microgranitoid enclaves in granites—globules of hybrid magma quenched in a plutonic environment. *Nature* **309**, 438–439.

Vernon, R. H. (1990). Crystallization and hybridism in microgranitoid enclave magmas: microstructural evidence. *Journal of Geophysical Research* **95**, 17849–17859.

Wall, V. J., Clemens, J. D. & Clarke, D. B. (1987). Models for granitoid evolution and source compositions. *Journal of Geology* **95**, 731–750.

Wasserburg, G. J., Craig, H., Menard, H. W., Engel, A. E. J. & Engel, C. J. (1963). Age and compositions of a Bounty Islands granite and age of a Seychelles Islands granite. *Journal of Geology* **71**, 785–789.

Wegener, A. (1924). *The Origin of Continents and Oceans.* London: Methuen, 212 pp.

Weil, A. B., Van der Voo, R., MacNiocaill, C. & Meert, J. G. (1998). The Proterozoic supercontinent Rodinia: paleomagnetically derived reconstructions for 1100 to 800 Ma. *Earth and Planetary Science Letters* **154**, 13–24.

Weis, D. & Deutsch, S. (1984). Nd and Pb isotope evidence from the Seychelles granites and their xenoliths: mantle origin with slight upper-crust interaction for alkaline orogenic complexes. *Isotope Geoscience* **2**, 13–35.

Whalen, J. B., Currie, K. & Chappell, W. (1987) A-type granites: geochemical characteristics, discrimination and petrogenesis. *Contributions to Mineralogy and Petrology* **95**, 407–419.

Whalen, J. B., Syme, E. C. & Stern, R. A. (1999). Geochemical and Nd isotopic evolution of Palaeoproterozoic arc-type granitoid magmatism in the Flin Flon Belt, Trans-Hudson orogen, Canada. *Canadian Journal of Earth Sciences* **36**, 227–250.

White, A. J. R. & Chappell, B. W. (1977). Ultrametamorphism and granitoid genesis. *Tectonophysics* **43**, 7–22.

Wiebe, R. A. (1980). Commingling of contrasted magmas in the plutonic environment: examples from the Nain Anorthosite Complex. *Journal of Geology* **88**, 197–209.

Wiebe, R. A. (1993*a*). Basaltic injections into floored silicic magma chambers. *EOS Transactions, American Geophysical Union* **74**, 1–3.

Wiebe, R. A. (1993*b*). The Pleasant Bay layered gabbro–diorite, coastal Maine: ponding and crystallization of basaltic injections into a silicic magma chamber. *Journal of Petrology* **34**, 461–469.

Wiebe, R. A. (1996). Mafic–silicic layered intrusions: the role of basaltic injections on magmatic processes and the evolution of silicic magma chambers. *Transactions of the Royal Society of Edinburgh: Earth Sciences* **87**, 233–242.

Wiebe, R. A. & Collins, W. J. (1998). Depositional features and stratigraphic sections in granitic plutons: implications for the emplacement and crystallization of granitic magma. *Journal of Structural Geology* **20**, 1273–1289.

Wiebe, R. A., Holden, J. B., Coombs, M. L., Wobus, R. A., Schuh, K. J. & Plummer, B. P. (1997). The Cadillac Mountain intrusive complex, Maine: the role of shallow-level magma chamber processes in the generation of A-type granites. In: Sinha, A. K., Whalen, J. B. & Hogan, J. P. (eds) *The Nature of Magmatism in the Appalachian Orogen. Geological Society of America, Memoir* **191**, 397–418.

Wyllie, P. J. (1984). Constraints imposed by experimental petrology on possible and impossible magma sources and products. *Philosophical Transactions of the Royal Society of London, Series A* **310**, 439–456.

Yanagi, T., Wakizaka, Y. & Suwa, K. (1983). Rb–Sr whole rock ages of granitic rocks from the Seychelles Islands. *Eighth Preliminary Report on African Studies, Nagoya University*, pp. 23–36.